A-Tech Corporation *d.b.a.*
Applied Technology Associates
1300 Britt Street SE
Albuquerque, NM 87123
Cage Code: 6M566
www.atacorp.com
Phone: (505) 767-1200
Fax: (505) 768-1379

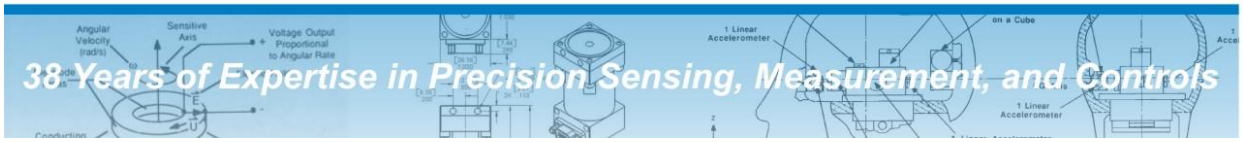

Rotation-Enabled 7-Degree of Freedom Seismometer for Geothermal Resource Development

Phase 1 Final Report

Award #: DE-EE-0005511

Report Period: 30 September 2011 to 31 October 2013

A-Tech Corporation *d.b.a.* Applied Technology Associates
with Team Members: Sandia National Laboratories and Nanometrics, Inc.

ATA Patentable and Proprietary data removed per DOE Final Report submission requirements. Full content available by request from ATA for authorized government reviewers for purposes of review and evaluation.

Prepared by:
Program Manager:
Bob Pierson
Applied Technology Associates
(505) 767-1210
Bob.Pierson@atacorp.com

Principal Investigator:
Darren Laughlin
Applied Technology Associates
(505) 767-1224
Darren.Laughlin@atacorp.com

Customer Distribution:
William A. Vandermeer
U.S. Department of Energy
Golden Field Office
1617 Cole Blvd
Golden, CO 80401-3393
(720) 356-1806
William.Vandermeer@go.doe.gov

Table of Contents

Table of Contents

List of Figures

List of Figures

List of Tables

1.0 EXECUTIVE SUMMARY

Under this Department of Energy (DOE) grant, A-Tech Corporation *d.b.a.* Applied Technology Associates (ATA), seeks to develop a seven-degree-of-freedom (7-DOF) seismic measurement tool for high-temperature geothermal applications. The Rotational-Enabled 7-DOF Seismometer includes a conventional tri-axial accelerometer, a conventional pressure sensor or hydrophone, and a tri-axial rotational sensor. The rotational sensing capability is novel, based upon ATA's innovative research in rotational sensing technologies. **Figure 1** diagrams the 7-DOF tool in its geothermal context.

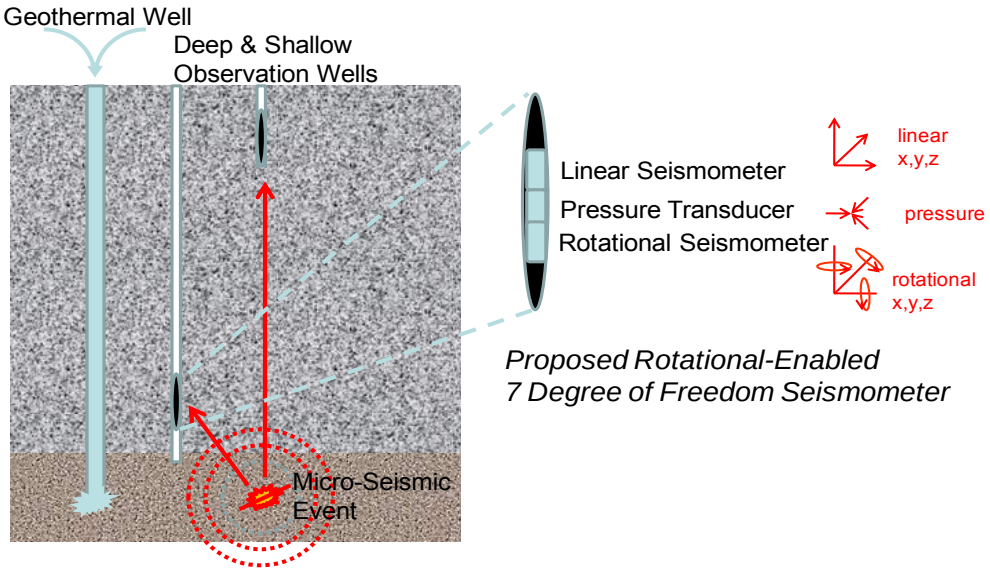

Figure 1. The ATA Tool Adds Rotational Measurement to Traditional Seismometry

The geothermal industry requires tools for high-precision seismic monitoring of crack formation associated with Enhanced Geothermal System (EGS) stimulation activity. Currently, microseismic monitoring is conducted by deploying many seismic tools at different depth levels along a "string" within drilled observation wells. Costs per string can be hundreds of thousands of dollars. Processing data from the spatial arrays of linear seismometers allows back-projection of seismic wave states. In contrast, a Rotational-Enabled 7-DOF Seismometer would simultaneously measure p-wave velocity, s-wave velocity, and incident seismic wave direction all from a single point measurement. In addition, the Rotational-Enabled 7-DOF Seismometer will, by its nature, separate p- and s-waves into different data streams, simplifying signal processing and facilitating analysis of seismic source signatures and geological characterization.

By adding measurements of three additional degrees-of-freedom at each level and leveraging the information from this new seismic observable, it is likely that an equally accurate picture of subsurface seismic activity could be garnered with fewer levels per hole. The key cost savings would come from better siting of the well due to increased information content and a decrease in the number of confirmation wells drilled, also due to the increase in information per well. Improved seismic tools may also increase knowledge, understanding, and confidence, thus

removing some current blocks to feasibility and significantly increasing access to potential geothermal sites.

During the Phase 1 effort summarized in this final report, the ATA Team modeled and built two TRL 3 proof-of-concept test units for two competing rotational sensor technologies. The two competing technologies were based on ATA's angular rate and angular displacement measurement technologies:

- *Angular rate*: ATA's Magnetohydrodynamic Angular Rate Sensor (Seismic MHD)
- *Angular displacement*: ATA's Low Frequency Improved Torsional Seismometer (LFITS)

In order to down-select between these two technologies and formulate a go / no go decision, the ATA Team analyzed and traded scientific performance requirements and market constraints against sensor characteristics and components, acquiring field data where possible to validate the approach and publishing results from these studies of rotational technology capability.

Based on the results of Phase 1, the ATA Team finds that the Seismic MHD (SMHD) technology is the best choice for enabling rotational seismometry and significant technical potential exists for micro-seismic monitoring using a downhole 7-DOF device based on the SMHD. Recent technical papers and field data confirm the potential of rotational sensing for seismic mapping, increasing confidence that cost-reduction benefits are achievable for EGS.

However, the market for geothermal rotational sensing is small and undeveloped. As a result, this report recommends modifying the Phase 2 plan to focus on prototype development aimed at partnering with early adopters within the geothermal industry and the scientific research community. The highest public benefit will come from development and deployment of a science-grade SMHD rotational seismometer engineered for geothermal downhole conditions and an integrated test tool for downhole measurements at active geothermal test sites.

2.0 ACCOMPLISHMENTS

ATA met or exceeded all Phase 1 goals for the Rotational-Enabled 7-Degree of Freedom Seismometer for Geothermal Resource Development. This section summarizes Phase 1 accomplishments and compares actual progress to the goals and objectives of the program Statement of Project Objectives (SOPO) both at high level and on a task-by-task basis.

2.1 PHASE 1 PROJECT OBJECTIVES AND ACCOMPLISHMENTS

Per the program SOPO for the Phase 1 effort, the ATA Team originally proposed to model and construct a TRL 3 laboratory proof-of-concept for two competing rotational sensor technologies: ATA's angular rate sensor technology (SMHD) and ATA's angular displacement sensor technology (LFITS). As part of the down-select and go / no go decision, the ATA Team proposed to analyze and trade scientific performance requirements and market constraints against sensor characteristics and components, publishing results of these studies and rotational technology capability.

The ATA Team met all Phase 1 program objectives. In particular, the ATA Team:

- Modeled and built two TRL 3 proof-of-concept units
  - A triaxial unit for the SMHD angular rate technology, and
  - A single axis unit for the LFITS angular displacement technology
  - *See Tasks 3 and 4 in following paragraphs for details*
- Down-selected to the SMHD angular rate technology based on
  - Analysis of scientific performance requirements and component availability
  - Analysis of market opportunity and constraints, and
  - A trade study of the two rotational sensor technologies for geothermal application
  - *See Tasks 1, 2, 5, and 6 in following paragraphs for details*
- Published initial results base on analysis and rotational seismic data collection
  - *See Task 7 in following paragraphs for details*

2.2 TASK 1: REQUIREMENTS

ATA worked with its partners, Sandia National Laboratories and Nanometrics, Inc. to establish and refine the key performance parameters and device constraints based on prior scientific field observations, analysis, and knowledge of industry standards and the EGS environment. See **Table 1** for key accomplishments.

Table 1. Task 1: Elicit Detailed Requirements

SOPO Text	Phase 1 Accomplishments
Task 1: ELICIT DETAILED REQUIREMENTS: This task will establish and refine threshold and objective performance requirements, environmental limits and commercial constraints for the rotational seismometer with focus on the EGS context. ATA will collaborate with national laboratory and industry partners to establish seismic rotational noise floors, industrial need, manufacturability, and data systems interfaces.	The ATA Team: • Established key performance parameters (KPP), particularly rotational measurement capability • Evaluated and refined the KPP based on available scientific field observations • Bounded EGS environmental constraints, particularly thermal environment • Constrained packaging format and interfaces to match existing downhole instruments See technical sections 3.1, 3.2 and Attachment A.

2.3 TASK 2: HIGH TEMPERATURE COMPONENTS

ATA and its partner, Sandia National Laboratories, surveyed high-temperature components for the rotational seismometer, linear sensors, pressure sensors and electronics. The team identified availability of all necessary technology for 7-DOF downhole tool. In addition, ATA analyzed its MHD rotational sensor, established the material and component changes necessary for high-temperature seismic applications, and built up a test article to prove the sensor fluid choice. See **Table 2** for key accomplishments.

Table 2. Task 2: Establish High-Temperature Components

SOPO Text	Phase 1 Accomplishments
Task 2: ESTABLISH HIGH TEMP COMPONENTS: This task involves gathering industry knowledge for high-temperature electronics, auxiliary linear and pressure sensors, and packaging. ATA's project team will identify components that are feasible for use in the rotational seismometer at 200°C, including signal conditioning and digitization.	The ATA Team: • Surveyed electronics, linear and pressure sensors for the 7-DOF downhole application • Identified high-temperature material and components for the SMHD rotational sensor • Built and validated an SMHD test article based on the new high-temperature sensor fluid See technical Section 3.3 and Attachment D.

2.4 TASK 3: MODELING

ATA developed models of both rotational seismometer technologies sufficient to project performance in the downhole geothermal application. See **Table 3** for key accomplishments.

Table 3. Task 3: Model Sensor Technology

SOPO Text	Phase 1 Accomplishments
Task 3: MODEL SENSOR TECHNOLOGY: This task will simulate and analyze the two alternative ATA technologies for rotational sensing in both near-surface and geothermal downhole conditions. ATA will collaborate with its partners on development and verification of models, including Matlab/Simulink models for the MHD ARS and LFITS, Altium models for the high temperature electronics, and Solid Works / Cosmos models for structural/thermal analysis.	The ATA Team: • Developed LFITS technology computer models • Updated MHD technology computer models to analyze new SMHD format and materials • Simulated the LFITS brassboard configuration • Simulated the MHD test units • Projected performance for both technologies as part of downselect for geothermal application See technical sections 3.4.1 and 3.5.1.

2.5 TASK 4: BRASSBOARDS

ATA developed brassboards to validate performance for both of the candidate rotational seismometer technologies. For angular displacement sensing, ATA designed and built a new rotational seismometer based on the LFITS technology. For angular rate sensing, ATA deployed existing MHD units for both laboratory characterization and field proof-of-concept measuring seismic rotational motion data. See **Table 4** for key accomplishments.

Table 4. Task 4: Rotational Sensing Proof-of-Concept

SOPO Text	Phase 1 Accomplishments
Task 4: ROTATIONAL SENSING PROOF-OF-CONCEPT: ATA will build laboratory proof-of-concepts brassboards for the two ATA rotational sensor alternatives and validate their performance relative to modeled predictions.	The ATA Team: • Built an LFITS brassboard for laboratory test • Benchmarked LFITS simulation models based on brassboard laboratory characterization data • Configured, characterized and deployed single axis and tri-axial MHD rotational sensors • Validated rotational sensing of seismic events See technical Sections 3.4.2, 3.4.3, 3.5.2, 3.5.3, and Appendices B and C.

2.6 Task 5: Trade and Down-Select

Based on test results from the brassboards, simulations of the respective rotational sensing technologies, and analysis of required performance and geothermal physical and environmental constraints, ATA selected the SMHD technology for Phase 2 development. ATA projects that an SMHD-based rotational seismometer will fit the size constraints for a downhole instrument while meeting resolution, bandwidth, dynamic range, temperature range, and reliability requirements. The LFITS technology, while not recommended for further development under this grant, may have applications in a less constrained and lower frequency bandwidth near-surface environment. See **Table 5** for key accomplishments.

Table 5. Task 5: Trade and Down-Select

SOPO Text	Phase 1 Accomplishments
Task 5: TRADE AND DOWN-SELECT: ATA will trade the two rotational sensor technologies based on the requirements, component availability, modeled sensor performance, and proof-of-concept results, leading to a down-select and recommendation of technologies for the Phase 2 build. ATA will lead the trade analysis and down select with our project partners participating in the analysis and evaluation.	The ATA Team: • Used simulation and analysis, benchmarked by brassboard results, to project performance for LFITS and SMHD in geothermal applications • Evaluated both technologies against the Key Performance Parameters identified in Task 1 • Selected the SMHD technology for further development, build and integration in Phase 2 See technical Section 3.6 and Attachment E.

2.7 Task 6: Development Plans

ATA's commercial partner, Nanometrics, Inc., completed a market assessment and worked with ATA to identify obstacles to product development and market acceptance. As a result of these studies, ATA has shifted its proposed Phase 2 plans towards a science grade instrument and initial deployment in partnership with geothermal monitoring activities. See **Table 6** for key accomplishments.

Table 6. Task 6: Solidify Initial Development Plans

SOPO Text	Phase 1 Accomplishments
Task 6: SOLIDIFY INITIAL DEVELOPMENT PLANS: In this task, we will analyze the market, develop plans, and solidify industry partnerships for development. ATA's industry partner(s) will lead the effort to develop a commercialization plan for the seismometer. This task also seeks to identify and clear hurdles to product development such as export agreements, U.S. production arrangements, and licensing agreements.	The ATA Team: • Completed a market assessment • Altered Phase 2 plans in response to small market and need to engage geothermal partners • Identified and addressed barriers to acceptance due to sensor materials and potential commerce department restrictions See technical Section 3.7 and Attachment F.

2.8 Task 7: Documentation

In addition to other contract documentation, this final report, and Geothermal Peer Review presentations in 2012 and 2013, ATA Team member, Sandia National Laboratories, published a paper "Observations of Volcanic Activity at Kilauea Volcano, Hawaii, Using Rotational Seismometers" which included Phase 1 findings validating the rotational seismometry approach and SMHD brassboard technology at the Seismological Society of America (SSA) annual meeting in Salt Lake City, April, 2013. See **Table 7** for key accomplishments.

Table 7. Task 7: Document and Publish

SOPO Text	Phase 1 Accomplishments
Task 7: DOCUMENT AND PUBLISH: ATA will develop and present technical papers and/or presentations summarizing Phase 1 results and Phase 2 prospects. ATA's national laboratory partner(s) will take a strong role in results analysis and interpretation. ATA will produce a Phase 1 Interim Technical Report.	The ATA Team: • Documented Phase 1 results in this Final Report • Presented Phase 1 results at the 2012 and 2013 Geothermal Peer Reviews in Denver, CO • Presented an SNL poster paper summarizing SMHD technology rotational seismometry observations at the SSA Annual Meeting See technical Section 3.2 and Attachment C.

2.9 Go / No Go / Re-Direct Decision Point

Per the Statement of Project Objectives (SOPO), the Phase 2 go / no go / re-direct decision will be made by DOE based on "sufficiency of Phase 1 modeling analysis and brassboard testing to demonstrate the feasible development of both a low-temperature and high-temperature pre-prototype rotational seismometer and high-temperature 7-DOF package capable of providing bandwidths at or exceeding 10-1,000 Hz, velocity sensitivity of 50-200 V/m/s, and practical operation of the high-temperature pre-prototype at 200^{o}C."

Section 3.0 of this Final Report provides the sufficiency of data and analysis to enable a "go" decision. As Section 3.5 shows, the projected SMHD bandwidth exceeds 10-1,000 Hz and provides a good match to expected source spectra of micro-seismic events. Section 3.3.2 describes a geophone option for the linear sensor for which the 50-200 V/m/s specification

applies; however, the ATA Team suggests a high-temperature accelerometer may better match the bandwidth of the SMHD rotational sensor. Finally, practical operation at 200°C depends upon the material and component selections described in Section 3.3.

The SOPO go / no go / re-direct paragraph further specifies that: "Phase 1 deliverables will include 1) a Phase 1 report documenting the results of the Phase 1 activities and analysis; 2) demonstration that the remaining budget and Recipient cost share are adequate to complete Phase 2 activities; and 3) documentation that permitting, site access, and environmental approvals required for Phase 2 are achievable within the remaining project budget and schedule."

The first deliverable constitutes sections 1 through 3 of this Final Report. The second deliverable is part of the Budget Performance and Phase 2 Plans, sections 4 through 5 of this Final Report. The third and last deliverable is also incorporated in the Phase 2 plan (Section 5.0) of this Final Report.

Thus, all requirements are fulfilled to enable a "go" decision for Phase 2. Note, however, that based on non-technical factors, particularly the market analysis completed under Phase 1, this Final Report recommends changes to the Phase 2 plan. The proposed changes lower government and corporate cost by reducing the emphasis on developing a commercial product, and concentrating instead on near-term high-value development of instruments to enable further scientific investigations and validation of the potential of the technology to achieve industrial cost savings goals.

2.10 Summary of Accomplishments

Phase 1 has demonstrated that ATA's SMHD rotational sensing technology enables a viable, low-risk development path for a rotational seismometer that matches the requirements for monitoring of micro-seismic events. In addition, the component electronic and sensor technologies have been identified for integration of a 7-DOF seismic measurement tool. The ATA Team met all requirements for a Phase 2 "go" decision within the Phase 1 budget and is suggesting a plan to lower Phase 2 costs to focus on highest value. Finally, the scientific analysis suggests that rotational seismometry provides additional information content that can potentially lower the number of deployed instruments and drilled holes needed for characterization of a fracture field, lowering cost of enhanced geothermal development.

3.0 TECHNICAL DISCUSSION

This section summarizes Phase 1 project technical activities including methods, results, and analysis. **Table 8** describes the technical subsections that follow and maps these subsections back to tasks within the original SOPO and program plan.

Table 8. Technical Subsections Mapped to SOPO Tasks

Technical Subsection	Description and Mapping to Original SOPO Tasks
Section 3.1 Requirements	Presents the key performance parameters for rotational-enabled seismometry based on analysis and elicitation of detailed requirements (Task 1)
Section 3.2 Rotational Seismometry Science	Summarizes methods, analyses and field observations that motivate rotational seismometry or define requirements (Task 1), including Phase 1 publications (Task 7)
Section 3.3 High Temperature Components	Names the key material and component choices enabling 7-DOF seismometry for high-temperature downhole geothermal application (Task 2)
Section 3.4 LFITS Development	Describes simulation models (Task 3) and brassboards (Task 4) for ATA's angular displacement technology: Low Frequency Improved Torsional Seismometer (LFITS)
Section 3.5 SMHD Development	Describes simulation models (Task 3) and brassboards (Task 4) for ATA's angular rate technology: Seismic Magnetohydrodynamic angular rate sensor (SMHD)
Section 3.6 Trade and Down-Select	Summarizes the trades of format and performance against requirements that led to selection of the SMHD technology for Phase II development (Task 5)
Section 3.7 Development Plan	Synopsizes findings of the commercial market research that have motivated changes to Phase II and the overall development plan (Task 6)
Section 3.8 Conclusions	Gathers key technical findings and products of the Phase I effort (all tasks)

3.1 REQUIREMENTS

ATA worked with its partners, Sandia National Laboratories and Nanometrics, Inc. to establish and refine the key performance parameters and device constraints based on prior scientific field observations, analysis, and knowledge of industry standards and the EGS environment.

Attachment A contains draft specification notes for a 7-DOF seismometer. This partial specification attempts to capture the key constraints and key performance parameters (KPP) for a 7-DOF downhole seismometer, with particular emphasis on defining requirements for the novel rotational sensing capability. Discussions and analysis between ATA and its commercial and industry partners focused on four major areas, which are summarized in the paragraphs that follow:

- Design Goals
- Physical Constraints
- Thermal Environment
- Seismometer Performance Requirements

Design Goals: The 7-DOF seismometer development effort addresses the need for high precision seismic monitoring described under Topic 4 of the Geothermal Technologies Program Funding Opportunity Announcement (FOA). The ultimate goal is to understand the evolution of a reservoir during Enhanced Geothermal System stimulation activities by developing new data collection techniques, temperature and pressure rated components and tools. **Table 9** lists seismometer goals from Topic 4 and relates them to flow-down goals for this 7-DOF seismometer program. It should be noted that the core of the 7-DOF seismometer effort is development of the novel rotational sensors and integration of a tool that includes existing linear and pressure sensors and associated 7-DOF data processing. This effort does not, for example, attempt to develop novel linear seismometers.

Table 9. Geothermal Technologies Program Topic 4 Seismometer Goals

Specification	Target	Flow-Down Goals for 7-DOF Seismometer
Cost	50% cheaper than 2011 model comparable sensor	There are no comparable rotational seismometers or 7-DOF tools. Initial price goal is based on the per-axis cost of linear sensors ($3K-$6K/axis). However 50% cost and power savings come from reduction of total number of sensors required.
Power	30% less power than 2011 comparable sensor	
Bandwidth	10-1,000 Hz	> 10-1,000 Hz (broader bandwidth preferred)
Endurance	> 1,000 hours at 200°C	> 1000 hrs @ 200°C
Sensitivity	50-200 V/m/s	Linear geophone 50-200 V/m/s. However, this is not a linear geophone development effort. Goal is matched sensitivity of rotational and linear sensor suite to micro-seismic signals.
Operation	years	> 5 years
Sample Rate	480 samples/s	> 480 samples/s (2kHz preferred)
Digitization	24 bit A/D per channel	24 bits A/D per channel
Data Transfer	Efficient data transfer module	Efficient data transfer module
Data Output	Easily recordable, displayable in standard industry formats	Easily recordable, displayable in standard industry formats

Physical Constraints: Maximum sensor size is a key constraint required to evaluate feasibility of the technology. Specifying this size depends upon identifying an existing downhole tool to serve as a nominal enclosure for the 7-DOF seismometer. For Phase 1 analysis, two downhole tool sizes were identified; the larger Trillium Borehole tool available from Nanometrics, and a smaller high-temperature package in use by Sandia National Laboratories.

Figure 2 shows the larger Trillium Borehole tool that sets the upper limit for sensor size. This tool is a 143 mm (5.6") diameter stainless steel pressure vessel with holelock for cased boreholes. Although assumed for the time being based on available systems like the Trillium, adequate holelock and orientation knowledge will ultimately be critical to device performance.

The Nanometrics tool is not currently rated for high-temperature geothermal operation. However, team member Sandia National Laboratories has a similar holelock device operating at up to 210°C and is developing tools for higher temperatures. The ATA Team considers the Nanometrics tool representative for packaging and considered specific issues related to high-temperature operations separately (see Section 3.3).

The crucial constraint imposed by downhole tool packaging is the 137mm (5.37") interior diameter, which constrains the maximum size of the seismometers and other instrumentation. Simulations of the two competing rotational sensors technologies (Sections 3.4 and 3.5) constrained both to a maximum sensor diameter of 3.8" to support tri-axial packaging in all three orientations within the nominal tool casing.

As noted above, phase 1 simulations also considered a smaller borehole tool format based on an existing high-temperature package in use by Sandia National Laboratories. That tool has an inner diameter of 2.25", and a resulting rotational seismometer diameter of 1.6" was used for simulating this configuration.

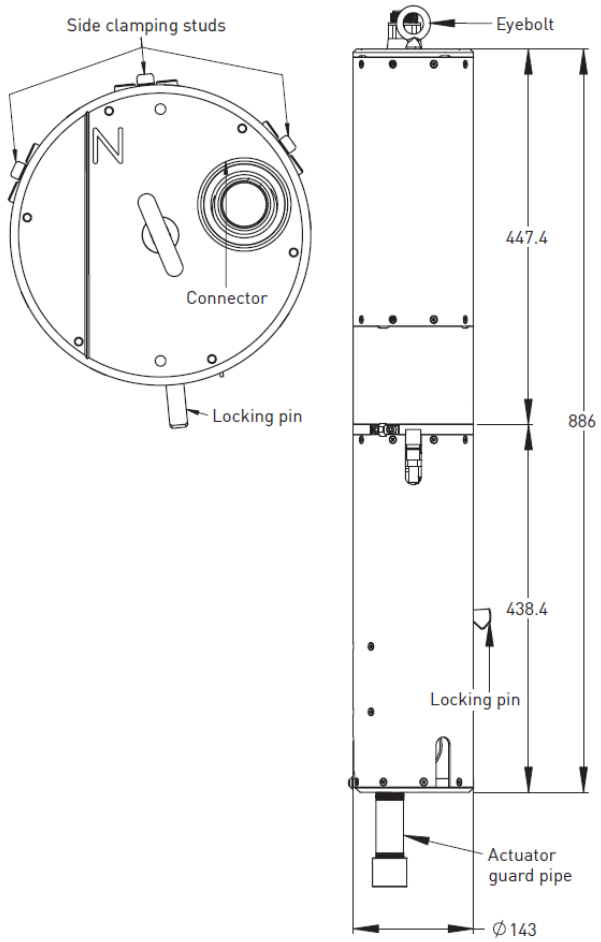

Figure 2. Nominal Downhole Package Based on the Nanometrics Trillium Tool

Thermal Environment: Per the original grant and SOPO, the 7-DOF seismometer is specified to operate at 200°C. This specification obviously drives material and components selections (see Section 3.3). Less intuitively, the thermal specification also drives required seismic sensor performance. For example, consider **Figure 3**, a geological and thermal cross-section of the Northwest Geysers EGS demonstration area. The temperatures at depth are above 400°C. The 7-DOF seismometer would thus be restricted to downhole locations both laterally separated from the fracture zone by observation well availability but also vertically separated due to the instrument's temperature limitations. As the next paragraph will indicate, distance between the seismometer and fracture zone will determine the magnitude of measurable micro-seismic events. There is a potentially complex trade between required instrument sensitivity and the cost and complexity associated with the instrument's thermal tolerance. Analyses in this report assume the 200°C requirement.

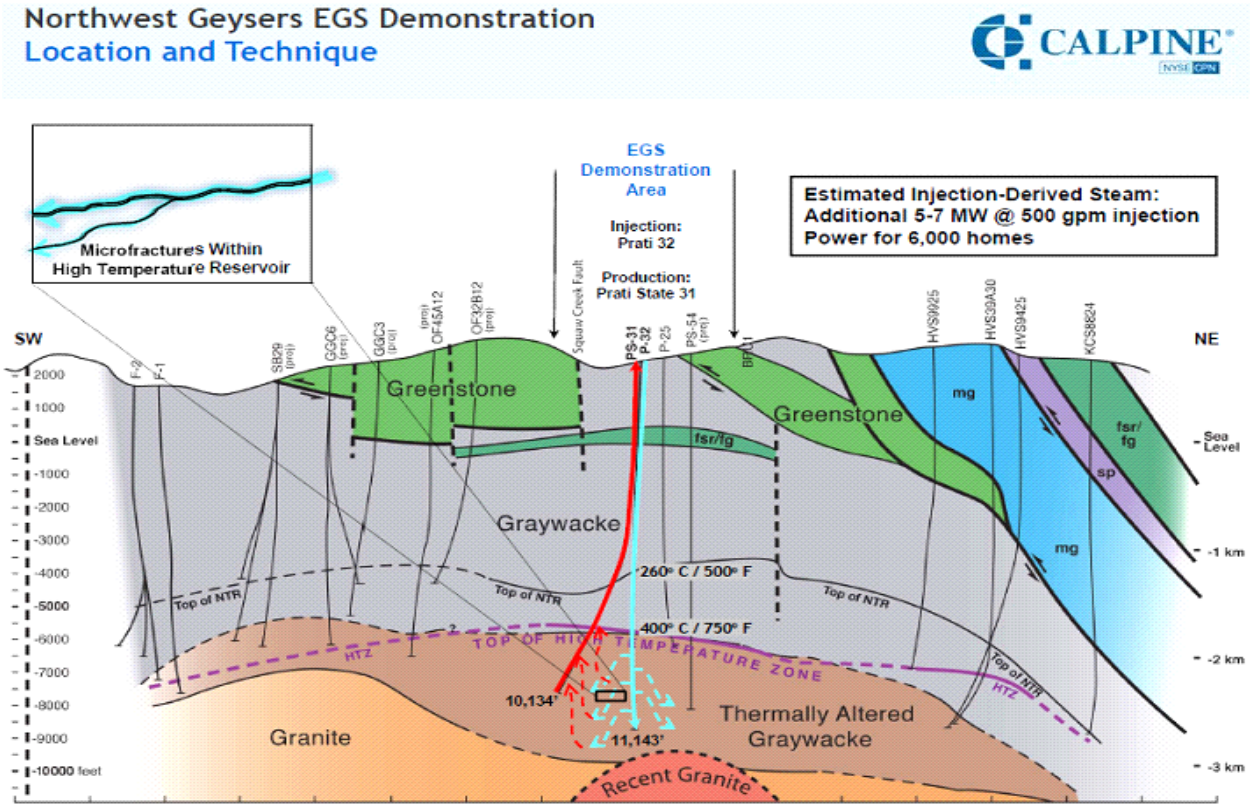

Figure 3. Thermal Cross-Section of the Northwest Geysers EGS Demonstration Area

Based on recent observations of micro-seismic swarms during EGS stimulation, the upper bound event (moment) magnitude was chosen at +3.5. The lower bound magnitude was set at -2.0. In other words, the seismometer was expected to have utility if it had sufficient signal-to-noise to measure a -2.0 event and would not saturate for a +3.5 event. Halliburton has summarized basic information on moment magnitude for microseismic events in relation to current linear seismometer recording range.[1] In addition, ATA Team member Nanometrics, Inc. recently published a key study on "Estimating the Spectra of Small Events for the Purpose of Evaluating Microseismic Detection Thresholds."[2] The methods described in the Nanometrics study form the basis for simulations and analyses presented in this section.

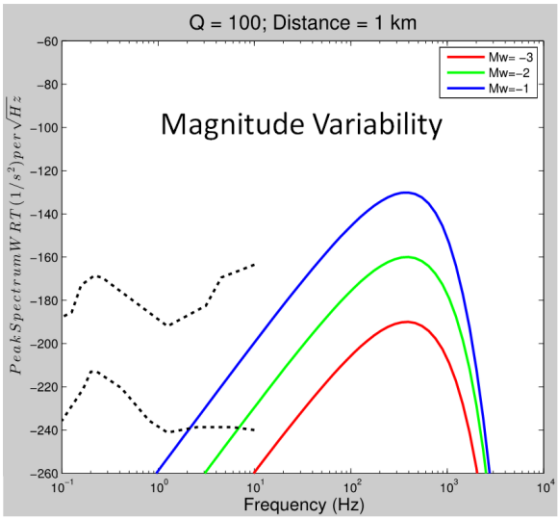

Figure 4. Seismic Signal as a Function of Wave Frequency and Event Magnitude

As an example of the analysis, **Figure 4** indicates sensitivity to seismic event magnitude (moment magnitude). The curves are power spectral density (PSD) for rotational motion at the sensor measured in dB for events of magnitude -3.0, -2.0, and -1.0, all at 1 km distance and with Q=100. Note that discussions of distance and Q follow. However, as one might expect, changes in event magnitude correspond directly to changes in rotational motion magnitude at the seismometer but do not affect the expected seismic wave frequency.

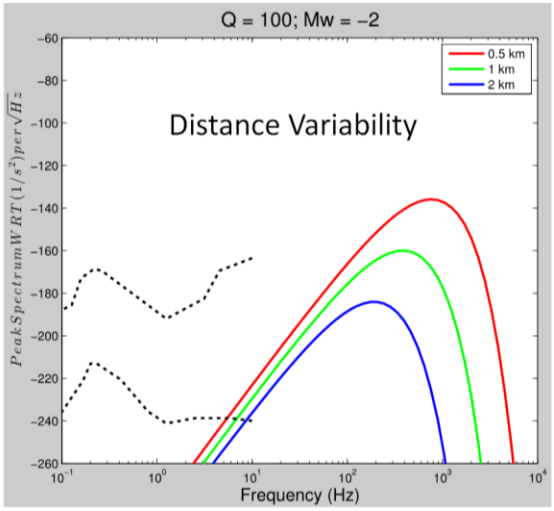

Figure 5. Seismic Signal as a Function of Wave Frequency and Distance

Figure 5 plots received signal dependence on distance. Optimally, observation wells would be drilled near the expected fracture, but based on considerations already mentioned in the preceding Thermal Environment paragraph, the lower-bound distance between seismic event and seismometer was set to 0.5 km and an upper-bound set to 2.0 km. Thus, **Figure 5** plots PSDs for rotational motion in units of dB for a magnitude -2.0 micro-seismic event at distances of 0.5, 1.0, and 2.0 km, with Q=100. As the plot indicates, both magnitude and seismic wave frequency change with distance. For most subsequent analyses, a distance range of 1.0 to 2.0 km was assumed.

Attenuation is characterized by the amplification factor, Q, for the material between the fracture and the sensor. The lower the Q, the more

[1] Halliburton, "Microseismic Events: How Big Are These Microseismic Events," available on-line at www.halliburton.com/public/pe/contents/Data_Sheets/.../H08325.pdf, last accessed September 2013.
[2] N. Ackerley, "Estimating the Spectra of Small Events for the Purpose of Evaluating Microseismic Detection Thresholds," GeoConvention 2012: Vision, Calgary, Canada (May 2012).

attenuation the seismic wave will exhibit as it passes through the rock. Q is highly variable from site to site. Estimates of Q for the Geysers geothermal site are in the mid-range of 100 to 200. At the high end, estimates of Q exceed 1,000 for the Fenton Hill geothermal site near Los Alamos, NM. **Figure 6** plots received signal dependence on Q. The curves trace PSD for rotational motion in units of dB for a magnitude -2.0 micro-seismic event at a distance of 1.0 km. Both magnitude and seismic wave frequency vary significantly with Q. Subsequent analyses consider both a "low Q" and "high Q" situation, with "low Q" corresponding to Q~100 and "high Q" corresponding to Q~1,000.

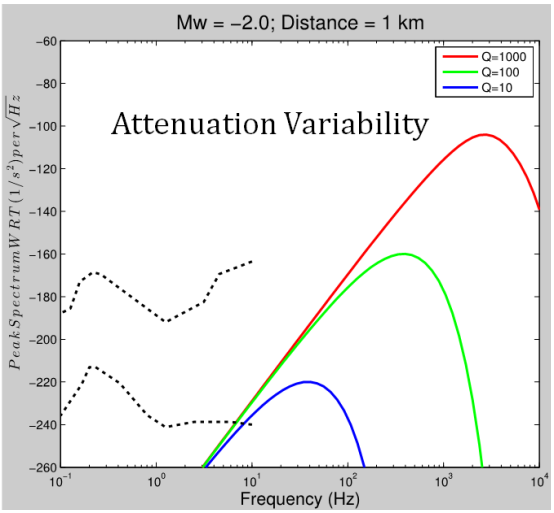

Figure 6. Seismic Signal as a Function of Wave Frequency and Attenuation

Finally, the signal at the rotational seismometer varies with seismic wave velocity. **Figure 7** indicates the variation in received signal due to changes in wave velocity. The plots trace PSDs for rotational motion in units of dB for a magnitude -2.0 micro-seismic event at a distance of 1.0 km and Q=100 with wave velocities of 2km/s, 3km/s, and 4 km/s. Shear wave velocity variations cause a relatively small change in signal magnitude and frequency relative to other factors, and a nominal value of 4 km/s was assumed in all other analyses and simulations.

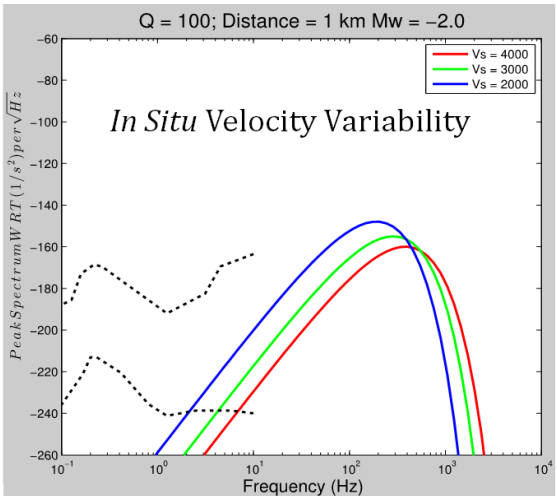

Figure 7. Seismic Signal as a Function of Wave Frequency and Velocity

Combining all the analyses of the micro-seismic signal environment, the ATA Team established expected rotational, linear, and pressure signal ranges for the 7-DOF seismometer based on the ensemble of "desired micro-seismic events" to be detected. **Figure 8** shows the low Q (left) and high Q (right) results for rotational motion. **Figure 9** shows similar low Q and high Q results for linear motion, and **Figure 10** presents corresponding results for pressure. In all of these plots, the gray area represents the range of expected signal magnitudes between a lower bound established by a small and distant seismic event (magnitude -2.0 at 2 km) and an upper bound representing a nearby large event (magnitude +3.5 at 1 km).

Subsequent sections of this report base their simulation and analyses on the physical constraints and requirements summarized in this section. In particular, the trade between the two candidate rotational seismometer technologies depends on the size and temperature constraints and comparisons of performance against expected micro-seismic signatures.

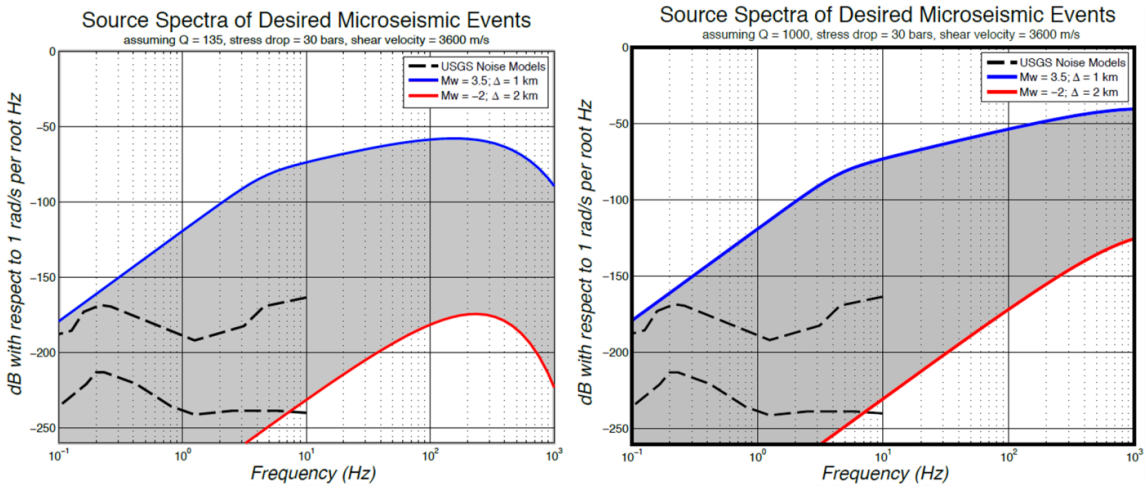

Figure 8. Desired Micro-Seismic Rotational Velocity Envelope

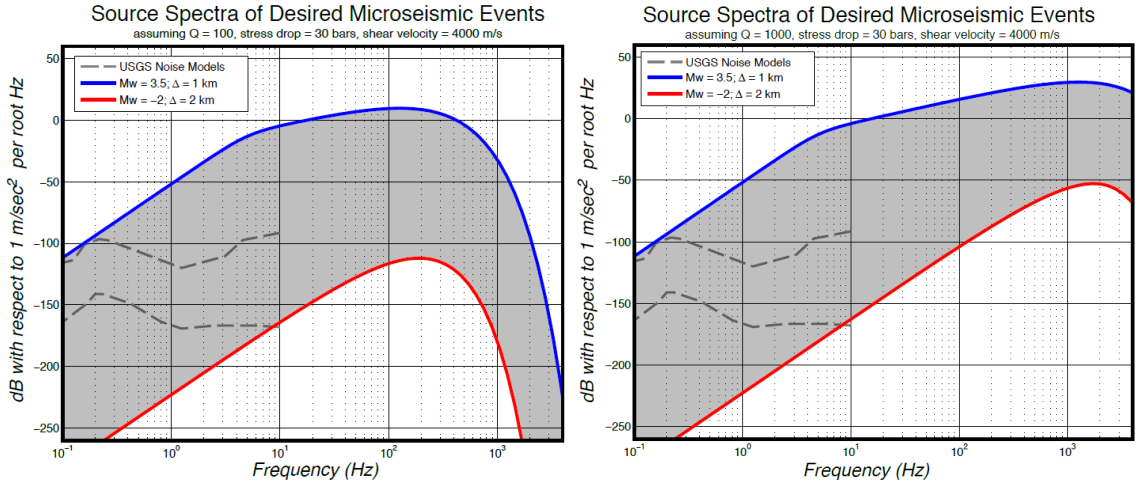

Figure 9. Desired Micro-Seismic Linear Acceleration Envelope

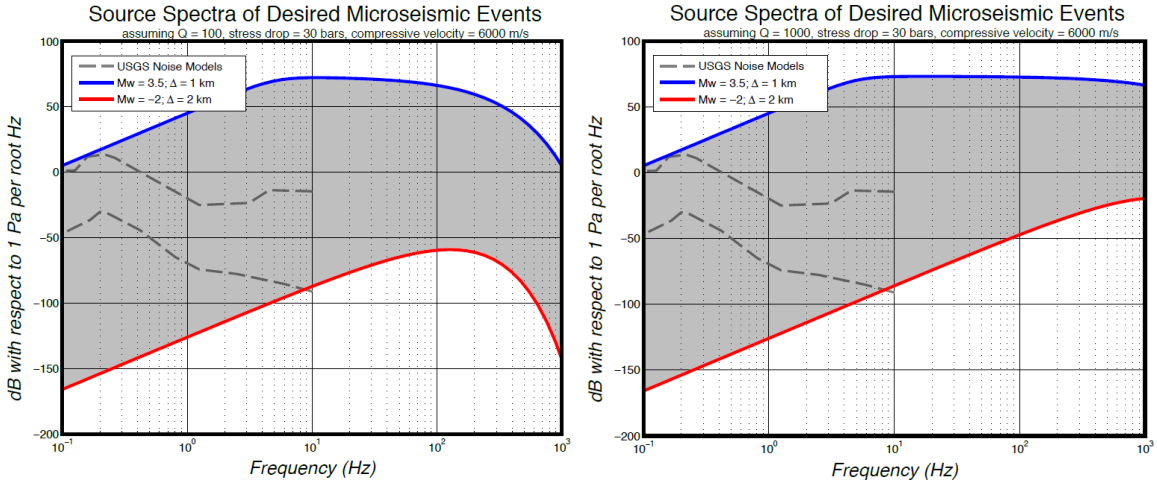

Figure 10. Desired Micro-Seismic Fluid Pressure Envelope

3.2 ROTATIONAL SEISMOMETRY SCIENCE

This section briefly recapitulates the science involved in combing linear and rotational seismic motion sensors to enable point measurement of incident seismic waves, then presents recent encouraging field tests and validations of the approach. The reader is referred to the referenced papers for additional detail.

ATA Team member Sandia National Laboratories has been at the forefront of research on the "point seismic array" concept. According to geophysical theory and seismic modeling results, a 7-DOF sensor that includes the rotational degrees of freedom will be able to determine wave speed for both pressure (p) waves and shear (s) wavers, as well as the incident direction of both wave types. The ability to measure all these quantities with a single tool would allow fewer monitoring holes and fewer tools per borehole. The essence of these claims can be derived from the propagation of a plane wave in isotropic media following the derivation in Aldridge.[3] A simple derivation is reproduced below from Abbott, et al.[4]

Consider a plane wave propagating in direction of unit vector **n** with speed c. The particle displacement vector **u**(x,t) is given by

$$\bar{u}(\bar{x},t) = U\hat{p}w\left(t - \frac{\bar{x}\cdot\hat{n}}{c}\right), \qquad (1)$$

where U is the displacement amplitude scalar, $\boldsymbol{p}$ is a dimensionless unit polarization vector, and **w**(**x**,t) is the displacement waveform. For a plane shear wave p·n = 0 and c = β, for a plane compressional wave $\boldsymbol{p} = \boldsymbol{n}$ and $c = \alpha$. Since our instrumentation measures particle acceleration and rotation rate, we need expressions for those quantities. The associated particle acceleration vector **a**(**x**,t) is given by

$$\bar{a}(\bar{x},t) = U\hat{p}\ddot{w}\left(t - \frac{\bar{x}\cdot\hat{n}}{c}\right), \qquad (2)$$

and the particle rotation rate vector is given by the time derivative of *curl* **u**(**x**,t)

$$\dot{\bar{\omega}}(\bar{x},t) = \frac{U}{c}\ddot{w}\left(t - \frac{\bar{x}\cdot\hat{n}}{c}\right)(\hat{p}\times\hat{n}). \qquad (3)$$

Note that particle rotation rate is a dimensionless quantity, and is perpendicular to both $\boldsymbol{p}$ and $\boldsymbol{n}$.

[3] David F. Aldridge and Robert E. Abbott, "Investigating the Point Seismic Array Concept with Seismic Rotation Measurements," Sandia National Laboratories, SAND2009-0798 (2009).
[4] Robert E. Abbott, Darren Hart, and Weston A. Thelen, "Observations of Volcanic Activity at Kilauea Volcano, Hawaii, Using Rotational Seismometers," poster paper at the Seismological Society of America annual meeting, Salt Lake City, April, 2013. See Attachment C of this document.

The vector product of (2) and (3) via the "Bac-Cab" Rule is:

$$\bar{a}(\bar{x},t) \times \dot{\bar{\omega}}(\bar{x},t) = \frac{U^2}{c}\left(\ddot{w}\left(t - \frac{\bar{x}\cdot\hat{n}}{c}\right)\right)^2 [(\hat{p}\cdot\hat{n})\hat{p} - \hat{n}]\,. \qquad (4)$$

For a shear wave $\mathbf{p}\cdot\mathbf{n} = 0$, leading to

$$\bar{a}(\bar{x},t) \times \dot{\bar{w}}(\bar{x},t) = -\frac{U^2}{c}\left(\ddot{w}\left(t - \frac{\bar{x}\cdot\hat{n}}{c}\right)\right)^2 \hat{n}\,, \qquad (5)$$

and

$$\frac{\bar{a}(\bar{x},t) \times \dot{\bar{w}}(\bar{x},t)}{\|\bar{a}(\bar{x},t) \times \dot{\bar{w}}(\bar{x},t)\|} = \hat{n}\,. \qquad (6)$$

Thus, measurement of both acceleration and rotation rate at the same receiver location allows the determination of the propagation direction of the incident wave. Furthermore, using equations (2) and (3), the wavespeed of the incident wave is given by

$$\frac{\|\bar{a}(\bar{x},t)\|}{\|\dot{\bar{w}}(\bar{x},t)\|} = c = \beta\,. \qquad (7)$$

Attachment C contains Sandia National Laboratories' paper: "Observations of Volcanic Activity at Kilauea Volcano, Hawaii, Using Rotational Seismometers" from which the preceding derivation is excerpted. That poster paper, presented at the April 2013 Seismological Society of America (SSA) annual meeting, provides recent seismic observations combining measurements from tri-axial accelerometers and ATA's ARS-16 and ARS-24 brassboard rotational sensors deployed as part of this Phase 1 effort at Uwekahuna, Hawaii, on Kilauea Volcano.

Many high-amplitude seismic events were recorded at the Hawaii site and processed for back azimuth and in-situ shear velocity. The measurements demonstrated high correlation between vertical-axis rotation rate and transverse horizontal acceleration signals; however, the result back azimuth calculations were highly variable, perhaps due to wave scattering. Calculation of in-situ shear velocity is not sensitive to scattering and yielded velocities of 350-450 m/s at 10 Hz, in agreement with previous seismic array studies. Thus, initial results with the SMHD technology brassboards are encouraging for point seismic measurements (see also Section 3.5.4).

Other research teams are also validating 6-DOF seismometry in the field. Lee et al. provide background information on the potential for rotational seismometry and a survey of recent advances.[5] In a more recent article in the Journal of Seismology, Hadziioannou et al. demonstrate, in practice, the ability to combine measured rotation rate with transverse to fully reconstruct the seismic wave field.[6] The authors combine rotational data from a sensitive ring laser and linear measurements from a broadband seismometer that are co-located at the Wettzell

[5] William H. K. Lee, Heiner Igel, and Mihailo D. Trifunac, "Recent Advance in Rotational Seismology," *Seismological Research Letters*, vol. 80 (May/June 2009), p. 479-490.
[6] Celine Hadziioannou, Peter Gaebler, Ulrich Schreiber, Joachim Wasserman, and Heiner Igel, "Examining ambient noise using collocated measurements of rotational and translational motion," J Seismol (2012) 16:787-796.

Geodetic Observatory in Germany. They obtain both local phase velocity and the back azimuth of the strongest background seismic noise source during two different time periods, and they validate these point measurements against classic array beamforming analysis. The final paragraph of their conclusion is worth quoting in its entirety:

> We have shown that the measurements of rotational and translational motions in ambient noise at a single location can be used to make observations consistent with traditional methods, which require arrays of translational instruments. However, currently, only very expensive instruments such as the Wettzell ring laser are sensitive enough to detect the rotational motions in ambient noise. This illustrates the importance of developing less expensive rotational sensors with low noise levels.[7]

Later sections of this final report suggest that the SMHD technology may offer precisely the combination of low noise and low cost desired in Hadziioannou. It is safe to say that published scientific results strongly motivate development of both the rotational seismometer and an integrated 7-DOF instrument during Phase 2 of the current project.

3.3 High Temperature Components

ATA and its partner, Sandia National Laboratories, surveyed high-temperature components for the rotational seismometer, linear sensors, pressure sensors, and electronics. The team identified availability of all critical components for a 7-DOF downhole tool. In addition, ATA analyzed its SMHD rotational sensor, established the material and component changes necessary for high-temperature seismic applications, and built up a test article to prove the sensor fluid choice.

The results in this section are divided up into three subsections according to the type of material or components under discussion. Section 3.3.3 describes relevant high temperature electronics options. Section 3.3.1 focuses on the critical material and component changes needed to enable a high-temperature SMHD sensor, and Section 3.3.2 surveys the availability of high-temperature sensors (linear and pressure) needed to complete a 7-DOF downhole instrument.

3.3.1 High-Temperature SMHD Rotational Seismometer

The rotational seismometer brassboards build in Phase 1 validated the concepts of rotational seismometry and benchmarked computer models at earth surface temperatures. High-temperature downhole sensors will require changes to both components and materials. Both the SMHD angular rate sensor and LFITS angular displacement sensor were analyzed for high temperature design challenges during the trade study between the two technologies. However, this section focuses specifically on the SMHD technology that was selected for development in Phase 2 and the feasibility of available materials to support the high-temperature application.

ATA currently designs, builds and sells angular rate sensors (ARS) based on the magneto-hydrodynamic (MHD) technology. Attachment D documents a comprehensive analysis of the issues associated with modifying the existing technology for the high-temperature seismic applications. Thermal expansion, material degradation, and performance degradation are assessed for each material and component within the SMHD.

[7] Ibid, 795.

The following list summarizes material issues (from most critical to least critical) relevant to designing a high-temperature SMHD for downhole applications. Items 1-7 are expected to influence SMHD design choices and require detailed analysis and trades during the Phase 2 design effort. Items 8-12 have known solutions with minimal implications for the SMD design.

Most Critical

1)
2)
3)
4)
5)
6)
7)
8)
9)
10)
11)
12)

Least Critical

ATA Proprietary data removed per DOE Final Report submission requirements. Content available from ATA for authorized government reviewers for purposes of review and evaluation.

Overall, no insurmountable obstacles were discovered to a high-temperature SMHD design.

MHD Fluid: The most fundamental change and highest risk in SMHD high-temperature design is replacing the mercury sense element with another fluid. This change is motivated as much by environmental concerns as high-temperature operations. The report in Attachment D indicates the potential for using a Gallium-Indium-Tin eutectic (often referred to in shorthand by the product name, Galinstan). However, the viscosity of Galinstan is very different from mercury, which raised the question of how well Galinstan retained uniform properties above its freezing temperature (-19^{o}C).

To assess the performance and mitigate risk for Phase 2, ATA built a Galinstan test article based on an existing ATA MHD sensor design (**Figure 11**). Essentially, ATA built a prototype ARS-16 sensor using standard processes and procedures except that the sensor was filled with Galinstan instead of mercury. Although Galinstan will support operation at 200^{o}C, the other standard assembly elements of the ARS-16 test aricle will not. Thus, testing was to verify the behavior at the low end of Galinstan's range, i.e., for near earth-surface operations.

Figure 11. Galinstan Test Article Based on ARS-16

Galinstan is known to have a large freeze-thaw hysteresis, which introduced uncertainty about its performance over temperature. To resolve the uncertainty, ATA performed a series of frequency response measurements from approximately 10ºC up to 50ºC and recorded the 10Hz scale factor at 10 Hz and -3 dB point at each temperature. **Figure 12** plots the resulting scale factors and -3 dB frequencies as a function of temperature.

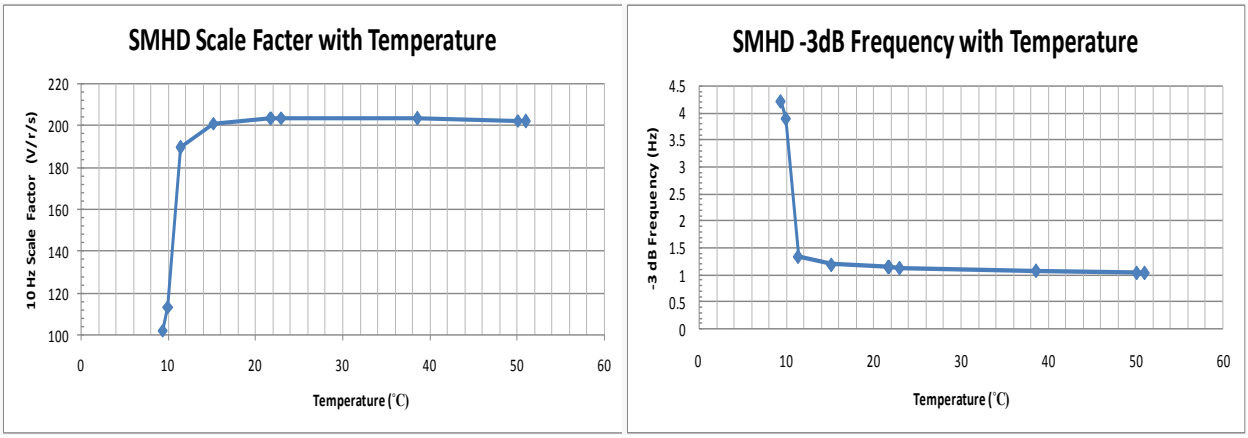

Figure 12. Galinstan Test Article Performance Over Temperature

Above 12°C, the Galinstan test article demonstrated excellent stability of response. In other words, an SMHD based on this material would operate well down to room temperature. In fact, at room temperature the Galinstan ARS-16 had lower noise from 1 to 1,000 Hz and a flatter frequency response function magnitude than the standard mercury model. However, the frequency response magnitude dropped sharply at temperatures below 11°C indicating that the viscosity of the Galinstan fluid was changing dramatically as it approached its freezing point.

High-temperature tests will be performed in Phase 2. However, the early work with the Galinstan test article has demonstrated feasibility, removed numerous questions, and validated the basic approach to a high-temperature SMHD sensor for Phase 2 development.

3.3.2 High-Temperature Linear and Pressure Sensors

In addition to the SMHD rotational sensor analyzed in Section 3.3.1, the 7-DOF downhole seismometer requires 3 linear motion sensors and a pressure sensor. Linear and pressure sensor technology is much more mature than the rotational seismometer, so this section represents a survey of suitable sensor types and candidate models.

Linear Motion Sensors: Both linear accelerometers and geophones are candidate technologies for linear motion sensors in the 7-DOF seismometer. The ATA Team identified candidate linear accelerometers and geophones based on Sandia National Laboratories' high-temperature geophysical field experience. Two representative models are:

- ***Endevco 7703A-1000 Accelerometer (Figure 13)*:** This piezoelectric accelerometer manufactured by Meggitt Aerospace provides temperature-compensated operation to +288°C. As a result, it is a strong candidate for meeting the 1,000 hours at 200°C operational goal. Its sensitivity is 1,000 pC/g, not directly comparable to the geophone-oriented 50-200 V/m/s program goal. Using an accelerometer would require local high-temperature signal conversion electronics. Bandwidth exceeds the 10-1,000 Hz program goal and the accelerometer provides a better match to the rotational seismometer than a geophone. Size and weight are compatible with the downhole application: 120 gm (4.2 oz); 23.1 mm (0.91") height x 25.4 mm (1.0") hexagonal width with a protruding cable connector.

Figure 13. Endevco 7703A-1000 Accelerometer

- ***OYO Geospace SMC-1850 Geophone (Figure 14)*:** This geophone from Geospace Technologies has been tested at 200°C up to 300 hours. Therefore, endurance for 1,000 hours at the 200°C operational goal is uncertain and requires further qualification in Phase 2. Frequency response is normally reported in a lower frequency range up to 500 Hz, but the geophone is expected to meet the 10-1,000 Hz program goal. It may not be as good a match to the rotational seismometer bandwidth as an accelerometer. The intrinsic sensitivity is 40 V/m/s, requiring a high-temperature amplifier circuit to increase gain to the 50-200 V/m/s goal. Size and weight are compatible with the downhole application: 43 gm (1.52 oz); 26.4 mm (1.04") height x 22.2 mm (0.875") cylindrical base.

Figure 14. OYO Geospace SMC-1850 Geophone

The trade between geophone and accelerometer will be part of the Phase 2 design effort. A key consideration in that trade will be the desire to match the frequency band between the linear and rotational sensors to maximize the range of correlation analysis. More specifically, the SMHD has a frequency response from 1 to 1000 Hz. If a geophone were chosen with a frequency response from 10 to 1000 Hz then the rotational information from 1 to 10 Hz might not be as useful to the analyst as it might have been if the linear sensor were an accelerometer with a 1 to 1000 Hz response. However, the desire to match sensors has to be traded against cost and complexity. The linear accelerometer is more expensive and requires additional electronics to convert the signal from capacitance to volts for digitization.

Pressure Sensor: A wide variety of high-temperature, high-pressure combination pressure and temperature transducers are available on the market. The ATA Team identified candidate pressure sensors based on Sandia National Laboratories' high-temperature geophysical field experience. A representative model is:

- ***Paine 211-55-010 Series Downhole Pressure Transducers (Figure 15)*:** These ruggedized pressure sensors from Paine Electronics measure pressures up to 30,000 PSIA and can operate in temperatures above 300°C. They have a calibrated range up to +260°C, easily satisfying the 1,000 hours at 200°C operational goal. Size and weight are compatible with the downhole application: 2.85" height and 0.75" cylindrical diameter.


Figure 15. Paine 211-55-0110 Pressure Sensor

The exact model to be employed in the 7-DoF instrument will be chosen during the Phase 2 design effort.

3.3.3 Ancillary High Temperature Electronics

The rotational seismometer and the 7-DOF tool will require additional high-temperature electronics for signal conditioning and transmission. The ATA Team surveyed available commercial of the shelf (COTS) components and identified availability of key components from Texas Instruments, Honeywell, Analog Devices, and Linear Technology. **Table 10** summarizes key active components rated for >200°C operations. High-temperature passive components

(resistors, capacitors, inductors, diodes, etc.) are also readily available from Vishay and others for 200°C operation.

Table 10. Survey of Relevant High-Temperature Rated Electronic Components

Electronic (IC) Type	Part Number	Rating
12 bit A/D Converter	Honeywell HTADC12	>5 yrs @ 225°C
24 bit A/D Converter	Texas Instruments ADS1243-HT	>1000 hrs @ 210°C
Low Noise Dual Op-Amp	Honeywell HTOP01	>5 yrs @ 225°C
Positive Linear Regulator	Honeywell HTPLREG	>5 yrs @ 225°C
Quad Analog Switch	Honeywell HT1204	>5 yrs @ 225°C
Dual 8 Channel Analog Multiplexer	Honeywell HT507	>5 yrs @ 225°C
Low Power Op-Amp	Analog Devices AD8634	Up to 210°C operation
High Temperature Instrumentation Amplifier	Analog Devices AD8229	Up to 210°C operation
High Temperature Precision Voltage Ref.	Analog Devices ADR225	Up to 210°C operation

As part of the trade study between the SMHD and LFITS rotational sensing technologies, ATA evaluated the required signal conditioning circuitry for both sensors. The SMHD technology chosen as a result of this trade study has much simpler signal conditioning. The SMHD requires power conditioning, amplification via a low noise op amp with relatively straight forward low pass filtering, and then digitization via a high resolution analog to digital converter (ADC). The most challenging high-temperature component is the analog to digital converters (ADCs). The TI ADS1243-HT is the only 24-bit ADC available that will operate above 200°C but has a limited life with no margin on the 7-DOF system goal (1000 hr). The Honeywell HTADC12 12 bit ADC will tolerate 225°C for more than 5 years, but a 12-bit ADC does not provide sufficient dynamic range for the full range of desired applications.

3.3.4 Summary of High-Temperature Components

The 7-DOF seismometer program is focused on development of a novel rotational seismometer technology and integration of these rotational seismometers with existing linear and pressure transducers into a 7-DOF tool for geothermal downhole applications. Detailed design of both sensors and system will occur in Phase 2.

The results in this section indicated the feasibility of an SMHD sensor for high-temperature downhole applications based on available materials and components. A test article was built to demonstrate the new Galinstan approach. This section also surveyed the available linear sensors, pressure sensors, and associated electronics for integration of the high-temperature 7-DOF instrument. Overall, feasibility of 1,000 hour operation at 200°C looks very promising.

3.4 LFITS DEVELOPMENT

ATA's Low Frequency Improved Torsional Seismometer (LFITS) is an angular displacement sensor and the first of two candidate rotational sensing technologies. This section describes development and test of the LFITS models and brassboard. Section 3.5 describes the corresponding models and brassboards for the other technology, the SMHD.

3.4.1 LFITS Principle of Operation

ATA Patentable material removed per DOE Final Report submission requirements. Content available from ATA for authorized government reviewers for purposes of review and evaluation.

3.4.2 LFITS Modeling (See Title Page for Restrictions)

ATA developed two computer performance models: the first for the LFITS brassboard and a second representing the high-temperature LFITS concept for the 7-DOF seismometer. The brassboard computer model allowed comparison with brassboard test results, and the high-temperature model informed the trade study between alternative rotational sensing technologies.

LFITS Brassboard Model: The LFITS is modeled as a rotational spring, mass, damper system. Equation 8 is the fundamental transfer function for the LFITS based on the proof mass inertia, $J_{\theta,}$ about the sensitive axis (z-axis), the rotational viscous damping term, B_{θ}, and the rotational

spring constant, K_θ, the sense element gain, K_{SE}, and the signal conditioning frequency response, H_{ELEC}.

$$H_\theta(S) = \frac{H_{ELEC}(S)\, K_{SE}\, S^2}{J_\theta S^2 + B_\theta S + K_\theta} \quad \text{(Volts/radian)} \qquad (8)$$

The LFITS dynamic performance estimation model was implemented in Matlab/Simulink. The device diameter is the key physical dimension affecting performance, and for the LFITS Brassboard, the diameter was set to 5.0". The sensor's dynamic performance also depends on several other key component and material properties. These include the mechanical properties of the neutrally buoyant proof mass (i.e. inertia J_θ), and the fluid physical properties, i.e. density, viscosity, dielectric constant, and resistivity versus temperature.

The LFITS Brassboard was designed, built, and characterized to model basic principles in the laboratory. Deionized water is an excellent fluid choice for the LFITS Brassboard operating near room temperatures. **Figure 17** through **Figure 20** document the relevant properties of deionized water over a range of temperatures from 10°C to 70°C. The plots indicate measured data points and a fitted curve for deionized water density, viscosity, resistivity, and permittivity.

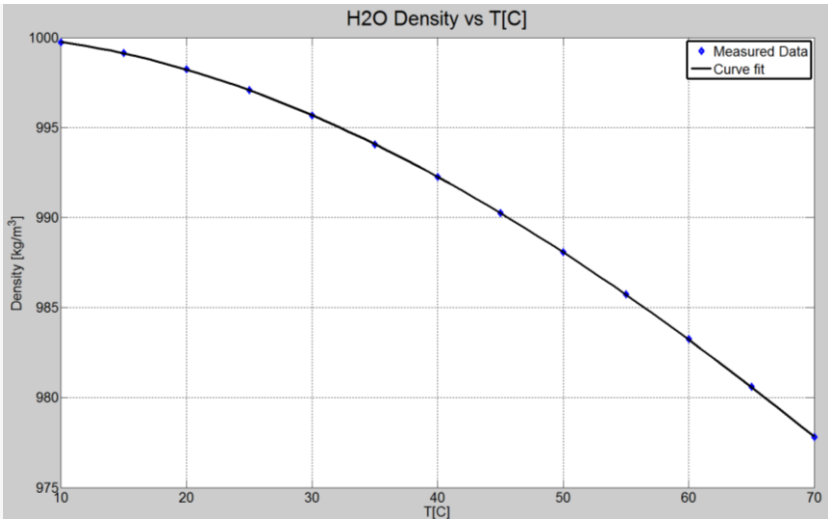

Figure 17. Deionized Water Density Versus Temperature

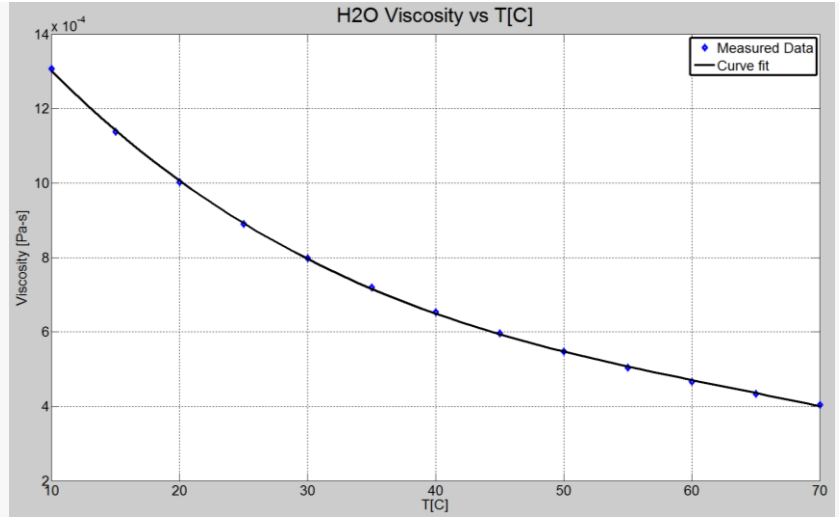

Figure 18. Deionized Water Viscosity Versus Temperature

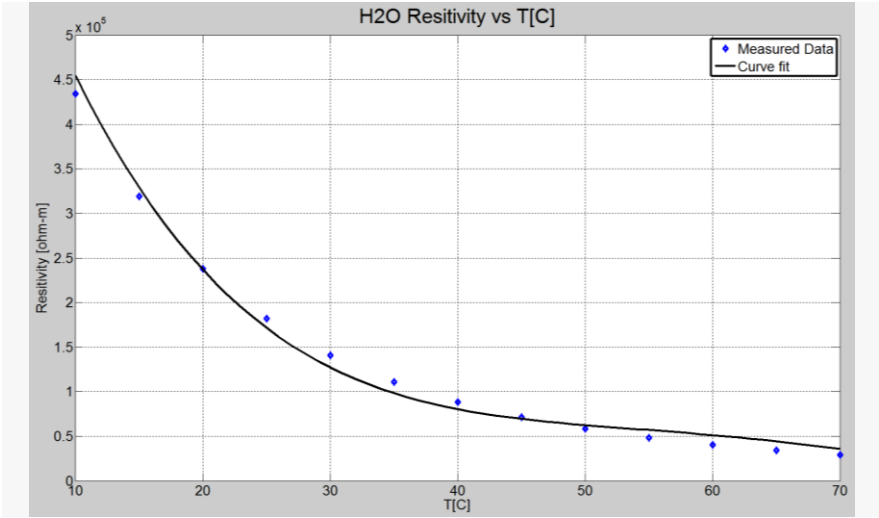

Figure 19. Deionized Water Resistivity Versus Temperature

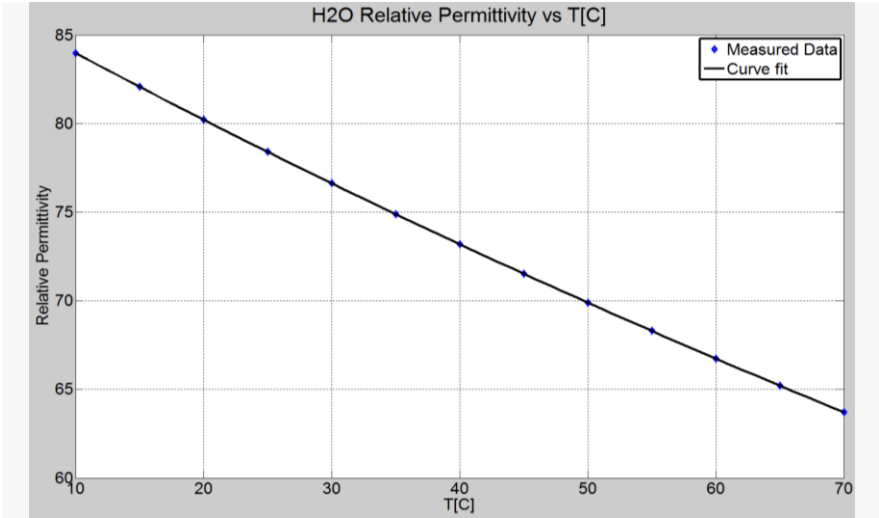

Figure 20. Deionized Water Permittivity Versus Temperature

Having set the Brassboard diameter (5.0") and established the key material properties of deionized water, these parameters were entered into the performance models to predict the brassboard frequency response and angular displacement noise. These projections depend both on the frequency response H_θ (S) of the sensor and its electronic signal conditioning noise.

Figure 21 and **Figure 22** are the estimated magnitude and phase response. Note that a family of curves is plotted representing temperatures from 10°C to 70°C. The main variations in both the phase and magnitude responses are due to changes n in viscosity of the deionized water.

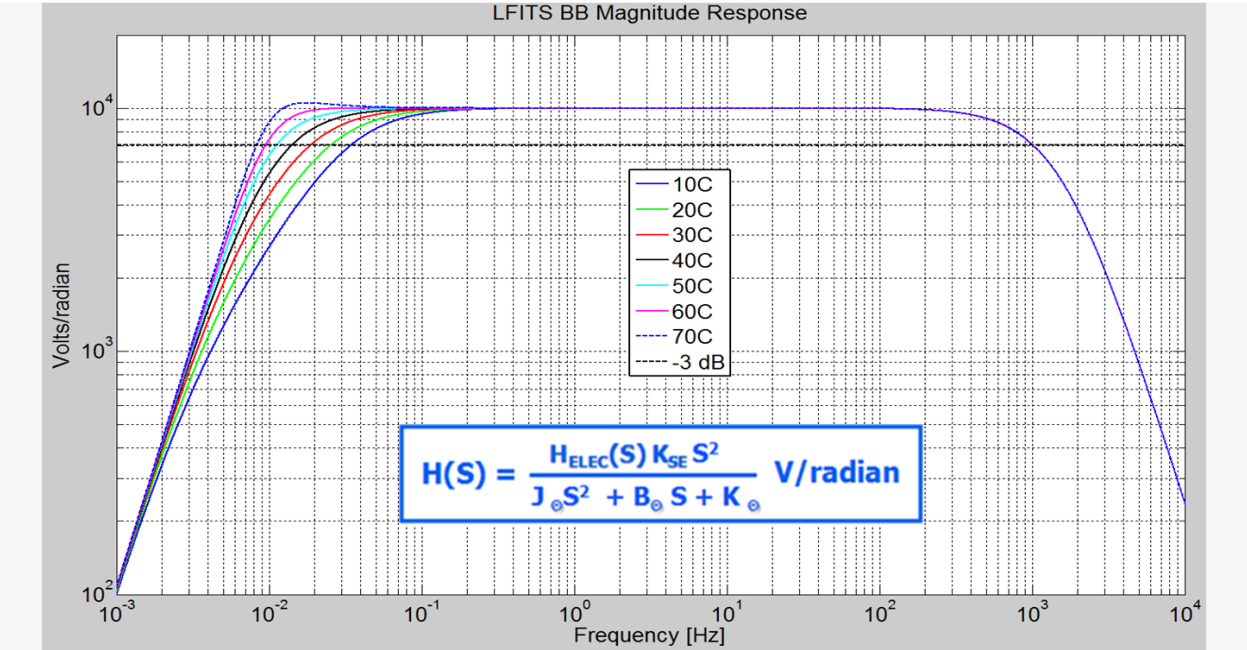

Figure 21. Modeled LFITS Brassboard Magnitude Response

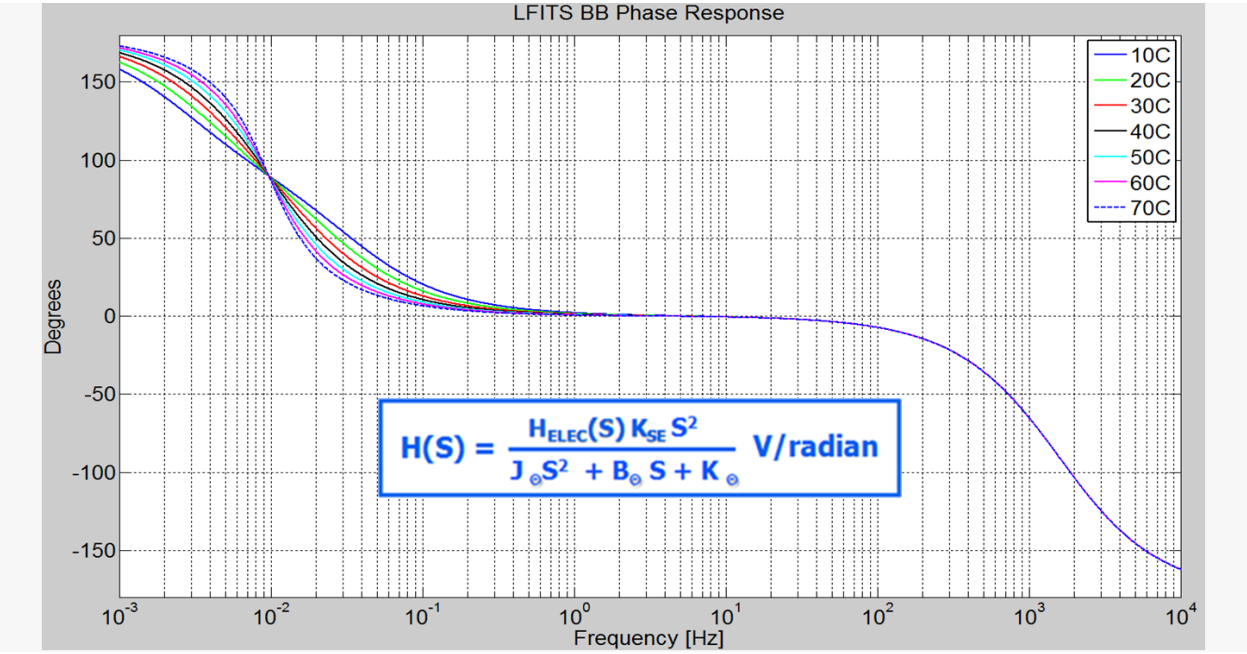

Figure 22. Modeled LFITS Brassboard Phase Response

Figure 23 is the estimated LFITS Brassboard angular displacement noise PSD. Note that in addition to the family of modeled curves over temperature, there are two "goal" curves superimposed on the plot. The higher "Original LFITS PSD" curve was the earliest estimate of LFITS technology performance from the ATA Team's proposal effort. The even lower "Desired LFITS PSD" represents a level of performance desired for LFITS, given the seismometer performance requirements analysis in Section 3.1 of this report.

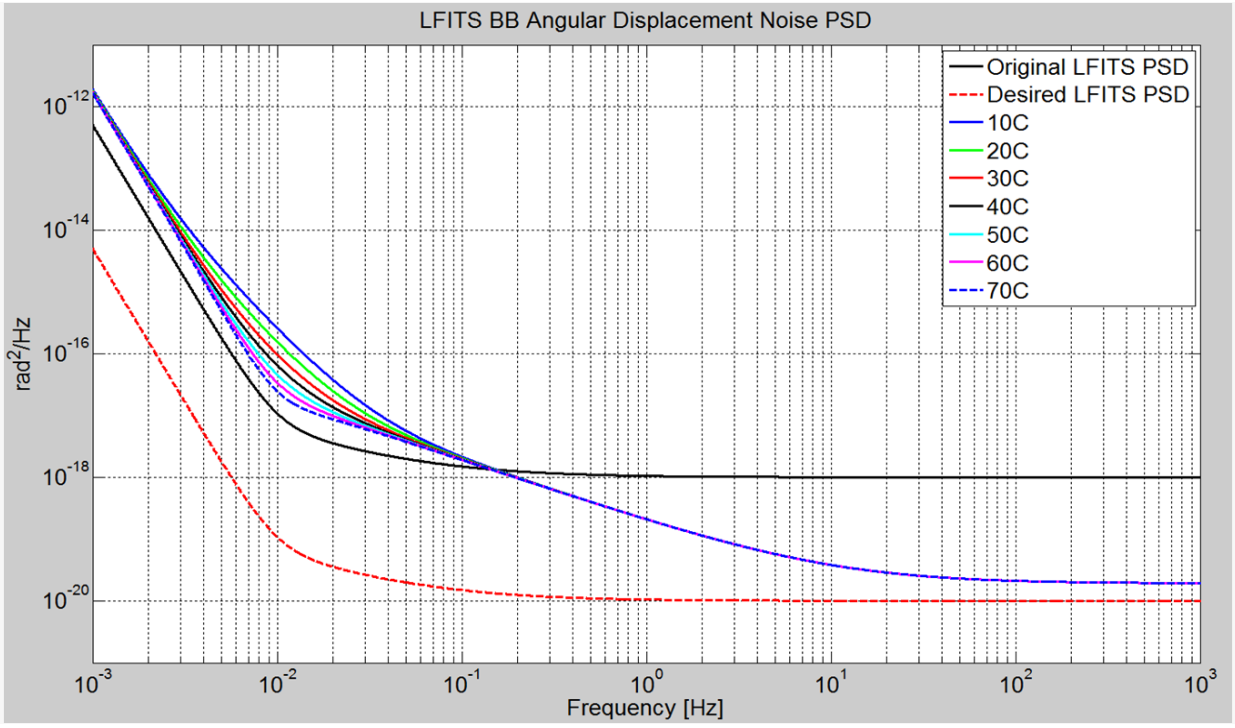

Figure 23. Modeled LFITS Brassboard Angular Displacement Noise

The predicted LFITS Brassboard performance lies between the two goal curves from 0.2 Hz to 1,000 Hz, and thus the brassboard was predicted to be in the range useful for establishing technical feasibility of the technology.

LFITS High-Temperature Performance Estimates: Deionized water is not an appropriate sensor fluid for downhole applications greater than 100°C. ATA analyzed alternative fluids but did not finalize a choice for high-temperature operation. In fact, there appear to be few good choices for a high-temperature dielectric fluid above 200°C. The material issues contributed to the decision to down-select for the SMHD rather than the LFITS technology.

However, in order to project representative performance for high-temperature units, ATA chose the fluid properties of pure ethylene glycol – density, viscosity, permittivity, and resistivity at 190°C, even though pure ethylene glycol boils at 197.3°C.

As noted in Section 3.1, ATA modeled two different unit sizes corresponding to downhole tools for smaller and larger boreholes. The modeled high-temperature sensor diameters are 1.6" and 3.8". A 1.6" diameter LFITS corresponds to the 2.25" inner diameter Sandia pressure vessel and a 3.8" diameter LFITS corresponds to the 5.27" inner diameter Nanometrics pressure vessel.

Figure 24, **Figure 25**, and **Figure 26** plot the predicted magnitude response, phase response, and equivalent angular displacement noise PSD respectively for the 1.6" and 3.8" diameter high-temperature LFITS. The Brassboard response is also plotted for comparison, although it is not discussed until Section 3.4.4.

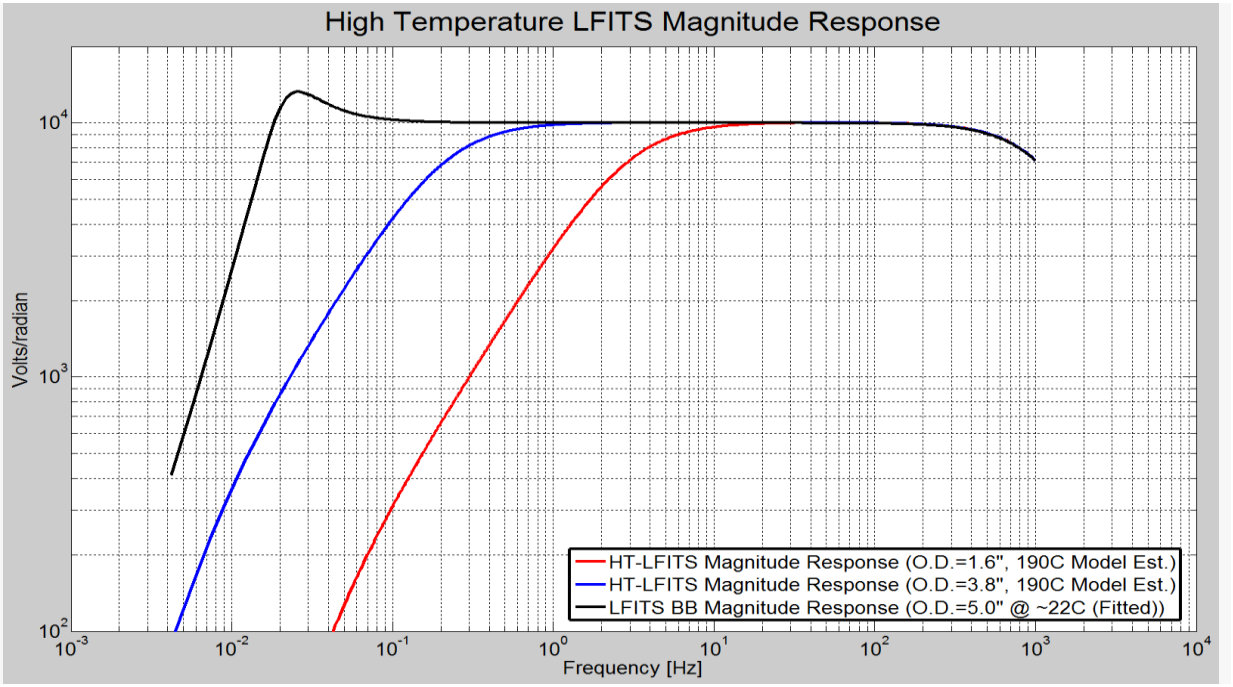

Figure 24. Modeled High-Temperature LFITS Magnitude Response

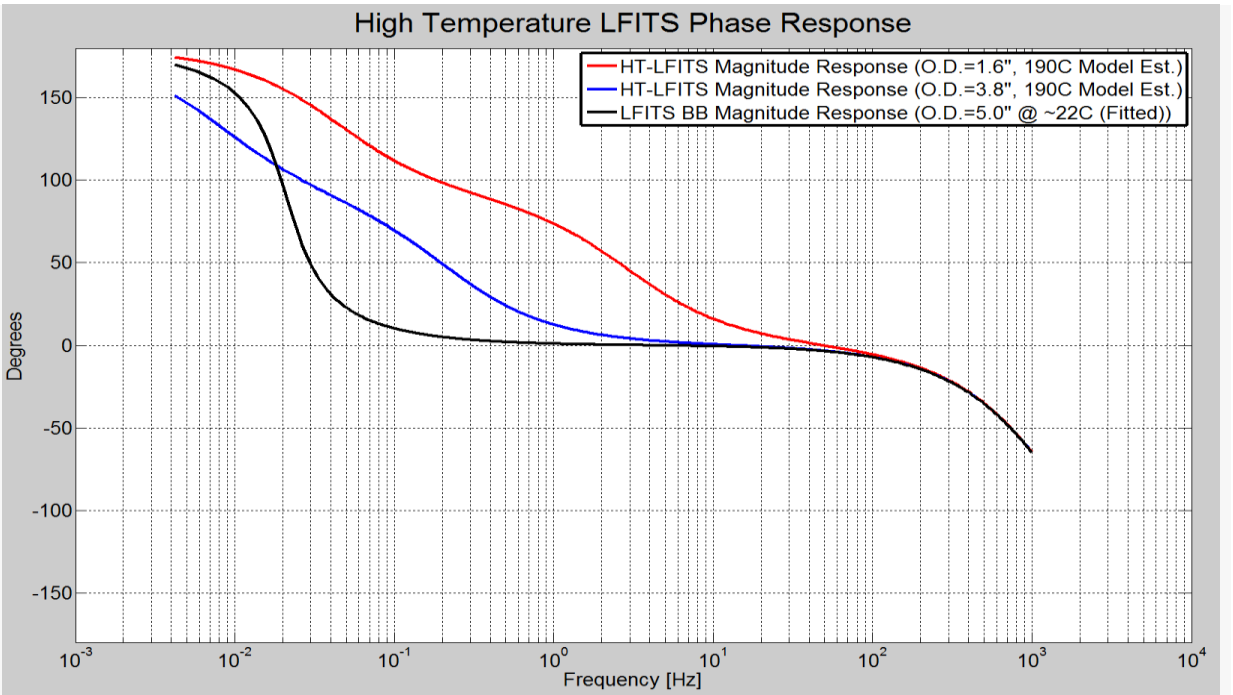

Figure 25. Modeled High-Temperature LFITS Phase Response

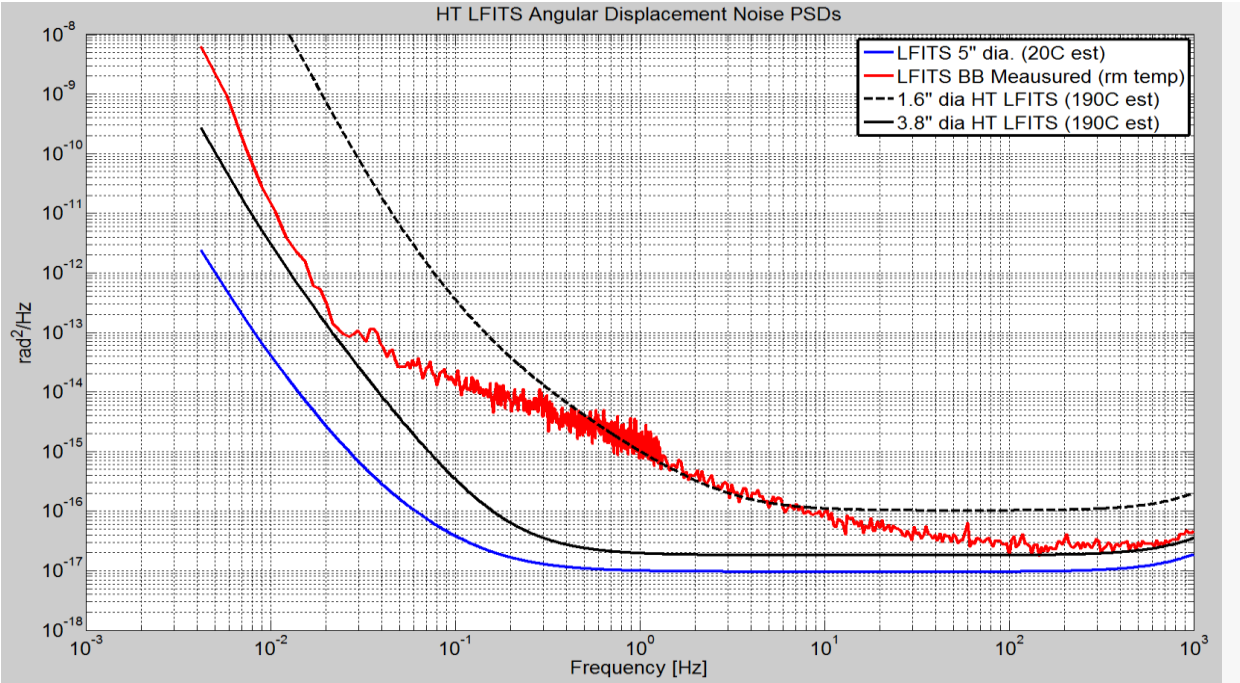

Figure 26. Modeled High-Temperature LFITS Angular Displacement Noise

Note that, in addition to the high temperature fluid choice challenges, the modeled high-temperature transfer functions, and noise spectra suggests potential performance challenges, particularly for smaller diameter devices. In short, modeling indicates that the LFITS Brassboard should be a good representative for evaluating the feasibility of the technology for seismic applications, but simulation suggests that downhole high-temperature devices will have based on the LFITS technology will have trouble meeting performance goals over the desired micro-seismic measurement bandwidth.

3.4.3 LFITS Brassboard

ATA Patentable material removed per DOE Final Report submission requirements. Content available from ATA for authorized government reviewers for purposes of review and evaluation.

ATA Patentable material removed per DOE Final Report submission requirements. Content available from ATA for authorized government reviewers for purposes of review and evaluation.

3.4.4 LFITS Test Results

The goal of LFITS Brassboard testing was to validate the LFITS technology computer models. After initial check-out, ATA measured the magnitude and phase response versus frequency and the quiescent noise PSD of the LFITS Brassboard.

Figure 30 and **Figure 31** show the LFITS Brassboard magnitude and phase responses (taken at room temperature, ~22^{o}C) overlaid with the LFITS Brassboard 20°C and 30°C model estimates. The frequency response data was only measured up to 10 Hz due to a limitation with the frequency response of the test fixture used on the rate table, i.e. the test fixture exhibited resonances above 10 Hz. The measured response deviates from the modeled predictions at low frequency, suggesting a higher than estimated spring constant and slightly lower viscous damping. The lack of knowledge of the spring constant reflects some of the challenges encountered in implementing the suspension during assembly. The LFITS Brassboard phase response also deviates from the modeled prediction. However, this deviation is suspected to be due to the non-rigid behavior (resonance) of the LFITS Brassboard test fixture that could not be resolved during Phase 1 tests.

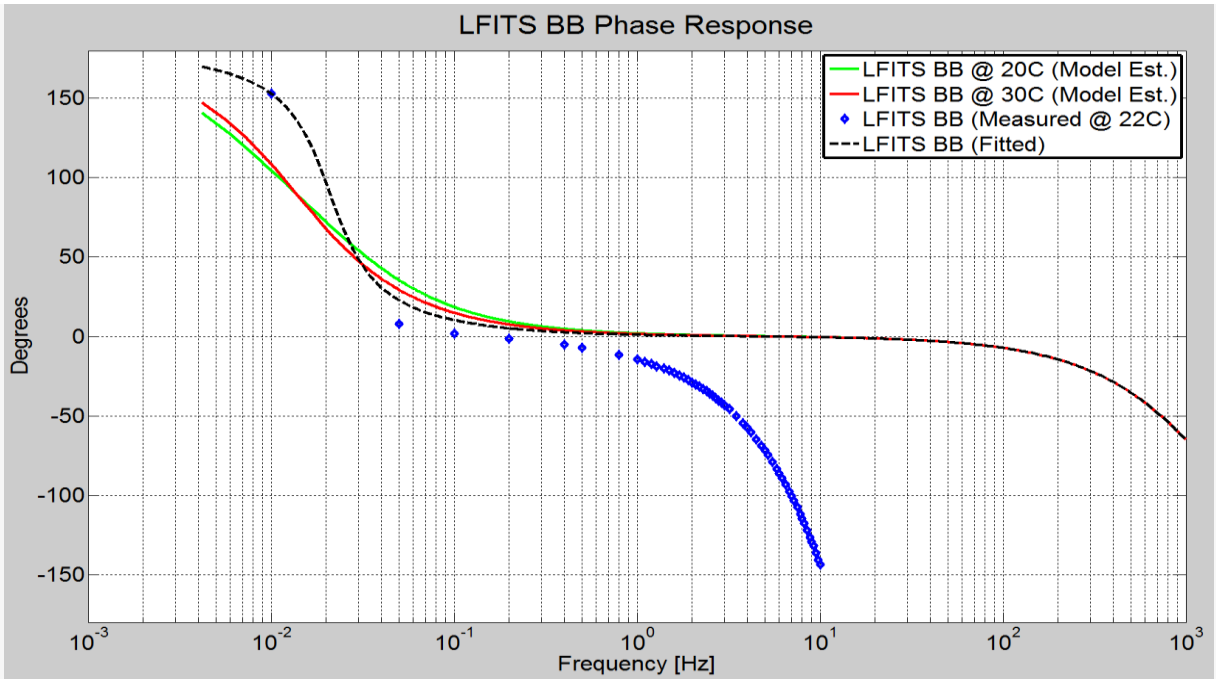

Figure 30. LFITS Brassboard Measured Phase Response Compared to Computer Models

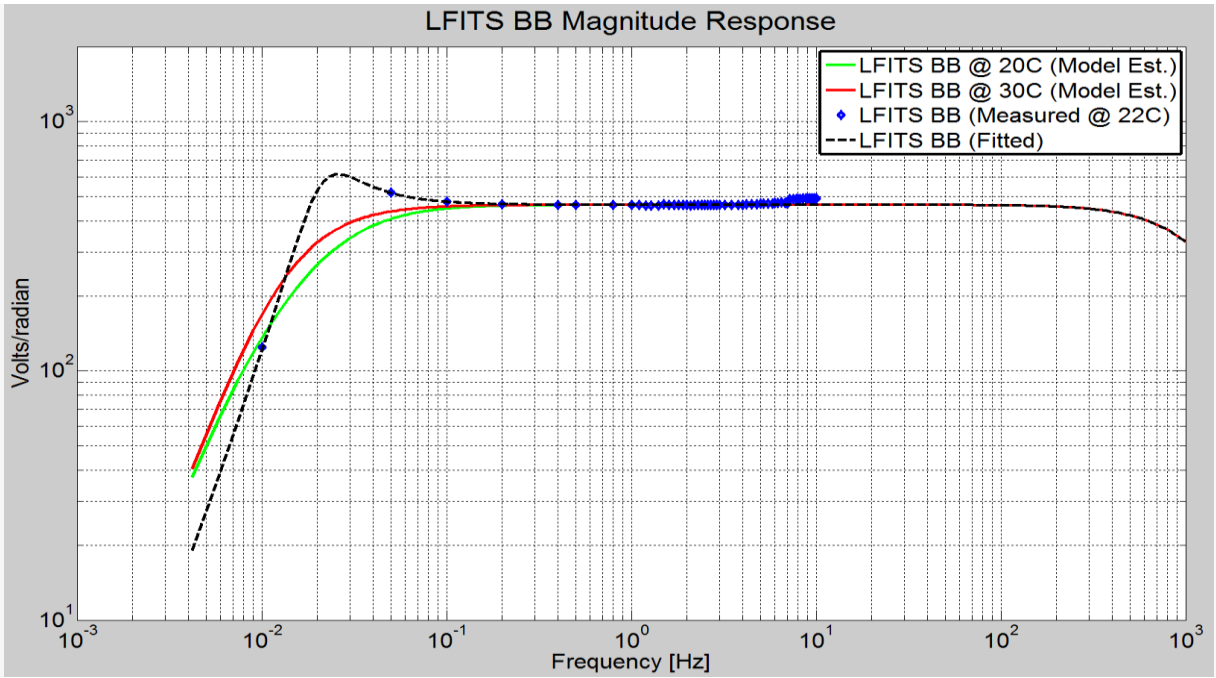

Figure 31. LFITS Brassboard Measured Magnitude Response Compared to Computer Models

Figure 32 shows the measured angular displacement noise PSD compared to the modeled predictions for the brassboard at 20°C and 30°C. The noise is higher than expected across all frequencies, apparently due to higher than expected noise in the signal processing electronics.

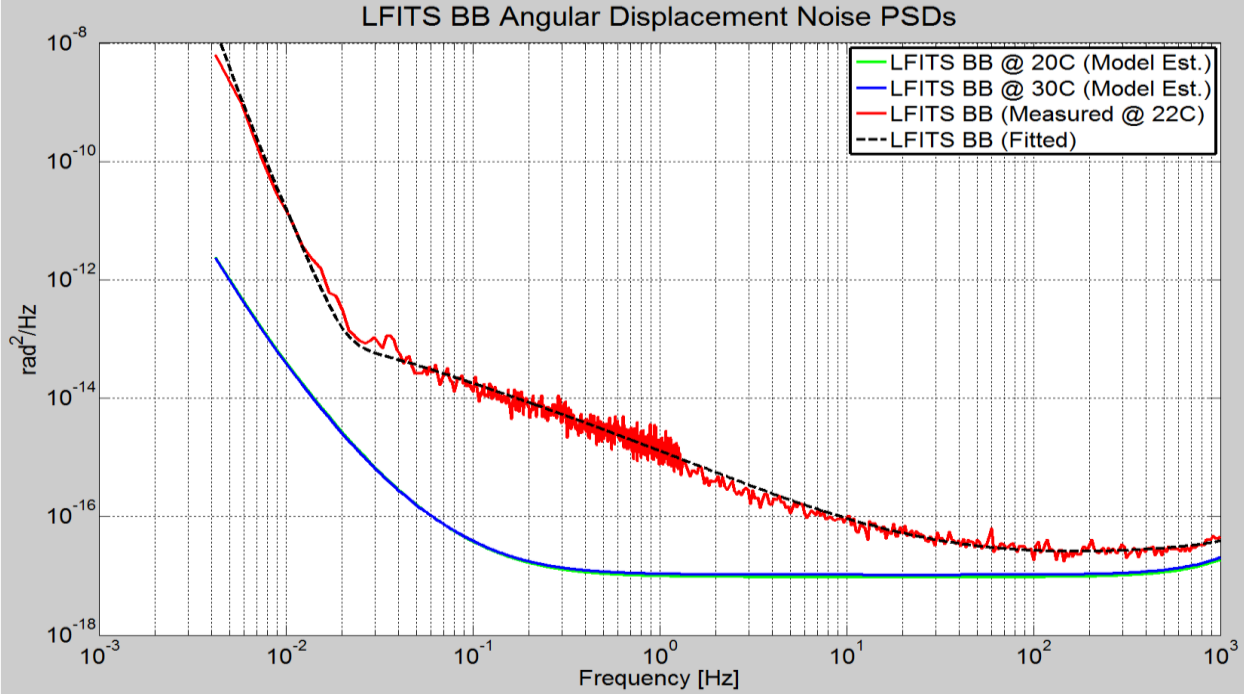

Figure 32. LFITS Brassboard Noise Floor Compared to Computer Models

Summary of LFITS Results: The LFITS Brassboard functioned as a rotational sensor, but test results were disappointing compared to modeled predictions. Although the frequency response suggests agreement with the modeled point design over a narrow band near 1 Hz, low frequency response suggests inaccurate model estimates of component and material properties, and high frequency response was lost or corrupted due to test issues. Angular displacement noise, a crucial measure of performance for micro-seismic signal detection, was measured over the full band buts is worse than predicted across all frequencies, potentially due to noise in the signal processing electronics. In short, the low technology readiness level of the LFITS was evident, suggesting risk in the amount of residual engineering required to achieve modeled performance levels for a 7-DOF seismometer even for earth surface applications. In addition, high-temperature analysis identified a difficulty in appropriate dielectric fluid choice for the hot downhole environment. These risks feed into the trade study analysis of Section 3.6.

3.5 SMHD DEVELOPMENT

ATA's Seismic Magnetohydrodynamic (SMHD) sensor is an angular rate sensor and the second of two candidate rotational sensing technologies. This section describes development and test of the SMHD models and brassboards. Section 3.4 describes corresponding models and brassboard for the other technology, the LFITS.

3.5.1 SMHD Principle of Operation

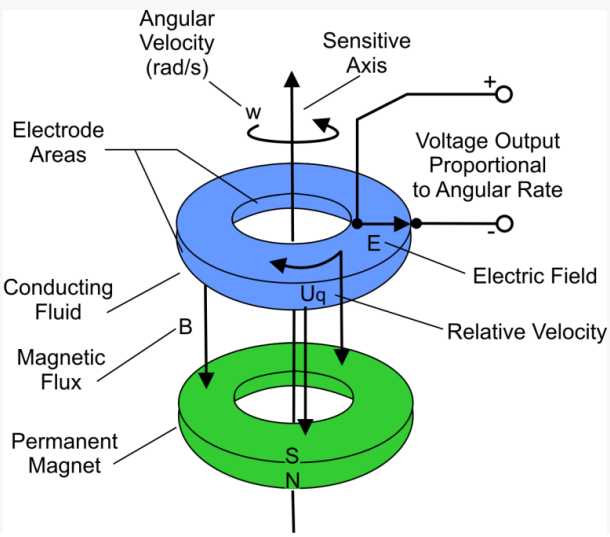

Figure 33. SMHD Principle of Operation

The SMHD technology is based on an evolution to an existing, relatively mature magneto-hydrodynamic sensor capability. ATA designs, builds, and sells commercial Angular Rate Sensors (ARS) based on this MHD technology for applications that demand wide bandwidth, low noise, and high sensitivity in a relatively compact format in ground and aerospace environments. Although the principle of operation remains the same for MHD and SMHD sensors, the SMHD application requires larger, very low-noise sensors with materials specifically adapted to geophysical conditions in hot downhole environments.

The principle of operation is depicted in **Figure 33** and is based on using a conductive fluid constrained in a void free annulus along with a static magnetic field applied through the conductive fluid, typically via permanent magnets. As the sensor is rotated about the sensitive axis, a relative velocity difference occurs between the conductive fluid and the magnetic field that moves with the case. This produces a voltage proportional to the relative circumferential velocity difference between the conductive fluid and the magnetic files and the width of the sense channel. The rate proportional output voltage can then be either picked off directly, or input to a high gain internal transformer that amplifies the sense channel output voltage by several thousand times proportional to the primary to secondary winding turn ratio. A low noise op-amp is typically the only additional electronics required to amplify the signal that is then typically digitized using a high resolution Analog to Digital Converter (ADC).

3.5.2 SMHD Modeling

ATA's existing MHD angular rate sensor technology is mature and well understood. Computer models have been developed that closely match measured data and are excellent predictors of the performance of new sensor designs. The frequency response function (Equation 9) is used to estimate the dynamic performance of the MHD ARS sense element before amplification by any signal processing electronics. Equation 9 is the basic model for calculating frequency response based on sensor component physical, electrical, and material properties.

ATA Proprietary data removed per DOE Final Report submission requirements. Content available from ATA for authorized government reviewers for purposes of review and evaluation.

The frequency response $H_{ars}(s)$ calculated by equation 9 is unamplified. The amplified reponse is the product of the sense element frequency response $H_{sense}(s)$ and the signal conditioning electronics response $H_{elec}(s)$.

$$H_{ars}(s) = H_{sense}(s) * H_{elec}(s) \quad \textbf{(10)}$$

All of the predicted phase and magnitude plot included in this section are based on the models of equation 9 and 10, substituting the appropriate materials and electronics for the brassboards and the high-temperature downhole application. Predictions also include the angular rate noise PSDs, which incorporate electronics noise models specific to the different sensors.

SMHD Brassboard Models: **Figure 34** and **Figure 35** are the modeled phase and magnitude response for the ARS-16 sensors used in the tri-axial brassboard. Since the ARS-16 is a new sensor design, the plot includes comparable curves for ATA's commercially available ARS-14. **Figure 36** plots the modeled ARS-16 and ARS-14 angular rate noise PSD.

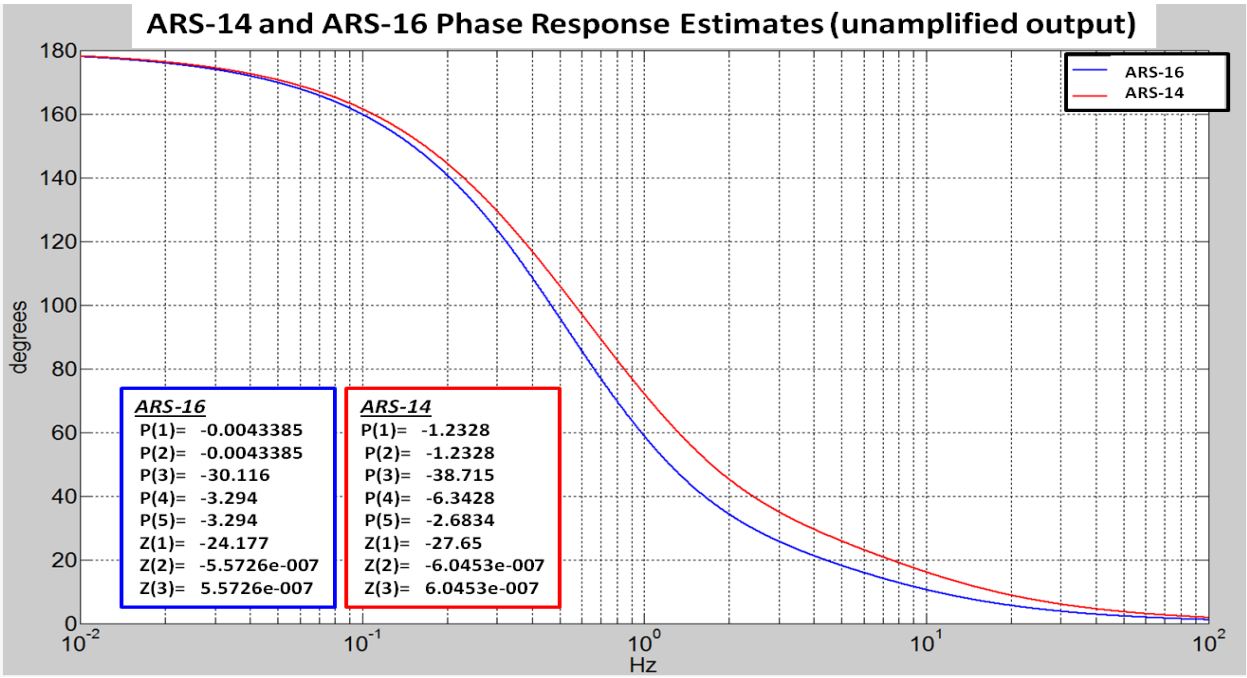

Figure 34. Modeled ARS-16 MHD Sensor Phase Response

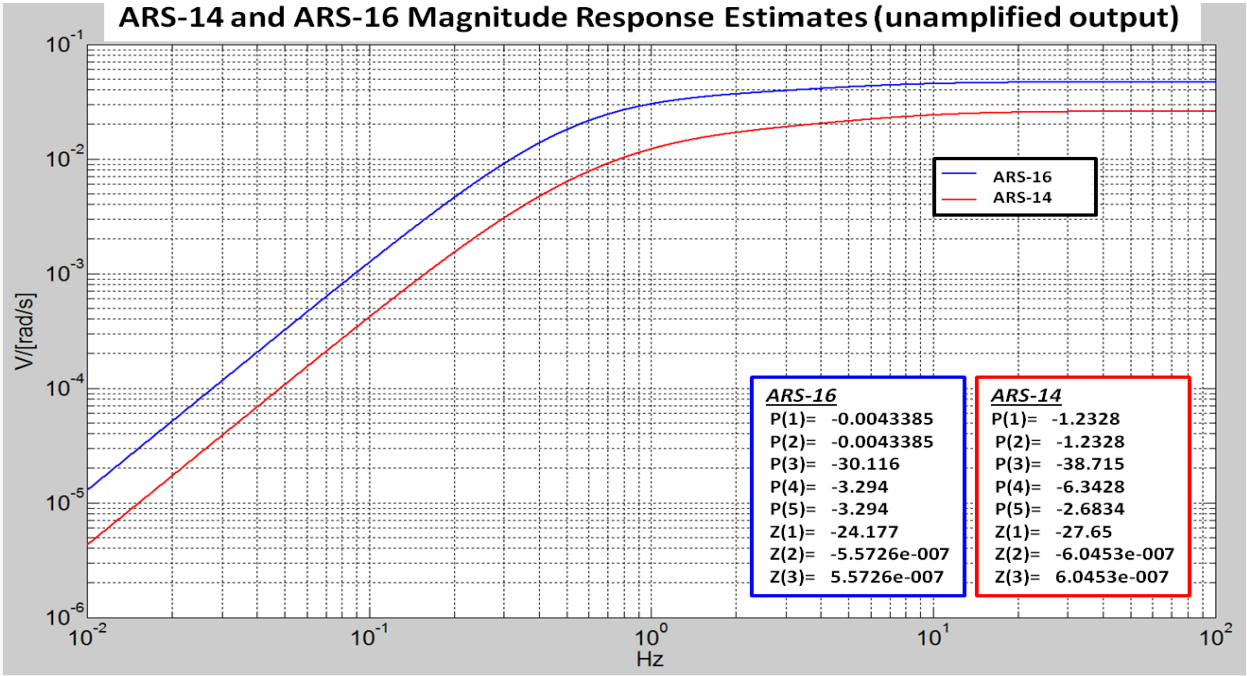

Figure 35. Modeled ARS-16 MHD Sensor Magnitude Response

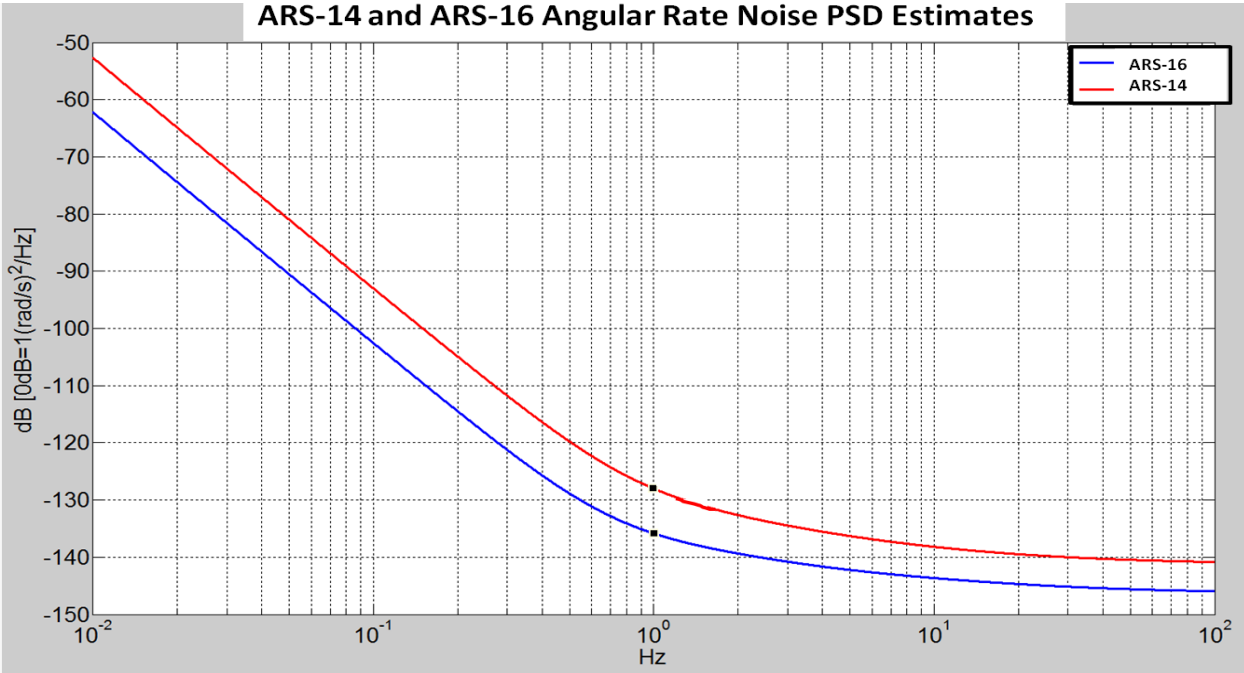

Figure 36. Modeled SMHD Brassboard Angular Rate Noise

SMHD High-Temperature Performance Estimates: ATA chose Galinstan as the high-temperature SMHD sense element, modeling sensor behavior based on its properties. Modeling for the electronics is based on the components described in Section 3.3.3.

As noted in Section 3.1, ATA modeled two different unit sizes corresponding to downhole tools for smaller and larger boreholes. The modeled high-temperature sensor diameters are 1.6" and 3.8". A 1.6" diameter SMHD corresponds to the 2.25" inner diameter Sandia downhole pressure vessel, and a 3.8" diameter SMHD corresponds to the 5.27" inner diameter Nanometrics vessel.

Figure 37, **Figure 38**, and **Figure 39** plot the predicted magnitude response, phase response, and equivalent angular displacement noise PSD for the 1.6" and 3.8" diameter high-temperature SMHD.

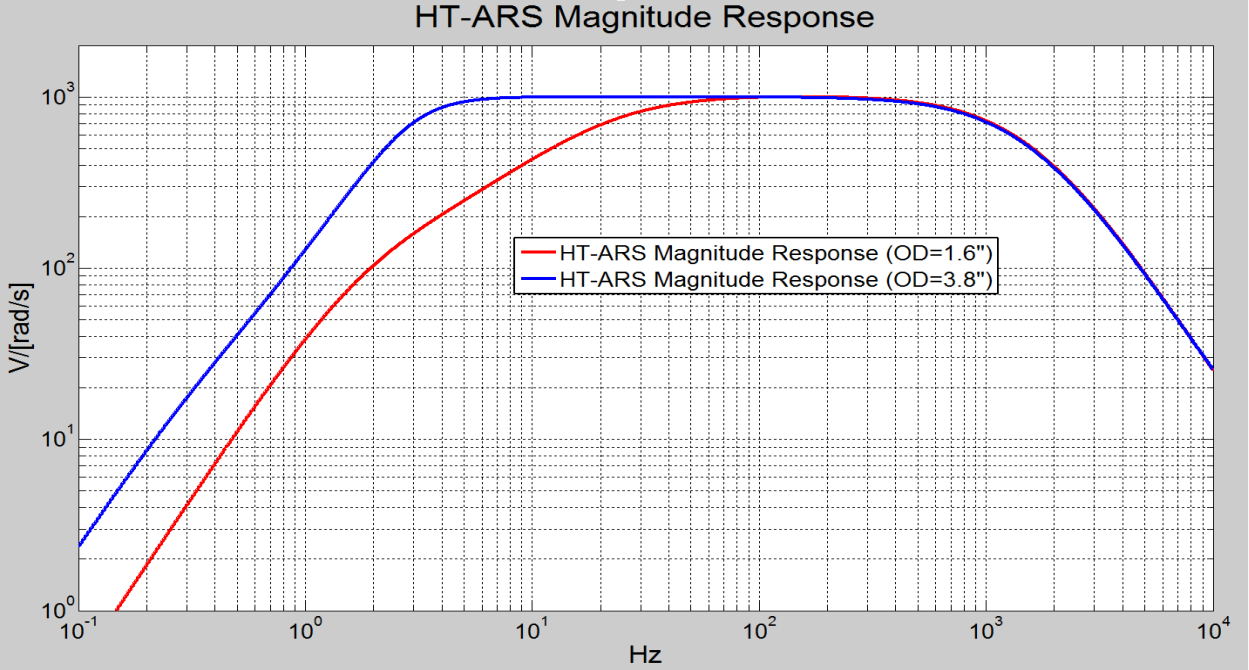

Figure 37. Modeled High-Temperature SMHD Magnitude Response

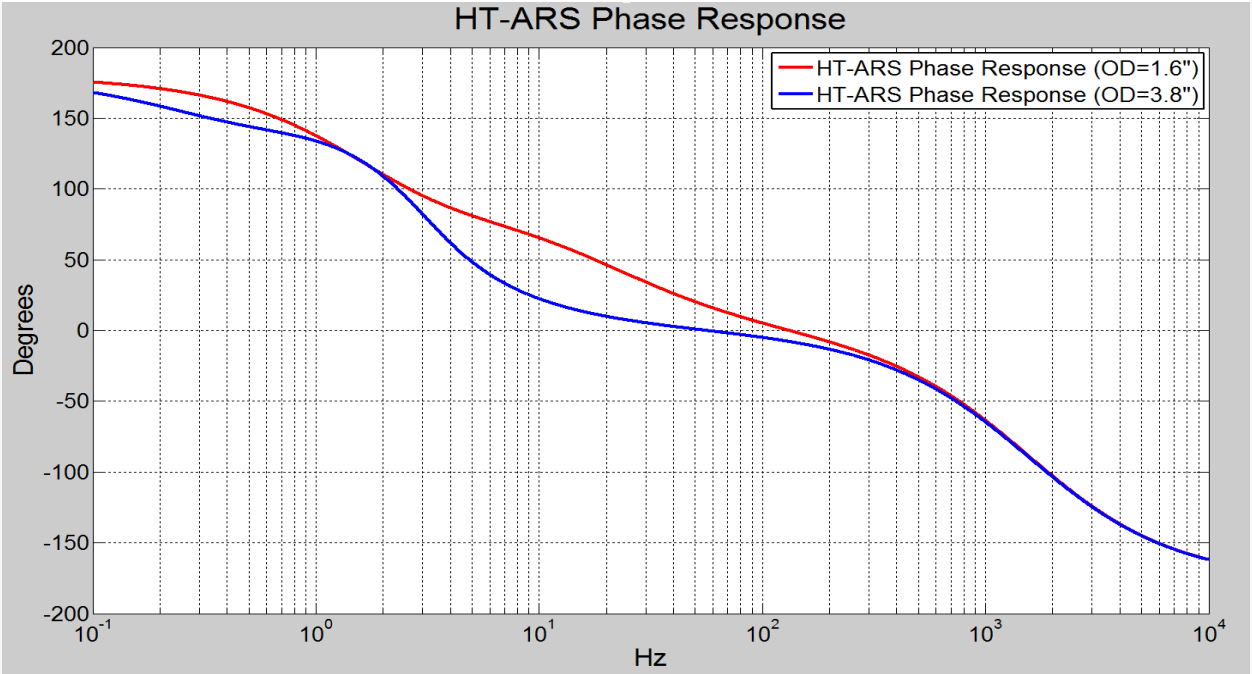

Figure 38. Modeled High-Temperature SMHD Phase Response

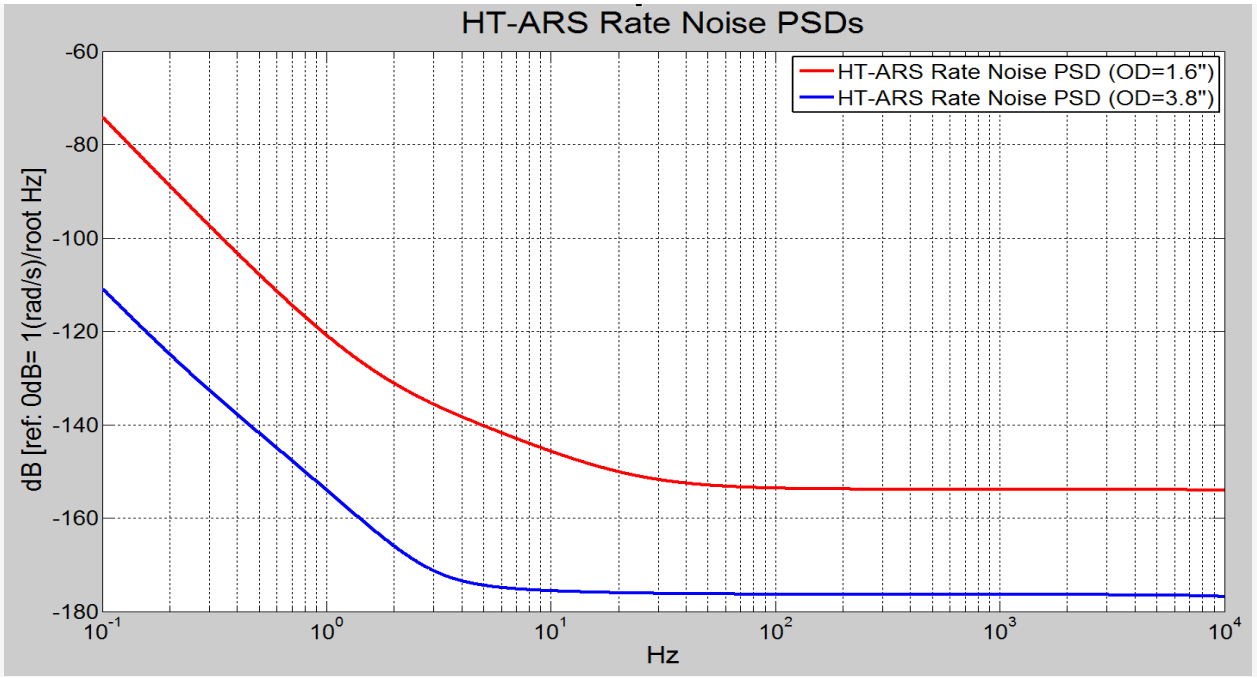

Figure 39. Modeled High-Temperature SMHD Rate Noise

3.5.3 SMHD Brassboards

As mentioned in prior sections, ATA's commercial ARS devices are based on MHD technology. The SMHD application requires larger, lower-noise sensors with materials specifically adapted to hot downhole environments. Thus, the SMHD brassboards made use of existing ARS devices and prototypes engineered for evaluation under earth-surface conditions, collection of field seismic data, and validation of SMHD material choices.

ATA maintains a small stock of sensors for rent to support field tests. From this stock, ATA provided two different sensor types for near-surface test and seismic characterization:

- An ARS-16 Tri-Axial Brassboard
- Two Single Axis ARS-24 Sensors

In addition, ATA built a proof-of-concept device for materials proposed for the SMHD design:

- One Galinstan Proof-of-Concept Sensor

ARS-16 Tri-Axial Brassboard: **Figure 40** shows the tri-axial brassboard with an individual ARS-16 sitting beside it. The ARS-16 sensor is ATA's latest rate sensor, not yet commercially released. The ARS-16 Tri-Axial Unit was designed so that the three ARS-16 sensors could be mounted parallel or orthogonally. The parallel configuration was used during sensor characterization efforts by Sandia National Laboratories when the brassboard was mounted on a rate table and driven with

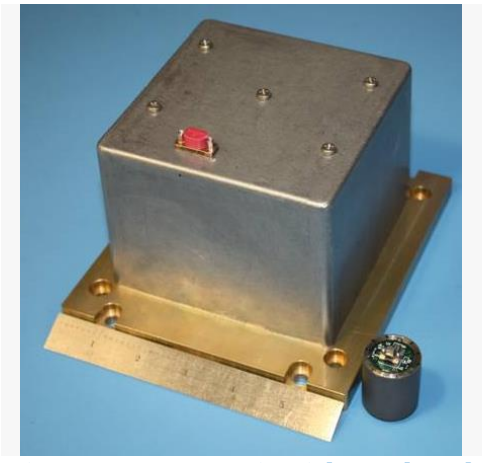

Figure 40. ARS-16 Tri-Axial Brassboard Box with an Individual ARS-16 Sensor

stepped-sine inputs, which imparted the same motion to all three sensors. Similarly, when the brassboard was placed in a quiet environment to measure the sensor noise, the parallel configuration imparted the same base motion to all three sensors. Later, the sensors were configured into an orthogonal triad for field measurements at the Hawaii Volcano Observatory.

Figure 41. Single Axis ARS-24 Sensor

ARS-24 Sensors: **Figure 41** shows a single one-axis ARS-24 sensor with push pins for scale. The ARS-24 is the highest resolution MHD sensor built by ATA but is not a commercially available product. Its noise is approximately 14 dB lower than the ARS-16, still not the levels needed for SMHD but closer to the level required to detect smaller seismic events.

Galinstan Proof-of-Concept Sensor: ATA built a single-axis proof-of-concept sensor using Galinstan (a gallium, indium, tin, and zinc eutectic) as the fluid sensor element. As shown in **Figure 42**, the unit is physically identical to the ARS-16 upon which it is based.

Figure 42. Single Axis Galinstan Sensor

The change from mercury to Galinstan addresses a number of concerns. First, it is non-toxic and eliminates the environmental hazards cited as a barrier in the market assessment summarized in Section 3.7. Second, it supports high-temperature downhole operation per Section 3.3.1 while making the sensor less applicable to military applications because of its limited low temperature performance. This should help remove any International Traffic in Arms Regulations (ITAR) restrictions (another market barrier summarized in Section 3.7).

The change from mercury to Galinstan addresses a number of concerns. First, it is non-toxic and eliminates the environmental hazards cited as a barrier in the market assessment summarized in Section 3.7. Second, it supports high-temperature downhole operation per Section 3.3.1 while making the sensor less applicable to military applications because of its limited low temperature performance. This should help remove any International Traffic in Arms Regulations (ITAR) restrictions (another market barrier summarized in Section 3.7).

Unlike the ARS-16 Tri-Axial unit and the ARS-24 units, the Galinstan sensor was not built for field data acquisition. It was used to evaluate fabrication challenges and validate performance of the novel material. For example, the assembly process allowed ATA to assess oxidation and wetting properties that differ substantially from mercury. Unlike mercury, Galinstan is reactive to oxygen and forms a black oxide immediately upon contact with air. Care must be taken to fill the sensor under a vacuum to prevent contact with oxygen. Also, unlike mercury, Galinstan instantly wets everything it touches which introduces considerable handling and clean up challenges. However, the assembly was successful and the learning process increases likelihood of successful Phase two SMHD design and fabrication.

3.5.4 SMHD Testing

The ATA Team conducted three distinct types of testing with the various SMHD brassboards. These were:

- Laboratory performance characterization of the ARS-16 and ARS-24 sensors
- Field measurements of rotational seismic signals using ARS-16 and ARS-24, and
- Laboratory characterization of the Galinstan proof-of-concept sensor

Results from each of these tests is summarized in the paragraphs that follow.

ARS Characterization: Sandia National Laboratories independently tested three ARS-16s and an ARS-24. Attachment B contains the resulting Sandia Report SAND2013-3674, "Evaluation of ARS16 and ARS24 Rotational Seismic Sensor Designed by Applied Technology Associates." ATA later built a second ARS-24 and supplied it to SNL for field deployment in Hawaii but it was not available for the characterization testing of the other four sensors.

The tests were conducted in collaboration with the United States Geological Survey (USGS) at the Albuquerque Seismic Laboratory in Albuquerque NM to evaluate sensitivity, linearity, self-noise, dynamic range, tonal and broadband frequency response, and cross-axis sensitivity. **Figure 43** shows the sensors under test in the Z-axis frequency response, the X-axis frequency response, and the self-noise test configurations. Results of these tests are summarized in **Table 11**.

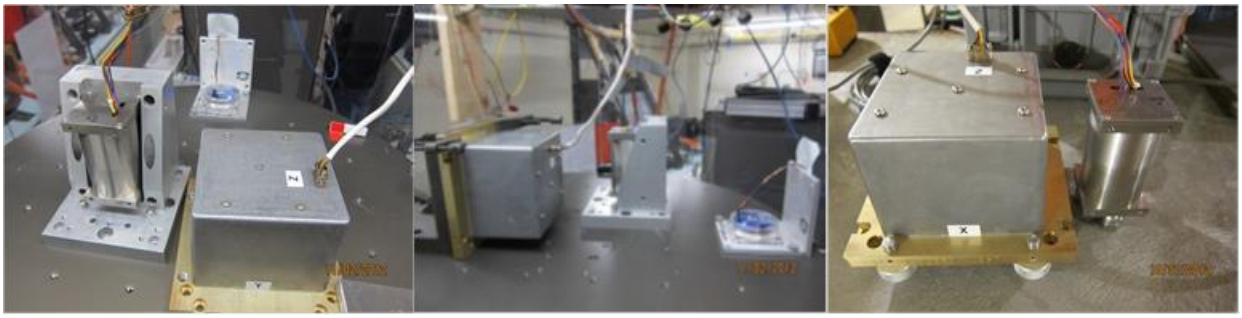

Figure 43. ARS Sensors Being Characterized at the USGS Albuquerque Seismic Laboratory

Table 11. Sandia National Laboratories Summary of Tests for ARS Rotational Sensors

Test Series	ARS-16	ARS-24
Static Performance	The isolation noise test showed the three transducers were well matched in self-noise levels. All three sensor had a noise floor at 10 Hz of -132 dB relative to one (radian/second) 2/Hz. The RMS noise of the three sensors for the 1-300 Hz passband were 10.80 µrad/s for ARS16z, 11.28 µrad/s for ARS-16y and 15.41 µrad/s for ARS16x. The associated dynamic ranges for the same passband are 62.7 dB ARS16z, 62.3 dB for ARS16y and 59.6 dB for ARS16x.	The ARS-24z sensor had a noise floor at 10 Hz of -152 dB relative to one (radian/second)2/Hz. The RMS noise of the 1 to 300 Hz passband was 3.12 µrad/s. The associated dynamic range for the same passband is 61.5 dB.

Test Series	ARS-16	ARS-24
Tonal Dynamic Performance	The 1 Hz linearity test showed stability in sensitivity for rotation rates of 0.14 to 24.4 radians/second. The 4 Hz linearity test showed stability in sensitivity for rotation rates of 0.14 to 17.4 radians/second. The 16 Hz linearity test showed stability in sensitivity for rotation rates of 0.14 to 14.0 radians/second.	The 1 Hz linearity test showed stability in sensitivity for rotation rates of 0.14 to 6.12 radians/second. The 4 Hz linearity test showed stability in sensitivity for rotation rates of 0.14 to 6.14 radians/second. The 16 Hz linearity test showed stability in sensitivity for rotation rates of 0.14 to 5.14 radians/second.
Broadband Dynamic Performance	The sensor passband was confirmed to be 0.1 to 60 Hz, below 2 Hz both amplitude and phase mismatch exists relative to the FOG reference sensor. The ARS-16 sensors were well phase-matched, showing less than 0.5 degrees variance, for the 0.1 to 60 Hz passband.	The sensor passband was confirmed to be 0.1 to 60 Hz, below 2 Hz both amplitude and phase mismatch exists relative to the FOG reference sensor.

Figure 44 plots the self-noise of the ARS-16 and ARS-24 as measured during test at the Albuquerque Seismic Laboratory. As expected, the ARS-24 has the lowest noise floor. Variation between the three ARS-16 sensors was minimal. Overall, the tests confirmed the modeled sensor performance and low cross-axis sensitivity for the technology.

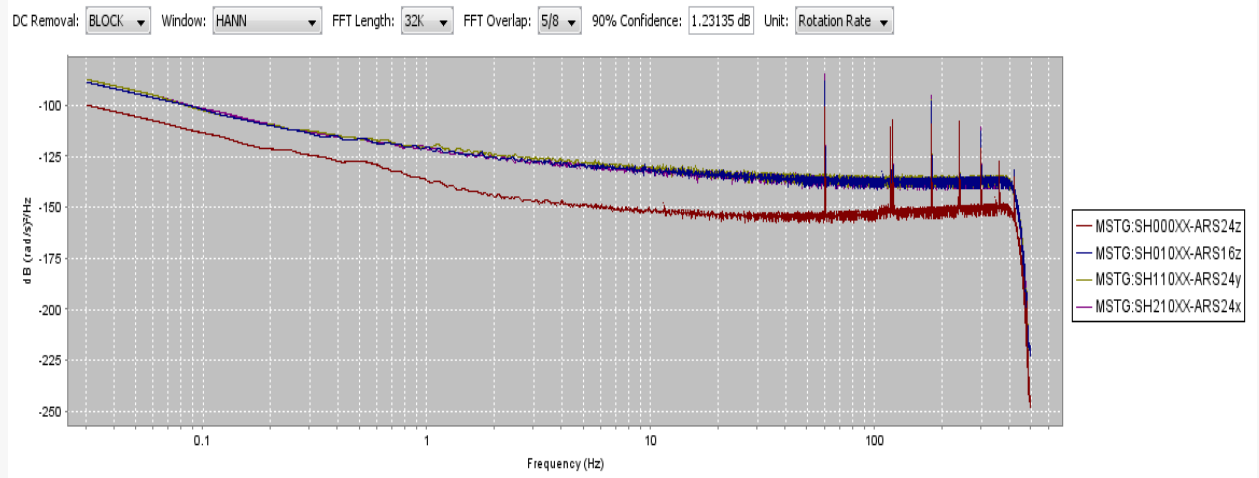

Figure 44. ARS Self-Noise Measured at the Albuquerque Seismological Laboratory

Field Measurements of Rotational Seismic Signals: As Section 3.2 indicated, it is only recently that geophysicists have attempted to measure and use rotational motion in seismic data collection, and there have been few rotational motion measurements in the field because high-quality rotational instrument have not existed or, like ring lasers, are exceedingly large and expensive. Using the existing SMHD Brassboard units, Sandia National Laboratories sought to prove the ability to record seismic rotational motion in the field and demonstrate associated processing algorithms to extract information from combined linear and rotational motion data.

Two ARS-24s and three ARS-16s were deployed by SNL to the Hawaii Volcano Observatory for two months, and a number of earthquakes were recorded. Attachment C contains Sandia National Laboratories' paper: "Observations of Volcanic Activity at Kilauea Volcano, Hawaii, Using Rotational Seismometers" The principal findings of the experiment were summarized in Section 3.2 of this report. Many high-amplitude seismic events were recorded and processed for back azimuth and in-situ shear velocity. Calculation of back azimuth may have been hampered by wave scattering and gave highly variable results. In contrast, calculation of in-situ shear velocity was successful, giving results in good agreement with previous seismic array studies.

The instruments were active between December 12th, 2012 and February 14, 2013. During that time, a number of high-amplitude events were detected. None of the rotational instruments were able to resolve ambient background noise above its own self-noise. Unfortunately, the two ARS-24 units began to malfunction a few days after deployment, and only operated until the 18th of December. This was not caught due to problems with telemetry. The Sandia researchers think the problem was related to a power supply common to both instruments. The three ARS-16's performed well throughout the deployment.

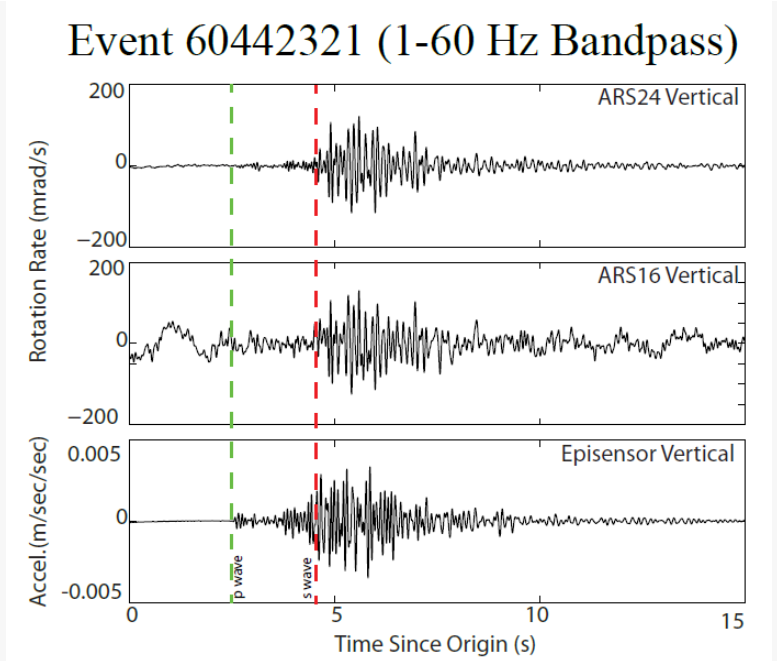

Figure 45. Vertical Rotation Rate and Acceleration Recorded for a Hawaiian Earthquake

Figure 45 reproduces a plot of vertical rotation rate measured by the ARS units and acceleration for a magnitude 1.85 event at 0.8 km distance. The plot demonstrates "the relative noise on the two rotation instruments, as well as relative lack of signal before the S wave. All of the signal before the S wave is caused by mode conversions from P to S, as sensitivity to translational motion on the rotational seismometers is essentially nil."

Galinstan Sensor Characterization: Section 3.3.1 summarized the tests and results for the Galinstan proof-of-concept unit. Standard testing included measuring the broadband frequency response and sensor noise floor. Results of both tests matched well to performance model predictions, and, at room temperature, the Galinstan sensor actually had lower noise from 1 to 1,000 Hz and a flatter frequency response function than the standard mercury ARS-16 model. Frequency response tests were repeated over a range of temperatures to evaluate the stability and behavior of the Galinstan sensor response near its freezing point. Results of these tests were shown and discussed in Section 3.3.1.

Summary of SMHD Results: The SMHD is based on a relatively mature MHD technology, but the technology requires modifications and enhancements for the high-temperature seismic application. ATA evaluated two types of brassboard sensors. The first included single axis

ARS-24 sensors and a tri-axial box of ARS-16 sensors used for both an assessment of sensor performance and field deployments to demonstrate measurement and processing of seismic rotational ground motion. The sensors performed as expected under earth surface conditions, validating models and increasing confidence in the science of rotational seismometry. The second type of brassboard was an SMHD device using Galinstan as the sensor fluid. This proof-of-concept unit validated the high-temperature SMHD sensor fluid choice, increased confidence in associated assembly processes, and validated excellent sensitivity and low noise in accordance with modeled results. These variable results figured heavily into the trade study analysis of Section 3.6.

3.6 TRADE AND DOWN-SELECT

ATA performed an assessment of the relative merits of the LFITS and SMHD rotational sensing technology for the high-temperature EGS fracture monitoring application. The study is based on test results from the brassboards, simulations of the respective rotational sensing technologies, and analysis of required performance and geothermal physical and environmental constraints. Attachment E contains the "SMHD-LFITS Trade Study" summarized in this section.

ATA identified sensor *resolution*, *bandwidth*, and *dynamic range* as the Key Performance Parameters (KPP) for the study. The trade study also considered Key System Attributes (KSA) including *size*, *operational temperature*, and *reliability*. **Figure 46** summarizes the study findings using a red / yellow / green system. Green indicates that the sensor technology can reasonably be expected to meet all of the requirements in that category. Yellow indicate that there are challenges due to the sensor meeting some but not all of the factors in that area, or there are unknowns that constitute residual risk to be addressed during detailed design and analysis in Phase 2. Red indicates significant shortfalls in the category and a high risk of failing to meet the requirement or attribute. The better sensor in each category is denoted with a checkmark. The following paragraphs summarize key findings from each category in the table.

Figure 46. Summary of Trade Between LFITS and SMHD Rotational Sensor Technology

Resolution (KPP): The SMHD technology measures angular rate. In contrast, the LFITS technology measures angular displacement. Thus, the SMHD has an inherent advantage at high frequency due to lower noise levels. **Figure 47** graphically illustrates the performance of the two sensor types relative to expected micro-seismic signal levels. The figure overlays the modeled high-temperature performance of LFITS and SMHD sensors onto the "low Q" (left) and "high Q" predicted micro-seismic signal spectra described in Section 3.1. As noted in the Requirements section, the grey region represents signals of interest between a lower bound set by a minimum seismic event (moment = -2 at 2 km) and an upper bound set by a maximum seismic event (moment = +3.5 @ 1 km).

The overlay curves for each LFITS and SMHD sensor are their noise floors, so the sensors detect signals above their respective curves. The ideal sensor would have a noise floor curve below the grey shaded area over as wide a frequency band as possible. Thus, the SMHD wins the trade due to its low noise floor at high frequency. However, both sensors are rated yellow in **Figure 46**. This rating reflects the critical nature of this requirement, the desire to push resolution as far as possible, and the uncertainties involved in defining the seismic signals of interest for such a new technology.

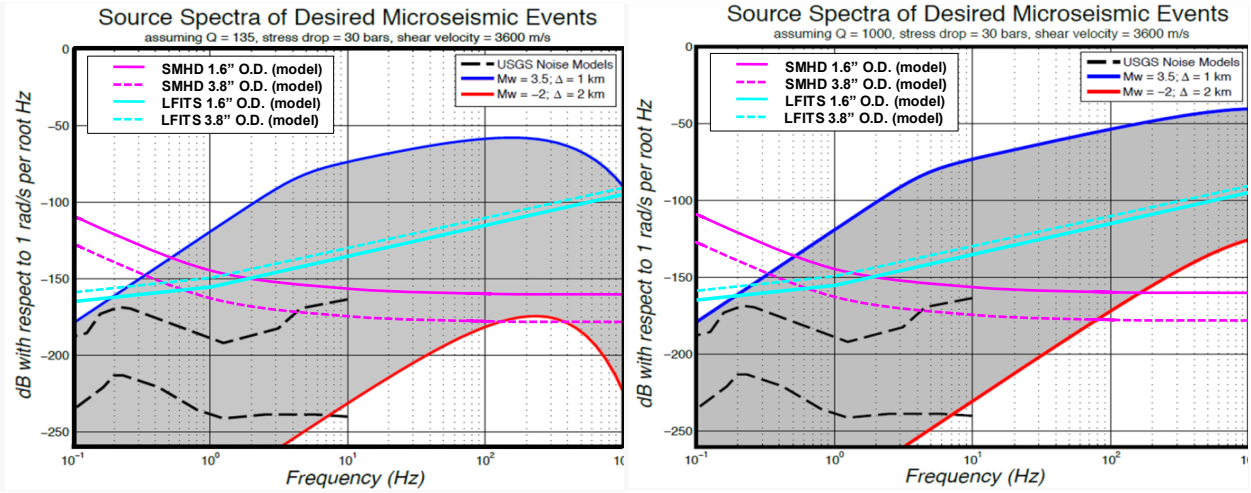

Figure 47. Modeled SMHD and LFITS Self Noise Overlain on Micro-Seismic Signal Plots

Bandwidth (KPP): The bandwidth goal specifies an upper limit of 1,000 Hz. Based on the brassboard, ATA believes it will be much more difficult to design an LFITS sensor that is rigid to high frequency. In addition, ATA is concerned at achieving the combination of adequate rotational sensitivity at high frequency while preventing sensitivity to cross-axis rotational motion and linear acceleration. This combination of concerns led to a yellow rating for the LFITS technology. In contrast, ATA's existing MHD-based sensors have been shown to operate at high frequencies with essentially no sensitivity to cross-axis rotation or linear acceleration. Thus, the related SMHD technology was rated green.

Dynamic Range (KPP): Modeling indicated that both sensors can be engineered for large dynamic range so both technologies are rated green and no clear winner is evident.

Size (KSA): As indicated in Section 3.1, the sensors are constrained to fit in a package suitable for hole-locked downhole deployment. Modeling indicated a sensor based on the LFITS technology was larger than the SMHD for the same approximate performance over the frequency band of interest. This creates a significant advantage for the SMHD. In addition, work with the brassboards indicates that there are considerable engineering challenges. Though promising work continues on the LFITS for another customer and application, the technology has too low a technology maturity to reliably achieve even the modeled sizes for a geothermal demonstration. Thus the SMHD was rated green and the LFITS given a yellow designation.

Operational Temperature (KSA): Analysis of the LFITS during modeling revealed challenges in identifying appropriate dielectric fluids for high-temperature operation. This and other residual engineering component and fabrication uncertainties earned LFITS a red rating. The SMHD was also rated yellow, but with far fewer concerns. ATA has built MHD-based sensors for more than

25 years and tested units up to 150°C without degrading their performance. During Phase 1, ATA performed a thorough assessment of each of the components of the high-temperature SMHD and demonstrated a test unit based on the proposed Galinstan sense element (see Section 3.3.1). As a result, the SMHD technology was considered much lower risk compared to LFITS.

Reliability (KSA): Reliability in the EGS environment depends primarily on the ability of the electronics to withstand high temperature. That means both that the electronic circuits have a long mean time to failure at high temperature and that the workmanship and manufacturing techniques are robust enough to prevent mechanical failure of solder joints, wiring connections, and liquid seals. As was noted in Section 3.3.3, the LFITS sensor would require many more electronic parts in the downhole device than the SMHD. In addition, the SMHD has intrinsic ruggedness due to a lack of moving parts aside from the sense fluid. Thus, although both technologies are rated yellow due to the need for additional qualification work, the SMHD's simplicity and toughness gives it the clear advantage.

Summary: ATA conducted a trade study to determine whether the LFITS or SMHD rotational sensing technology was more suitable for the EGS fracture monitoring application. The study considered performance as measured by resolution, bandwidth, and dynamic range plus the key attributes of size, operating temperature, and reliability. Based on this trade, ATA selected the SMHD technology for Phase 2 development.

The LFITS technology, while not recommended for further development under this grant, may have applications in a less constrained near-surface environment.

Looking forward to Phase 2, ATA projects that an SMHD-based rotational seismometer will fit the size constraints for a downhole instrument while meeting resolution, bandwidth, dynamic range, temperature range, and reliability requirements. In particular, the high sensitivity, technology maturity, simplicity, and ruggedness of the SMHD make it a good fit for the geothermal application.

3.7 DEVELOPMENT PLAN

Development planning integrates findings about the proposed technology with information about the geothermal application area, the associated markets, costs, and return on investment.

The Phase 1 investigations anchored the scientific theory, defined the required sensor capabilities, and determined the path to a 200°C downhole instrument. At the same time, ATA's commercial partner, Nanometrics, Inc., completed a market assessment and worked with ATA to identify obstacles to product development and market acceptance. Attachment F contains the market study, and this section summarizes the key findings that motivated Phase 2 planning.

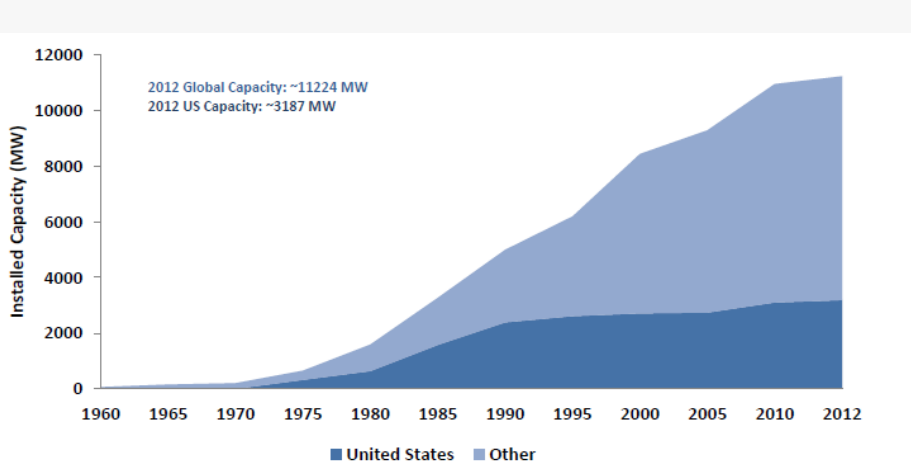

Figure 48. Geothermal Energy Capacity 1960-2012

The geothermal market is growing at approximately 8% per year with an estimated 4-6 new plants coming online per year in the U.S. and 8-12 plants coming online per year globally. **Figure 48** illustrates the recent growth in installed geothermal capacity both nationally and internationally.

Geothermal markets include low and high-temperature conventional extraction, and enhanced geothermal systems (EGS). Conventional extraction is growing but has limited downhole monitoring needs. The current grant is part of government investment in developing the EGS potential for substantially increasing geothermal generating capacity, and any resulting EGS sites will require downhole monitoring to understand the rock fracture structure. However, this market is five to ten years in the future. Near term interest will be limited to a few instruments for experimental or demonstration systems.

However, it should be noted that the microseismic studies required for geothermal fields are inherently similar to those required for shale oil and gas extraction, and the oil and gas microseismic monitoring market is 10 to 100 times larger than the geothermal monitoring market. The products and methods currently used for downhole monitoring are well-established in these markets with large companies such as Sercel and Schlumberger offering turnkey solutions. Any new instrument or 7-DOF method would need to demonstrate a clear competitive advantage over existing instruments and methods.

Competitive advantage for the new technology could be either cost saving or critical new knowledge. Since drilling wells is expensive ($1M - $2M per well), the 7-DOF seismometer will have a compelling advantage if it can demonstrate that it requires fewer installations and

fewer observation wells to locate micro-seismic events. The results to date are suggestive, but the science is still preliminary. Additional scientific studies and downhole demonstrations are required to establish the technology.

In addition, there are other barriers to market entry that must be overcome. The market study identified seven barriers, or requirements for market entry, summarized in **Table 12**. The ATA Team has established a corresponding approach to overcome each barrier. Some of the approaches are already underway, like replacing mercury as the SMHD rotational sensor fluid (Section 3.3.1 and 3.5.3) or teaming with a research organization (Sandia National Laboratories) for initial processing software and publication of results to the scientific community. Other elements of the approach motivate the Phase 2 plan (Section 5.0).

Table 12. Requirements for Market Entry and Associated Phase 2 Approach

Requirements for Market Entry	ATA Team Approach
(1) Acceptance of rotational sensor by scientific community	Engage the geophysical scientific community, particularly opinion setters, in testing the product and publishing results
(2) Processing and analysis software capable of handling rotational data	Team with a research organization to write processing software and then transition algorithms to a commercial partner
(3) Ability to sell sensor globally	Ensure instrument is not subject to U.S. Dept. of Commerce International Traffic in Arms Regulations (ITAR) restrictions
(4) Ability to deliver a turn-key solution	Offer a turn-key solution, preferably through a known provider
(5) Operational evidence of outperforming translational-only solutions	Team with a geothermal site operator for a demonstration project; publish papers comparing performance to translational sensors
(6) Reliability of the sensor	Design for robustness and rigorously test prototypes; establish manufacturing capability for high reliability
(7) Non-toxic sensing element	Eliminate mercury from the sensing element

To summarize, although there is a long-term potential for 7-DOF downhole seismometry in the geothermal industry (and other markets), there are also several barriers to market entry that must be overcome. The near-term geothermal market is too small to attract investment by a sensor manufacturing company, and Nanometrics, Inc. will withdraw from Phase 2 of this effort. The ATA and Sandia National Laboratories team will focus Phase 2 on developing a scientific grade downhole instrument to demonstrate and validate the technology, establish its cost advantages, and garner wider acceptance of rotational-enabled seismometry in the geothermal community.

3.8 Summary of Technical Discussions

Phase 1 demonstrated that ATA's SMHD rotational sensing technology enables a viable, low-risk development path for a rotational seismometer that matches the requirements for monitoring of micro-seismic events. The key specifications have been identified and the science confirms the expected advantage of adding rotational measurements to traditional seismometry. In addition, ATA identified the key electronic and sensor components for integration of a 7-DOF seismic measurement tool.

During Phase 1, ATA built brassboards of the two candidate rotational sensor technologies and compared modeled and measured results for both technologies. Rotational sensors were deployed for field data collection of rotational seismic signals, resulting in publication of scientific results. Combining the results of modeling, test, and analysis, ATA performed a trade study that selected the SMHD technology for Phase 2 development.

Finally, the ATA Team conducted a market assessment that identified barriers to market entry for the new technology. ATA has adjusted its Phase 2 plans to address the market need for a scientific-grade downhole instrument that allows early validation of the technology, establishes its cost advantages, and garners wider acceptance of rotational-enabled seismometry.

All work to date suggests that rotational seismometry provides additional information content that can potentially lower the number of deployed instruments and drilled holes needed for characterization of a fracture field, lowering cost of enhanced geothermal development. The prospects for Phase 2 development and subsequent demonstration of the technology look promising.

4.0 BUDGET PERFORMANCE

The Phase 1 program performed to budget, maintaining cost to plan. Neither funding delays at the outset nor staffing availability delays upon execution created any cost escalation

4.1 ORIGINAL CONTRACT NEGOTIATIONS

The grant contract was awarded in September 2011 with a one-year period of performance. However, negotiations on the total budget and the program plan were held through April 2012, including a government requested de-scope followed by a return to original full scope, at which point the plan was approved. When funds were released, the period of performance was extended through April 2013 to accommodate the start delays. At that time, the Phase 1 tasks and budgets were as shown in **Table 13**.

Table 13. Original Budget – April 2012

TASK NUMBER	TASK TITLE	PLANNED START DATE	PLANNED END DATE	BUDGET
1	Elicit Detailed Requirements	9/30/2011	10/31/2012	$127,098
2	Establish High Temperature Components	7/2/2012	10/31/2012	$126,059
3	Model Sensor Technology	8/9/2012	12/10/2012	$61,361
4	Rotational Sensing Proof-of-Concept	9/20/2012	3/27/2013	$226,370
5	Trade and Down-Select	9/3/2012	4/10/2013	$35,277
6	Solidify Initial Development Plans	9/20/2012	4/23/2013	$86,961
7	Document and Publish	5/7/2012	4/25/2013	$86,637
				$749,763

4.2 ADDITIONAL START DELAY

The late start due to extended contract negotiations disrupted original staffing plans, resulting in unavailability of key staff until October 2012. At that date, the program was re-planned to maintain cost and schedule, and execution began in earnest. In **Table 14**, the re-planned budgets show modifications to the "Budget" column and "Planned End Dates." ATA executed to this plan for the remainder of Phase 1 until Final Report preparations.

Table 14. Replanned Budget – October 2012

TASK NUMBER	TASK TITLE	PLANNED START DATE	PLANNED END DATE	BUDGET
1	Elicit Detailed Requirements	9/30/2011	11/30/2012	$141,982
2	Establish High Temperature Components	7/2/2012	10/16/2012	$54,554
3	Model Sensor Technology	8/9/2012	11/22/2012	$95,805
4	Rotational Sensing Proof-of-Concept	9/20/2012	3/27/2013	$164,117
5	Trade and Down-Select	9/3/2012	4/10/2013	$127,473
6	Solidify Initial Development Plans	9/20/2012	4/25/2013	$118,250
7	Document and Publish	5/7/2012	4/18/2013	$42,757
				$744,938

4.3 NO COST EXTENSION

In April 2013, ATA requested a no-cost extension (NCE) to the Phase 1 period of performance to allow completion of the Final Report. This was granted in June 2013, extending the Phase 1

period of performance through October 31, 2013. Budgets were not replanned at this point; however program execution did extend past the original end dates.

4.4 Final Performance to Budget

The Phase 1 activities conclude with the delivery of this Final Report. The final allocation of costs by task is shown in **Table 15**. High temperature component investigations, sensor modeling, and documentation (Tasks 2, 3, and 7) executed close to plan. Requirements elicitation (Task 1) ran under budget since it was pursued only to the point of establishing the fundamentals needed for trade studies between the two competing technologies. The critical task of developing and testing the rotational sensor brassboards (Task 4) ran well above budget. The additional efforts in both lab testing and field data collection were deemed critical to enabling a meaningful trade between the technologies and down-selection for Phase 2. Given the extensive brassboard results, the down-select itself (Task 5) was simplified and under-ran its budget. Similarly, as early market analysis results began to indicate that emphasis should be shifted towards a science grade instrument, ATA reduced costs allocated toward commercial development planning (Task 6). As a result, ATA was able to accomplish the SOPO goals and stay within budget by balancing funds and level of effort between tasks.

Table 15. Final Phase 1 Actual Performance to Budget

Task Number	Task Title	Budget	Final Actuals
1	Elicit Detailed Requirements	$141,982	$88,771
2	Establish High Temperature Components	$54,554	$53,670
3	Model Sensor Technology	$95,805	$97,573
4	Rotational Sensing Proof-of-Concept	$164,117	$349,975
5	Trade and Down-Select	$127,473	$34,200
6	Solidify Initial Development Plans	$118,250	$82,817
7	Document and Publish	$47,582	$42,757
		$749,763	$749,763

In summary, despite the delays at the start and the end of the program, all of the Phase 1 SOPO objectives and tasks were successfully completed within the total original budget.

5.0 PHASE 2 PLAN

5.1 PROGRAM PLAN

The results of the Phase 1 activities, particularly the identification of the limited size of the near-term geothermal market for a commercial 7-DOF Rotation Enabled Seismometer, resulted in the ATA Team's commercialization partner, Nanometrics, Inc., withdrawing from participation in Phase 2. While Nanometrics believes the geothermal market has great future potential, they did not see enough sales in the next 5-10 years to justify their investment in the program at this time.

Furthermore, after formal and informal interactions with the geothermal community, ATA concluded that there is still foundational scientific work to be done to demonstrate the value that rotational measurements can add to traditional linear seismic measurements. To this end, ATA proposes modifying the Phase 2 plan to work with Sandia National Laboratories on a scientific grade downhole instrument and the data processing to validate its utility. This revised plan better meets the original TRL 5 target for the technology, leaving additional production engineering efforts to a future stage of development.

In Phase 2, ATA will continue development of the crucial rotational sensor technology and its integration into a 7-DOF tool. Sandia National Laboratories has an existing downhole package suitable for demonstrating the 7-DOF Rotation Enabled Seismometer. Some seismic signal sensitivity is lost with smaller size, but, on the other hand, the instrument requires a smaller observation well. While it is not a commercial product, the Sandia package is already designed for high temperature operation, and so the effort that would have been required to migrate Nanometrics' Trillium instrument to high temperature capability will not be required.

ATA has reformulated the Phase 2 plan that follows, decreasing both scope and requested funding to focus on developing and demonstrating a scientific grade downhole instrument. The new plan has two major sub-phases: (1) developing and building the rotational seismometers capable of high-temperature operation, and (2) integrating the rotational seismometers with available linear sensors, pressure sensors and processing to create a downhole package that can validate the technology's utility in geothermal applications.

The re-scoped Phase 2 includes further development of rotational seismic signal processing and benchmarking of the processing with field data obtained by deployment of either the rotational sensors or the integrated instrument package. Environmental permitting issues are now minimal and well within the resources of Phase 2. The sensor itself is environmentally benign (due to Phase 1 efforts to investigate replacement of the mercury sense element), and the proposed deployment is to field sites that already have the infrastructure, permitting, site access, and environmental approvals in place for downhole data collection.

The revised Phase 2 tasks follow.

Task 8: Design Seismic MHD (SMHD) Sensor: ATA will develop the design for a rotational seismic sensor based on the SMHD technology characterized in Phase 1. The task will include initial risk reduction activities, modeling and simulation, and trades over design parameters culminating in preliminary and critical design reviews. The sensor will be designed to fit into Sandia National Laboratories' downhole instrument and be able to operate at 200^{o}C.

Task 9: Build and Characterize SMHD Sensor Prototypes: ATA will build multiple units of the SMHD sensor designed in Task 8 and characterize their performance relative to the models developed in Task 8. This task includes iterative development of pre-prototypes built in parallel with the design phase. After the final design review, ATA will build a batch of SMHD units sufficient to support characterization testing, development of a 7-DOF package in Task 12 and other opportunistic data collections per Task 13.

Task 10: Modify Sandia's Downhole Tool Package: Sandia National Laboratories will make design modifications to their existing downhole package to accommodate the sensors required for the Rotation Enabled Seismometer. This work will include mechanical, electrical and data acquisition enhancements.

Task 11: Develop Downhole Instrument Package: ATA will design the packaging for the integrated sensor suite such that it will fit into Sandia's downhole tool but can also be used standalone in surface applications. The initial instrument may be 6-DOF (three axes each of rotational and linear motion measurement) rather than 7-DOF (with pressure sensors) since the theory and analysis to date show highest value in combining linear and rotational signals. Engineering complexity, cost and risk for incorporating the pressure sensor will be traded against signal value. Either ATA or Sandia National Laboratories will acquire appropriate high temperature linear and pressure sensors depending on cost effectiveness and ATA and Sandia will jointly integrate and checkout the 6-DOF or 7-DOF sensor package. An initial mock-up using less expensive low-temperature linear sensors is anticipated which can also support opportunistic data collections per Task 13

Task 12: Integrate and Test 6-DOF/7-DOF Downhole Instrument: ATA will coordinate with Sandia National Laboratories to install the 6-DOF/7-DOF Sensor package into the downhole package and test it at Sandia's downhole test facilities. Data will be collected and analyzed to assess the value that rotational measurements provide in understanding microseismic events. Sandia will manage all permits and other regulatory requirements associated with these activities at existing test sites.

Task 13: Develop Rotational Seismic Processing: Sandia National Laboratories and ATA will continue development and implementation of processing algorithms that take advantage of rotational seismic signals. Where possible, ATA and Sandia National Laboratories will seek opportunities to obtain rotational seismic data to validate these processing algorithms through collaborative deployment of the rotational sensor prototypes, the sensor package, or the downhole tool at existing test sites. Operators of the existing installations will manage all permits and other regulatory requirements associated with these activities.

Task 14: Document and Publish Results: ATA will develop and present analyses, technical papers and/or presentations summarizing the Phase 2 results. Sandia National Laboratories will take a strong role in results analysis and interpretation. ATA will produce the Final Technical Report.

5.2 Financial Plan

Due to the revision of Phase 2 tasks described in preceding paragraphs, ATA is proposing a smaller total value for the Phase 2 effort than originally proposed. Our revised Phase 2 budget is shown in **Table 16**. Budget period 1 was Phase 1. Budget period 2 is Phase 2.

Table 16. Revised Phase 2 Budget

Budget Period	DOE Cost Share ATA (left) and FFRDC (right)		Recipient Cost Share ($ / %)	Total Estimated Costs
1 of 2	$599,812 / 52%	$400,000 / 35%	$149,953 / 13%	$1,149,765
2 of 2	$1,062,000 / 65%	$250,000 / 15%	$328,000 / 20%	$1,640,000
Total Project	**$1,661,812**	**$650,000**	**$477,953**	**$2,789,765**

ATA will provide all required supporting documents (Detailed Budget spreadsheet, modified Statement of Project Objectives, and environmental form EQ1) to the DOE as needed to support budget review for Phase 2 approval.

5.3 Phase 2 Summary

The revised Phase 2 plan reduces scope and lowers cost to the government by focusing on development of science-grade downhole instrumentation. At the end of Phase 2, ATA will have developed both a set of prototypes of the enabling SMHD rotational seismometer as well as an integrated tool for downhole seismic data collection in hot downhole geothermal applications. In addition, ATA and Sandia National Laboratories will continue to work together to collect, analyze, and publish data and processing methods demonstrating the utility of 7-DOF rotational-enabled seismometry in relation to geothermal site monitoring and characterization.

ATTACHMENT A: DRAFT SPECIFICATION NOTES FOR A 7-DOF SEISMOMETER

Document Description:	Document Number:	Applied Technology Associates
Draft Specification Notes for a 7-DOF Seismometer	0260000017	
Model:	**CAGE Code:**	Albuquerque, New Mexico
7-DOF Seismometer	6M566	

Draft Specification Notes for a 7-DOF Seismometer

Rev.	ECO #	Description	Date	Approved
A	1205	Original Release	10/10/2013	B. Pierson

APPROVALS	
PRINCIPAL INVESTIGATOR: Darren Laughlin	**Date:** 10/10/2013
PROGRAM MANAGER: Bob Pierson	**Date:** 10/10/2013
QUALITY MANAGER: Trish Kiker	**Date:** 10/10/2013

Table of Contents

List of Figures

1.0 SCOPE

Essentially all seismic measurements are currently acquired using linear seismometers and pressure sensors. Rotation is often calculated using the linear sensors but it is widely accepted that direct rotational measurements would provide additional information and utility. However, to date, no suitable rotational sensor has been developed. The purpose of this program is to define and demonstrate a 7-degree of freedom (7-DOF) motion measurement system (three linear sensors, three rotational sensors, plus pressure) designed for geothermal environments. This document defines the instrument proposed by Applied Technology Associates (ATA), Sandia National Laboratory (SNL), and Nanometrics for the Department of Energy. This specification attempts to capture the key requirements for the final downhole sensor suite. The Phase 1 effort will produce two candidate instruments; a Seismic MagnetoHydroDynamic angular rate sensor (SMHD) (similar to ATA's ARS-24 but specifically designed only for down-hole seismic measurements) and a Low-Frequency Improved Torsional Seismometer (LFITS) based on a capacitive sensing approach. These angular sensors will be performance tested in laboratory conditions. After a trade study, it is planned in Phase 2 for the angular sensor best suited for this application to be upgraded to include high-temperature electronics and materials and then be combined with high-temperature geophones and a pressure sensor to create a 7-DOF sensor package for monitoring downhole geothermal environments. Opportunities will be sought to make in-situ measurements with the prototype unit.

In addition to defining basic performance requirements, this specification attempts to recognize fundamental constraints that would define the path forward. For example, the sensors must be small enough to fit inside the geothermal borehole or a complete redesign would be required. Similarly, high-temperature electronics and materials availability must be considered to ensure that there is a path to the Phase 2 design.

2.0 REFERENCES

2.1 Customer Documents

2.1.1 DE-EE0005511/001 Attachment 2, Statement of Project Objectives

2.2 ATA Documents

2.2.1 "Seismological Magneto-Hydrodynamic (SMHD) Sensor High-Temperature Materials Analysis"

3.0 DEFINITIONS

3.1 None

4.0 UNIT DEFINITION

4.1 INTERFACE REQUIREMENTS (Entire 7-DOF sensor package)

4.1.1 Electrical Interfaces

Baseline Nanometric's Trillium downhole tool for all unspecified electrical and signal interfaces. Unspecified items are retained for completeness and traceability to full specification in Phase 2, but the currently unspecified items do not impact Phase 1 trade study analyses.

4.1.2 Power Interface

4.1.2.1 Normal Voltage Range

Input voltage range shall be 9 – 36 VDC.

4.1.2.2 Input Power Ripple

Power ripple shall be less than 10 mV 0-P.

4.1.2.3 Input Source Impedance

Baseline Nanometric's downhole instrument

4.1.2.4 Input Signal Definition

Baseline Nanometric's downhole instrument

4.1.2.5 Output Interfaces

Baseline Nanometric's downhole instrument

4.1.2.6 Output Signal Definition

Baseline Nanometric's downhole instrument

4.1.3 Command and Data Handling Interface

4.1.3.1 Discrete Command Inputs

Baseline Nanometric's downhole instrument

4.1.3.2 Discrete Command Outputs

Baseline Nanometric's downhole instrument

4.1.3.3 Serial Command/Telemetry Interfaces

Baseline Nanometric's downhole instrument

4.1.4 Software/Programming Interface

Baseline Nanometric's downhole instrument

4.1.5 Test Interfaces

Baseline Nanometric's downhole instrument

4.2 Mechanical Interfaces

The existing Nanometrics Trillium downhole tool is shown in Figure 1. The instrument housing (left) is easily reconfigured to accept additional instruments as necessary.

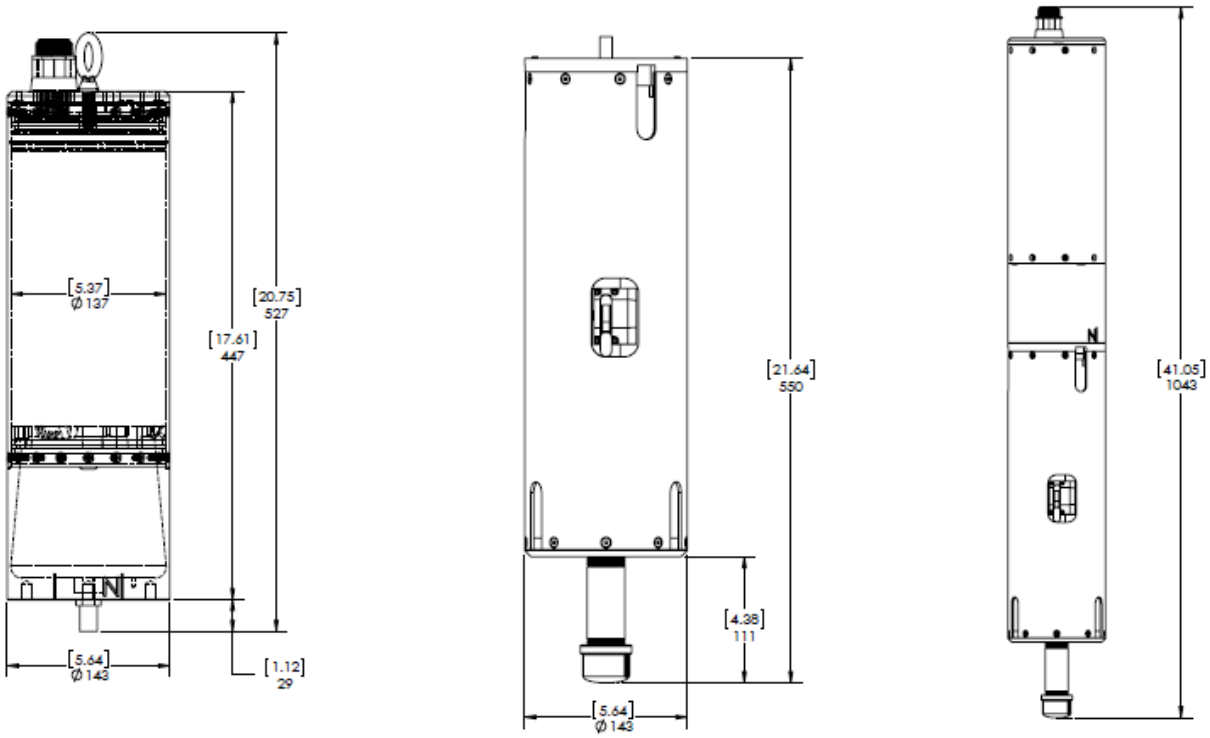

Figure 1. Nanometric's Wireline Tool Dimensions

4.3 Thermal Interfaces

The goal is for the instrument to be able to operate continuously at 200ºC. See Section 7.1 for a description of the thermal environment.

5.0 CHARACTERISTICS

5.1 Operating Requirements

The sensor package should be able to operate normally when tilted up to 90^{o} from vertical.

The 7-DoF sensor package should begin to generate signals within 1 second of power up. The sensor package should reach the ambient temperature within 12 hours of engaging the hole lock mechanism.

Ideally, the sensor package azimuth orientation relative to true north should be known to less than 1 degree.

The sensor package will be housed as shown in section 5.2. Sensors must be mounted sufficiently rigidly to enable 1,000 Hz measurements. The hole lock mechanism must be able to transmit 1,000 Hz motion to the sensors without introducing structural resonance effects.

5.2 Performance Requirements

5.2.1 Motion Environment

5.2.1.1 Rotational Motion

The expected rotational velocity motion is shown in Figure 2 below. The range shown in the shaded area is bounded by the minimum (red) and maximum (blue) expected motion. The minimum motion curve was defined as the smallest event magnitude of interest, Mw = -2, with the maximum expected separation from the event to the instrument, 2 km. The maximum motion curve was defined as the largest expected event magnitude, Mw = +3.5, with the minimum expected separation from the event to the instrument, 1 km. Cases are shown for two different values of Q. The motion is expected to be closer to the estimate with Q = 135 but could be higher if the rock is unexpectedly rigid. See Section 7.2 for a more thorough description of the environments.

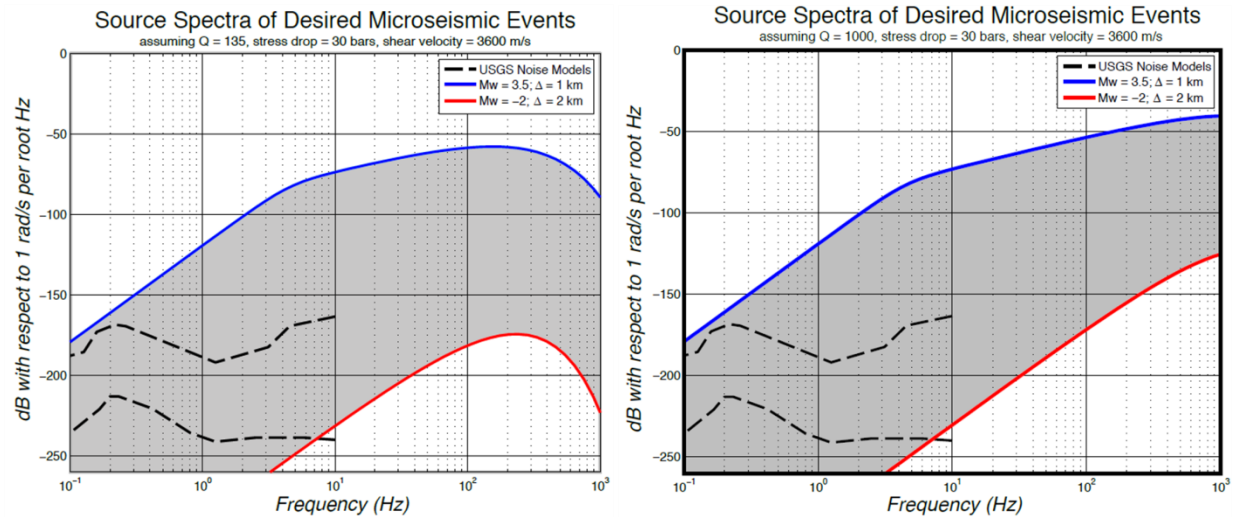

Figure 2. Predicted Rotational Velocity Envelope

5.2.1.2 Linear Motion

The expected linear motion is shown in Figure 3 below. Cases are shown for two different values of Q. Similar to the rotational motion estimates, the minimum motion of interest and the maximum expected motion bound the shaded region of the plots. The motion is expected to be closer to the estimate with Q = 100 but could be higher if the rock is unexpectedly rigid. See Section 7.2 for a more thorough description of the environments.

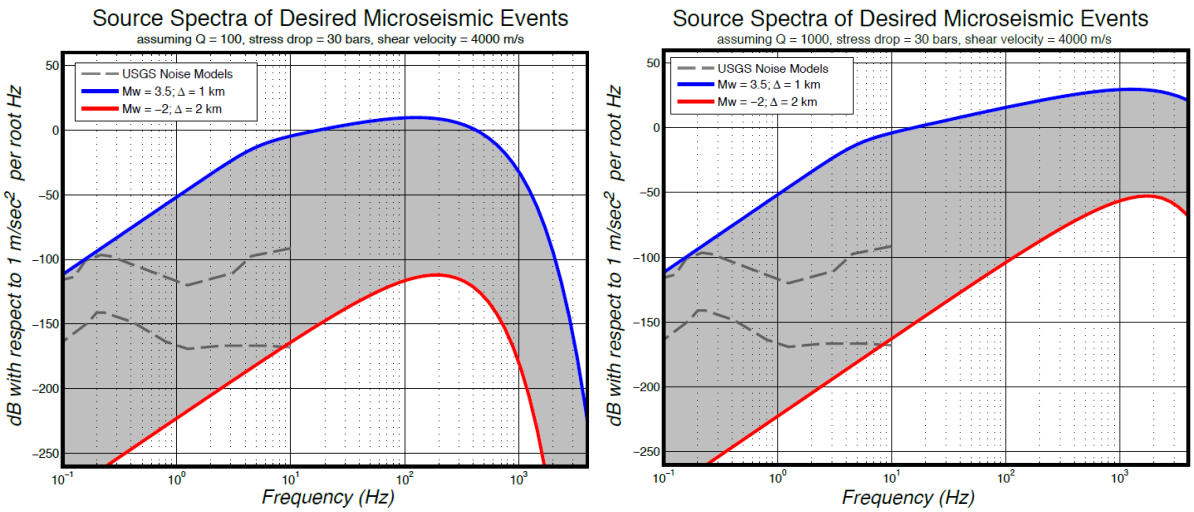

Figure 3. Predicted Linear Acceleration Envelope

5.2.1.3 Pressure

The expected pressures to be measured are shown in Figure 4 below. Cases are shown for two different values of Q for minimum and maximum ranges. The pressure is expected to be closer to the estimate with Q = 100 but could be higher if the rock is unexpectedly rigid. The pressure is measured in the center of a fluid filled borehole. See Section 7.3 for a more thorough description of the environments.

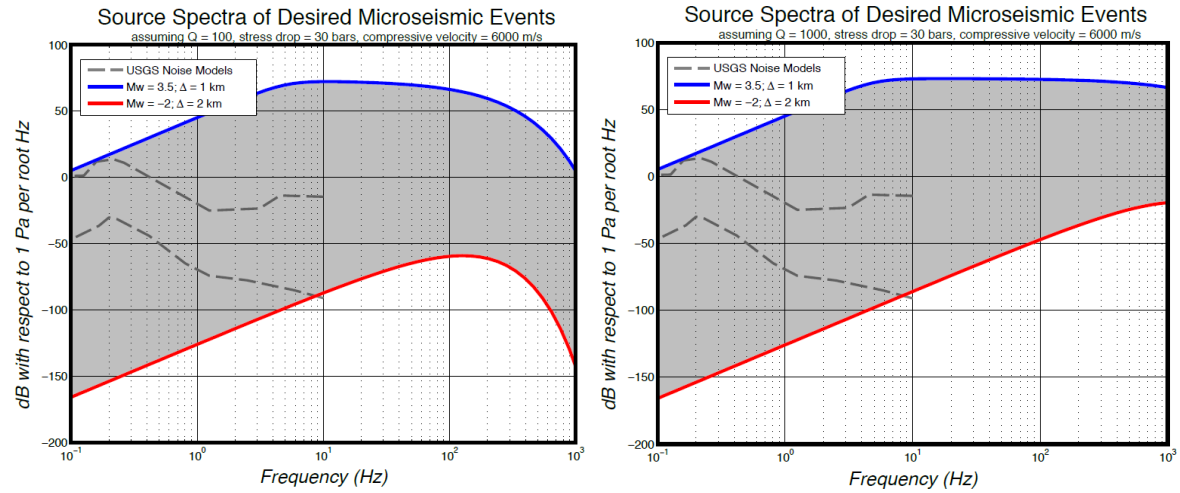

Figure 4. Predicted Fluid Pressure Envelope

5.3 Testability Requirements

The sensor shall be able to operate in any orientation. This will allow tests to be conducted with a vertical or horizontal sense axis.

6.0 PHYSICAL REQUIREMENTS

6.1 Mass Properties

Constrain based on Nanometric's downhole instrument

6.2 Dimensional Requirements

Constrain based on Nanometric's downhole instrument

6.3 Mounting Requirements

Constrain based on Nanometric's downhole instrument

6.4 Connector Requirements

Constrain based on Nanometric's downhole instrument

6.5 Unit Marking Requirements

Not currently specified

7.0 Environment

7.1 Thermal Environment

The 7-DOF sensor package will be designed to measure the motion, temperature, and pressure environment in geothermal monitoring bore holes. The downhole environment is extremely harsh with temperatures upwards of 400ºC, depending on the depth and location of the borehole. The 7-DOF instrument is not expected to operate up to the maximum temperature but rather will be located at a depth in the borehole that corresponds to temperatures up to 200ºC. For reference, a cross section of part of the Calpine Geysers facility is shown in Figure 5 below.

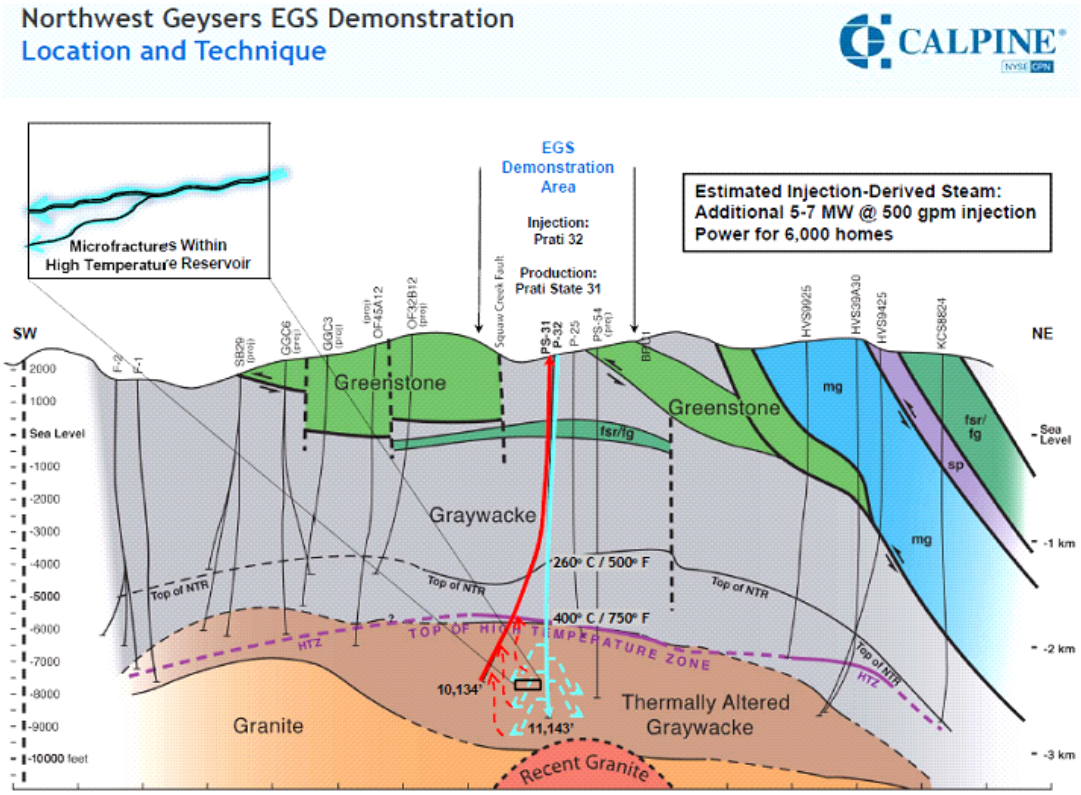

Figure 5. Cross section of a Calpine Geysers Geothermal Well Site

7.2 Motion Environment

The downhole geothermal motion environment has never been fully measured because a sensor suite has not existed heretofore. This is particularly true for rotational motions. A number of factors have been modeled to estimate and bound the expected range of motion that a 7-DOF geothermal monitoring sensor system might encounter.

Motions are highly dependent on the amplification factor, Q, for the material between the fracture and the sensor package location. More rigid and undamaged rock will produce higher values of Q. The lower the Q, the more attenuation the seismic wave will exhibit as it passes through the rock. Estimates of Q for the Fenton Hill geothermal site near Los Alamos, NM were above 1000. Estimates of Q for the Geysers geothermal facility are in the range of 100 to 200. A plot showing the effect of Q on motion magnitude is shown in Figure 6. The dashed lines on the plot show approximations of the USGS's New Low Noise Model (NLNM) and New High Noise Model (NHNM) converted to rotation.

Another factor required to estimate the expected motion environment is the shear wave propagation velocity. More rigid and undamaged rock will transmit waves at higher velocity. Many other factors such as porosity, fluid content and type, etc. also affect wave velocity. Changes in the rotation PSD with respect to shear wave velocity is shown in Figure 6. Though there is some change in frequency and rotational magnitude the effect is clearly less than the effect of Q.

Obviously, the magnitude and frequency of the measured shear wave rotations will vary with event equivalent earthquake magnitude and distance from the fracture to the instrument. Those relationships are shown in Figure 7.

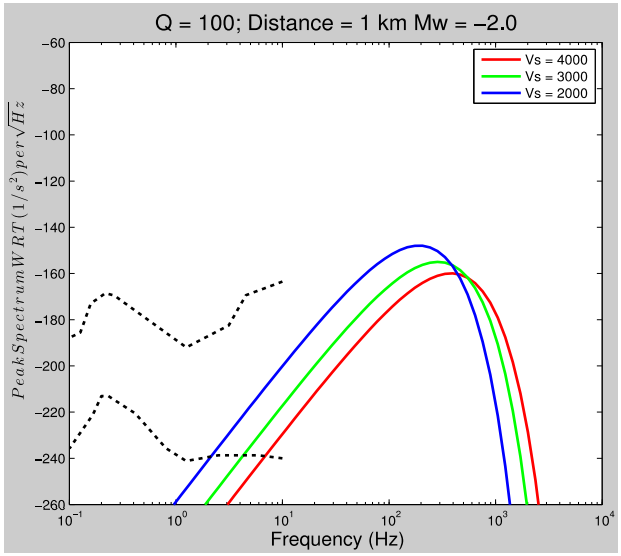

Figure 6. Effect of Changes in Attenuation, Q, (left) and Wave Velocity (right)

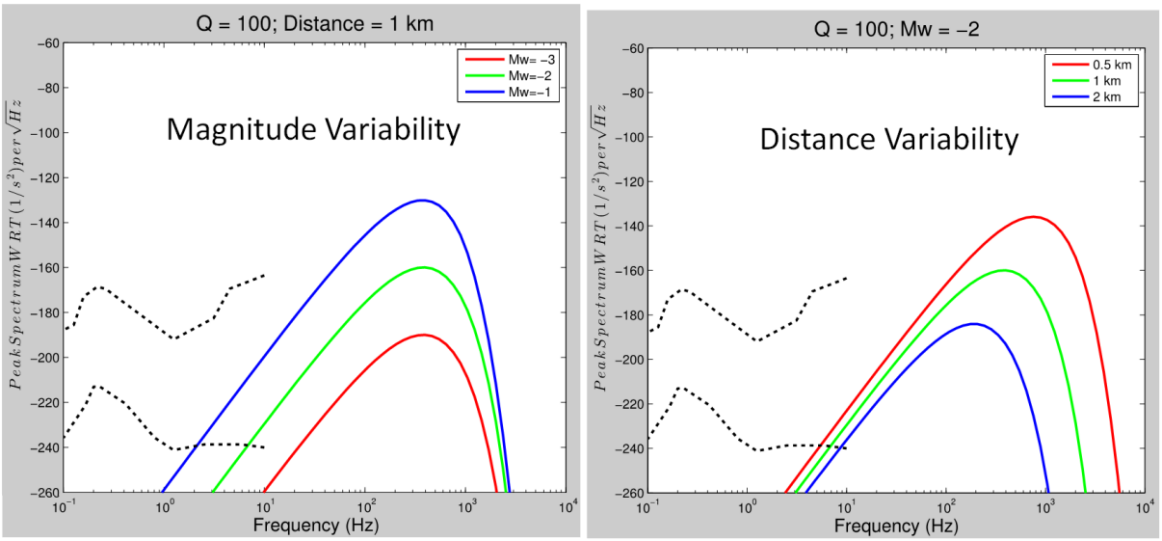

Figure 7. Effect of Earthquake Magnitude (left) and Distance to the Earthquake (right)

To bound the estimates of rotational motion expected in geothermal environments values were chosen for each of the parameters above and the maximum and minimum motion levels were plotted to display the expected PSD range. Earthquakes smaller than -2 are of less concern and the maximum measured earthquake shown in a recent Calpine presentation at The Geysers was 3.16. Bounding magnitudes were chosen as -2 < Mw < +3.5. Shear wave velocity variations do not affect the rotation PSD significantly in these conditions so a standard velocity of 4000 m/s was chosen. At these depths and material conditions it is unlikely that Q will be less than 100 and the Fenton Hill extreme of Q = 1000 was chosen as the maximum. Referring to Figure 5 above, it is expected that most of the

fractures will occur in the Thermally-Altered Graywacke but the instrument will be only about halfway down the well to limit the operating temperature and so will be between 1 and 2 km distant from the fracture events. Combining the high magnitude and minimal distance will cause maximum motion. Minimum magnitude with maximum distance produces the minimum motion. For clarity, two plots are presented that show the maximum and minimum motion with two different values of Q in Figure 8. The expected motion should fall between the two curves.

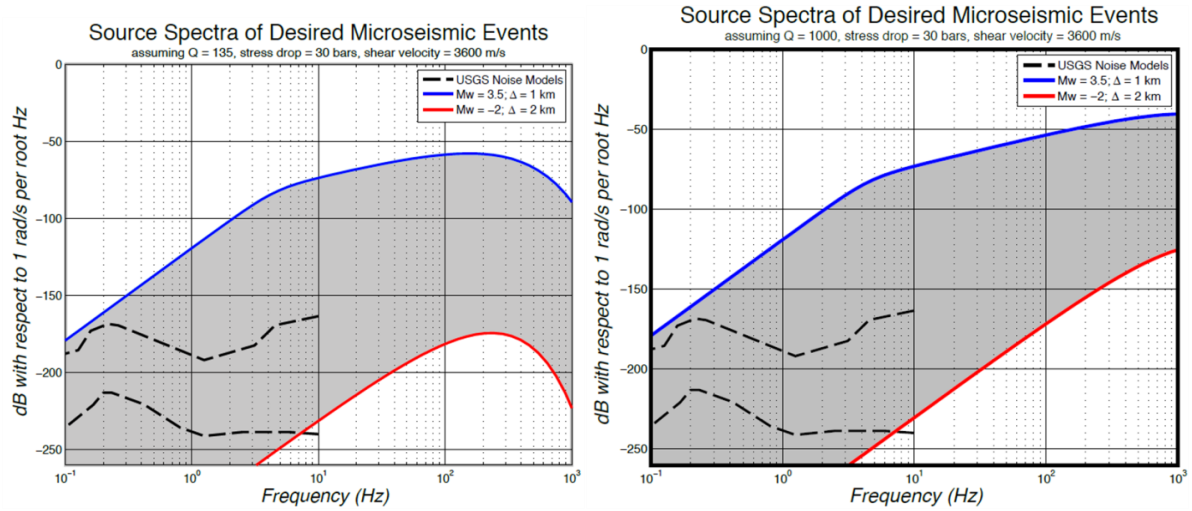

Figure 8. Predicted Rotational Velocity Envelope

Likewise, estimates have been made for linear acceleration expected at the 7-DOF sensor package. As with the rotational motion estimates, limits of high and low Q are shown in two plots in Figure 9 and absolute magnitude of the fracture event and distance from the event define the range of predicted linear accelerations.

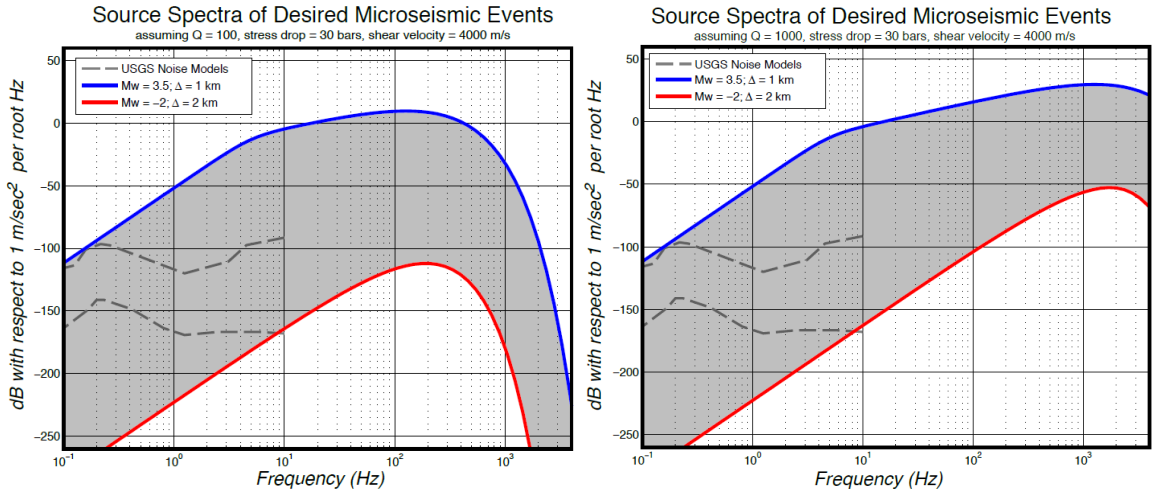

Figure 9. Predicted Linear Acceleration Envelope

7.3 Pressure Environment

The seventh degree of freedom is the dynamic pressure measured in the fluid-filled borehole as the pressure wave passes through the sensor location. The estimates shown in Figure 10 are for measurements at the cylindrical center of the borehole for a low and high value of Q. In a similar fashion as the linear and rotational measurements, the estimated pressure envelopes are defined for magnitudes -2 < Mw < 3.5 and distances from 1 to 2 kilometers from the fracture.

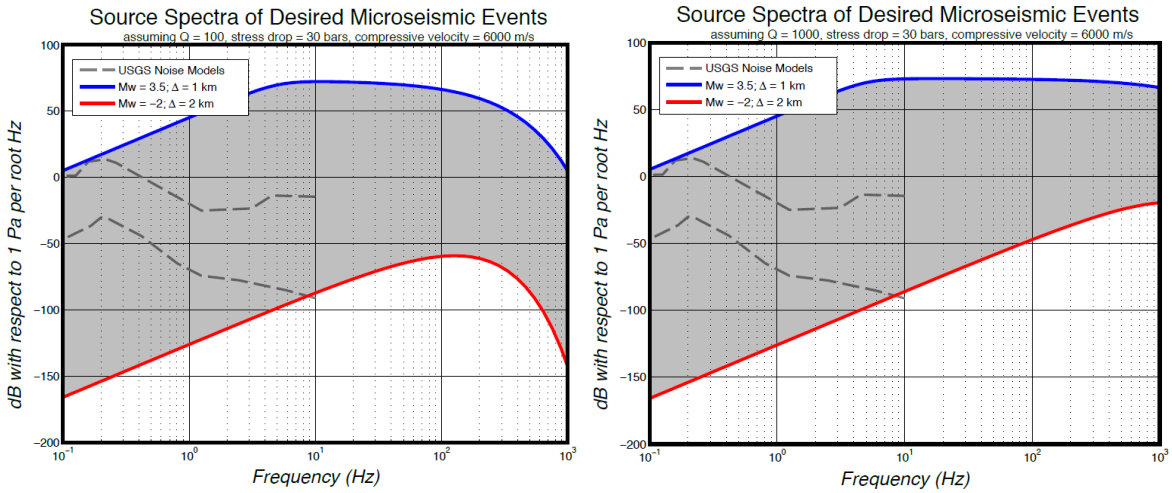

Figure 10. Predicted Fluid Pressure Envelope

ATTACHMENT B: EVALUATIONS OF ARS ROTATIONAL SEISMIC SENSORS

SANDIA REPORT
SAND2013-3674
Official Use Only ● Privileged Information
Printed May 2013

Evaluation of ARS16 and ARS24 Rotational Seismic Sensor Designed by Applied Technology Associates

Darren M. Hart
Bion John Merchant
Robert E. Abbott

Prepared by
Sandia National Laboratories
Albuquerque, New Mexico 87185 and Livermore, California 94550

Sandia National Laboratories is a multi-program laboratory managed and operated by Sandia Corporation, a wholly owned subsidiary of Lockheed Martin Corporation, for the U.S. Department of Energy's National Nuclear Security Administration under contract DE-AC04-94AL85000.

Issued by Sandia National Laboratories, operated for the United States Department of Energy by Sandia Corporation.

SAND2013-3674
Official Use Only – Privileged Information
May 2013

Evaluation of ARS16 and ARS24 Rotational Seismic Sensor Designed by Applied Technology Associates

Darren M. Hart, B. John Merchant and Robert E. Abbott
Ground-based Monitoring R and E
Sandia National Laboratories
P.O. Box 5800
Albuquerque, New Mexico 87185-0404

Abstract

Sandia National Laboratories has evaluated two rotational seismic sensor designs provided by Applied Technology Associates (ATA). The purpose of the rotational seismic sensor evaluation was to confirm sensitivity, transfer function, power, self-noise, full-scale, and dynamic range and to comment on any issues encountered during the evaluation. The test results included in this report were in response to tonal input signals. Whenever possible test methodologies used were based on IEEE Standards 1057 for Digitizing Waveform Recorders and 1241 for Analog to Digital Converters.

Table of Contents

1 EVALUATION SUMMARY

1.1 Applied Technology Associates: ARS16 Rotation Rate Sensor

Static Performance:

The isolation noise test showed the three transducers were well matched in self-noise levels. All three sensor had a noise floor at 10 Hz of -132 dB relative to one (radian/second)^2/Hz. The RMS noise of the three sensors for the 1-300 Hz passband were 10.80 µrad/s for ARS16z, 11.28 µrad/s for ARS16y and 15.41 µrad/s for ARS16x. The associated dynamic ranges for the same passband are 62.7 dB ARS16z, 62.3 dB for ARS16y and 59.6 dB for ARS16x.

Tonal Dynamic Performance:

The 1 Hz linearity test showed stability in sensitivity for rotation rates of 0.14 to 24.4 radians/second. The 4 Hz linearity test showed stability in sensitivity for rotation rates of 0.14 to 17.4 radians/second. The 16 Hz linearity test showed stability in sensitivity for rotation rates of 0.14 to 14.0 radians/second.

Broadband Dynamic Performance:

The sensor passband was confirmed to be 0.1 to 60 Hz, below 2 Hz both amplitude and phase mismatch exists relative to the FOG reference sensor. The ARS16 sensors were well phase-matched, showing less than 0.5 degrees variance, for the 0.1 to 60 Hz passband.

1.2 Applied Technology Associates: ARS24 Rotation Rate Sensor

Static Performance:

The ARS24z sensor had a noise floor at 10 Hz of -152 dB relative to one (radian/second)^2/Hz. The RMS noise of the 1 to 300 Hz passband was 3.12 µrad/s. The associated dynamic range for the same passband is 61.5 dB.

Tonal Dynamic Performance:

The 1 Hz linearity test showed stability in sensitivity for rotation rates of 0.14 to 6.12 radians/second. The 4 Hz linearity test showed stability in sensitivity for rotation rates of 0.14 to 6.14 radians/second. The 16 Hz linearity test showed stability in sensitivity for rotation rates of 0.14 to 5.14 radians/second.

Broadband Dynamic Performance:

The sensor passband was confirmed to be 0.1 to 60 Hz, below 2 Hz both amplitude and phase mismatch exists relative to the FOG reference sensor.

2 TESTING OVERVIEW

2.1 Objectives

The objective of this work was to evaluate technical specifications of two ATA supplied sensors. Basic sensor characterization includes determining sensitivity, linearity across a range of rotation inputs, self-noise, full-scale, dynamic range, verify nominal transfer function and cross-axis sensitivity.

2.2 Test and Evaluation Background

Sandia National Laboratories (SNL), Ground-based Monitoring R&E Department has the long-standing capability of evaluating the performance of sensors for geophysical applications.

2.3 Standardization/Traceability

Most tests are based on the Institute of Electrical and Electronics Engineers (IEEE) Standard 1057 [Reference 1] for Digitizing Waveform Recorders and Standard 1241 for Analog to Digital Converters [Reference 2]. The analyses based on these standards were performed in the frequency domain or time domain as required. When appropriate, instrumentation calibration was traceable to the National Institute for Standards Technology (NIST).

2.4 Test/Evaluation Process

2.4.1 Testing

Testing of the ATA supplied rotation rate sensors, models ARS16 and ARS24 (serial number 0110) were performed in November 2012, in conjunction with the United States Geological Survey (USGS) Albuquerque Seismic Laboratory (ASL). The USGS ASL provided the testbed used to test the sensors and Sandia National Laboratories provided the analysis of the test data.

2.4.2 General Performance Tests

The tests that were conducted on the ATA sensors were based on tests described in the test plans: *Test Definition and Test Procedures for the Evaluation of Seismic Sensors* [Reference 3].

The tests selected provide a high level of characterization for a rotation sensor.

Static Performance Tests
- Isolation Noise (RS-IN)
- Power (RS-P)
- DC-Offset (RS-DCO)

Tonal Dynamic Performance Tests
- Linearity Verification (RS-LV)
- Discrete Frequency Sweep (RS-DFS)

Broadband Dynamic Performance Tests
- Frequency Amplitude Phase Verification (RS-FAPV)

2.5 Test Configuration and System Specifications

2.5.1 Sensor Description and Test Configuration

The rotation-rate seismic sensors under evaluation were provided by Applied Technology Associates, of Albuquerque, NM. The sensor models under evaluation are the ARS16 and ARS24. The ARS16 was configured with three rotation rate transducers. The ARS16 transducers had all been aligned to measure rotation about a common axis, the Z-axis. Figure 2.5.1.1 is a picture of the ARS16 sensor. Data sheets from ATA were used to build the instrument response models for the unit under evaluation. The response models for the three transducers are given in Figures 2.5.1.2-4. The ARS24 consists of a single transducer and tested with its rotational axis aligned to the Z-axis. Figure 2.5.1.5 is a picture of the ARS24 sensor and Figure 2.5.1.6 is the response model for this sensor. The objective of this evaluation is to confirm sensor specifications provided by ATA.

The data for the evaluation was collected on a Quanterra Q330S high-resolution digitizer provided by USGS ASL. The Q330S was configured to acquire data at 1000Hz for six input channels. An HP 3458A multimeter provided a calibrated voltage reference for validating digitizer channel bit-weights prior to starting this sensor evaluation. The USGS rotation rate testbed uses a Fiber Optic Gyro (FOG) model VG 103LD as the rotation rate reference. A picture of the FOG is provided in Figure 2.5.1.7. The FOG has a flat response from DC to hundreds of Hz with a sensitivity of 0.6933 mV/radian/second at 10 Hz. More information can be obtained from the manufactures website http://www.fizoptika.com/product.php?id=27.

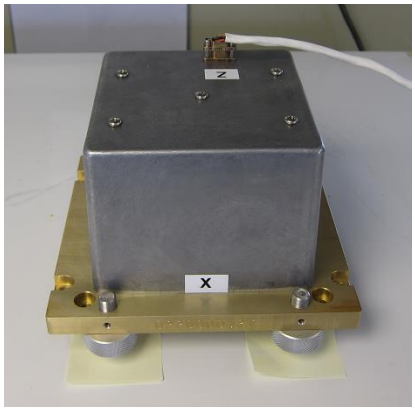

Figures 2.5.1.1 shows the physical characteristics of the ARS16 sensor. The sensor package is approximately 4”x4”x6”.

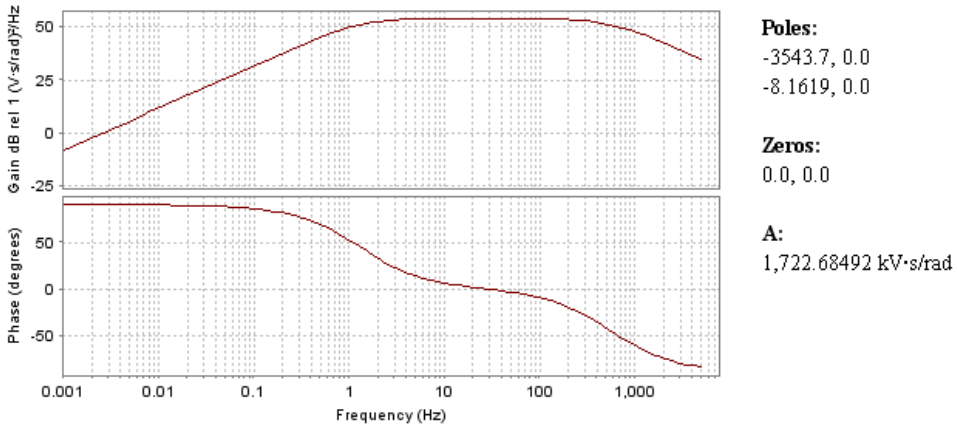

Figure 2.5.1.2 Instrument response model for ARS16-001Z-009, based on data sheets provided by ATA.

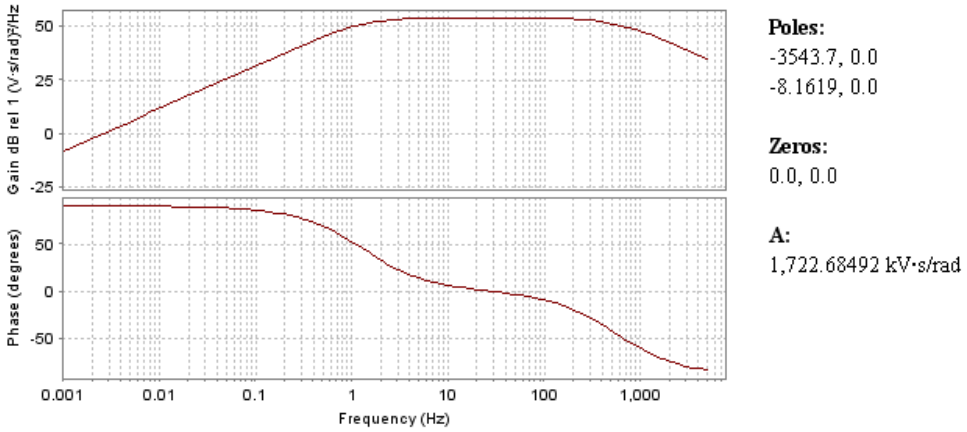

Figure 2.5.1.3 Instrument response model for ARS16-001N-008, based on data sheets provided by ATA.

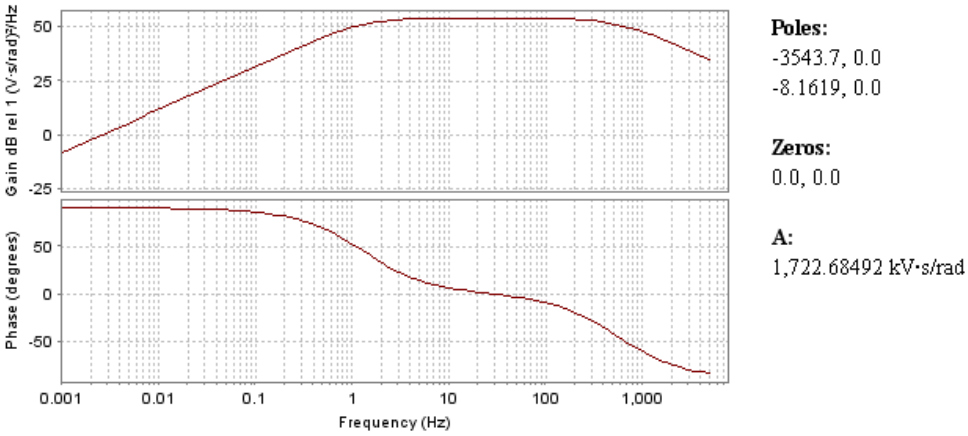

Figure 2.5.1.4 Instrument response model for ARS16-001E-007, based on data sheets provided by ATA.

Figure 2.5.1.5 shows the physical characteristics of the ARS24 sensor. The sensor package is approximately 2”x2” at square ends and 4 inches long.

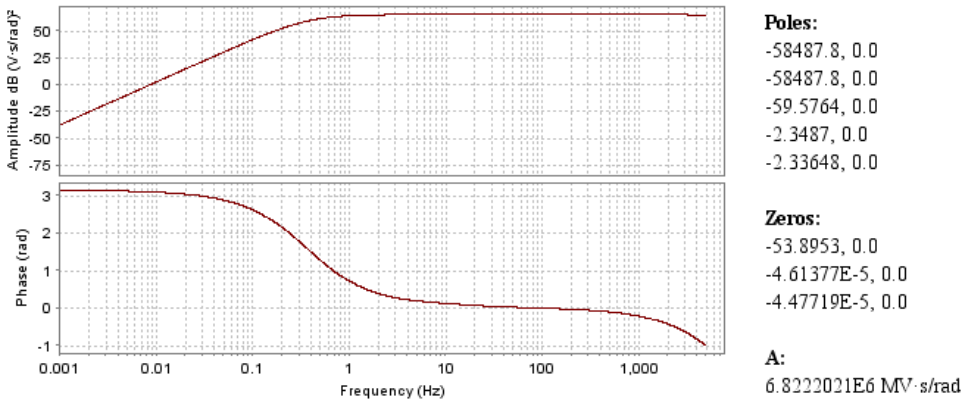

Figure 2.5.1.6 Instrument response model for ARS24-0110, based on measurements provided by ATA.

Figure 2.5.1.7 shows the Fiber Optic Gyro model VG 103LNrotation rate reference sensor. The physical dimensions of the sensor package is approximately 2.5”x2.5” at square ends and 0.8 inches thick.

3 EVALUATION

3.1 Linearity Verification 1 Hz:

Test description: Determine if the rotation rate sensors under evaluation have a linear voltage output versus increasing rotation rate.

The linearity test was conducted on the USGS rotational testbed with both ARS16 and ARS24 sensors present during the test. The input signal was a sinusoid with frequency 1 Hz and twenty amplitude steps, ranging from 7.812 mV to 5.04 Volts. The results are shown in Figure 3.1.1.

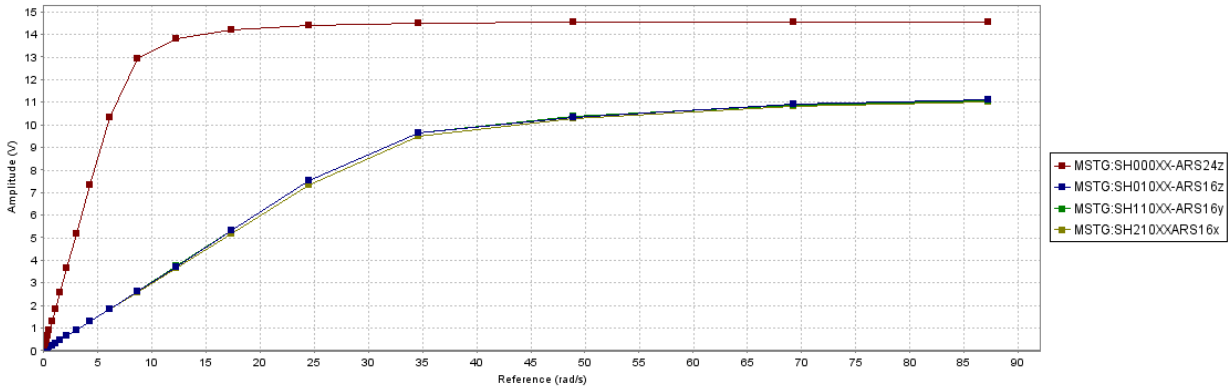

Figure 3.1.1 Rotation rate sensor linearity test results of voltage output versus input rotation rate.

The range of rotation rates spans 0.14 radian/second to 87.2 radian/second. Figure 3.1.2 is a plot of the estimated sensitivity of each rotation rate sensor at each test amplitude.

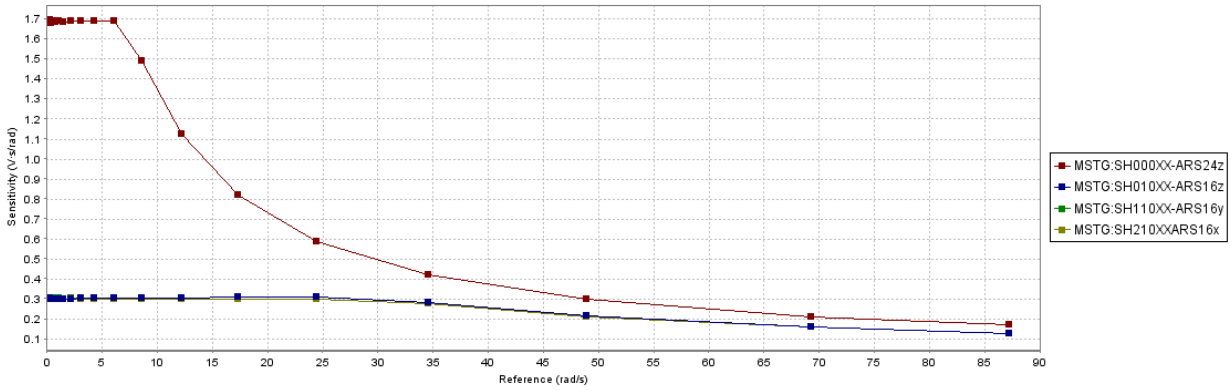

Figure 3.1.2 Rotation rate sensor linearity test results of sensitivity (V/radian/second) versus input rotation rate (radian/second) for ARS16 and ARS24.

The ARS16 sensors maintained a linear output up to 24.4 radian/second, where 24.4 radian/second is the full-scale output of the ARS16 at 1 Hz. Table 3.1.1 lists the average sensitivities for the ARS16 within its linear range of 0.14 to 24.4 radian/second. The ARS24 sensor maintained a linear output up to 6.12 rad/s, where 6.12 radian/second is the full-scale output of the ARS24 at 1 Hz. Table 3.1.2 gives the average sensitivity for the ARS24 within its linear range of 0.14 to 6.120 radian/second.

Sensor ID	Average Sensitivity (V/radian/second)	Standard Deviation (V/radian/second)
ARS16z	301.07	2.62
ARS16y	301.42	2.71
ARS16x	297.21	1.34

Table 3.1.1 Summary of ARS16 average sensitivity values for linearity test.

Sensor ID	Average Sensitivity (V/radian/second)	Standard Deviation (V/radian/second)
ARS24z	1688.1	4.01

Table 3.1.2 Summary of ARS24 average sensitivity values for linearity test.

3.2 Linearity Verification 4 Hz:

Test description: Determine if the rotation rate sensors under evaluation have a linear voltage output versus increasing rotation rate.

The linearity test was conducted on the USGS rotational testbed with both ARS16 and ARS24 sensors present during the test. The input signal was a sinusoid with frequency 4 Hz and twenty-four amplitude steps, ranging from 7.812 mV to 20.16 Volts. The results are shown in Figure 3.2.1.

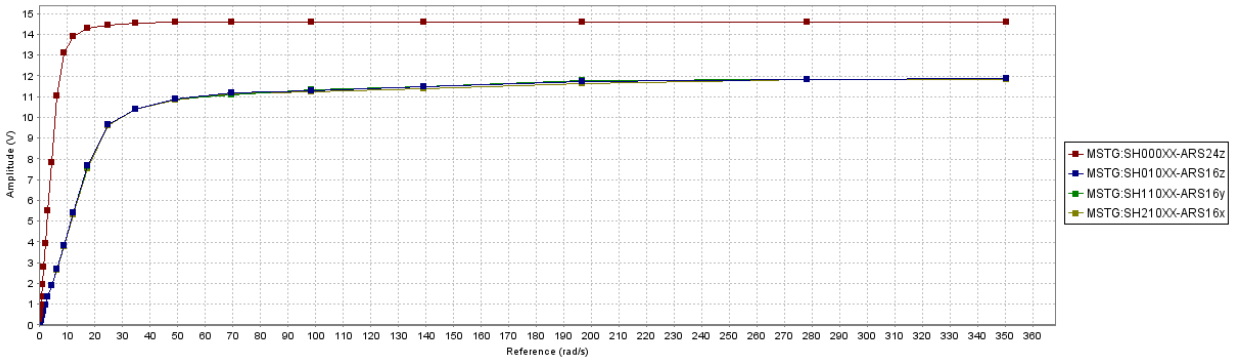

Figure 3.2.1 Rotation rate sensor linearity test results of voltage output versus input rotation rate.

The range of rotation rates spans 0.14 radian/second to 350.3 radian/second. Figure 3.2.2 is a plot of the estimated sensitivity of each rotation rate sensor at each test amplitude.

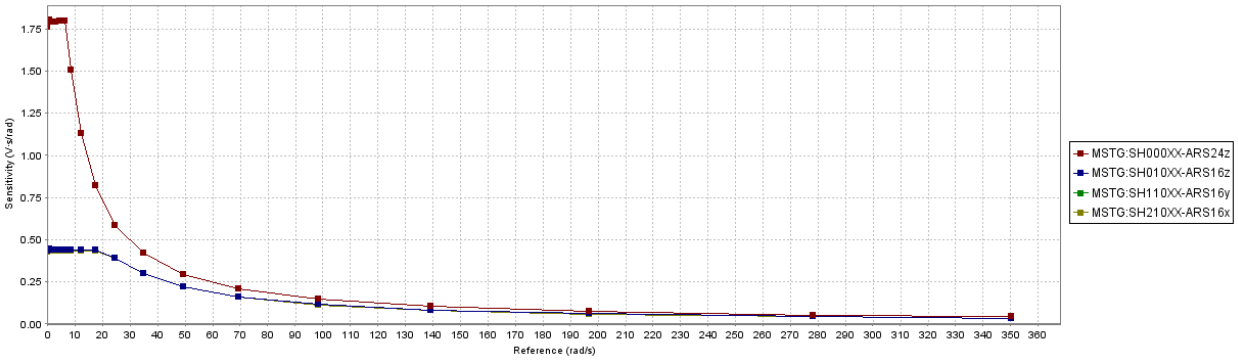

Figure 3.2.2 Rotation rate sensor linearity test results of sensitivity (V/radian/second) versus input rotation rate (radian/second) for ARS16 and ARS24.

The ARS16 sensors maintained a linear output up to 17.4 radians/second, where 17.4 radian/second is the full-scale output of the ARS16 at 4 Hz. Table 3.2.1 lists the average sensitivities for the ARS16 within its linear range of 0.14 to 17.4 radians/second. The ARS24 sensor maintained a linear output up to 6.14 rad/s, where 6.14 radians/second is the full-scale output of the ARS24 at 4 Hz. Table 3.2.2 gives the average sensitivity for the ARS24 within its linear range of 0.14 to 6.14 radians/second.

Sensor ID	Average Sensitivity (V/radian/second)	Standard Deviation (V/radian/second)
ARS16z	440.11	1.975
ARS16y	439.25	2.231
ARS16x	432.49	2.104

Table 3.2.1 Summary of ARS16 average sensitivity values for linearity test.

Sensor ID	Average Sensitivity (V/radian/second)	Standard Deviation (V/radian/second)
ARS24z	1790.5	10.2

Table 3.2.2 Summary of ARS24 average sensitivity values for linearity test.

3.3 Linearity Verification 16 Hz:

Test description: Determine if the rotation rate sensors under evaluation have a linear voltage output versus increasing rotation rate.

The linearity test was conducted on the USGS rotational testbed with both ARS16 and ARS24 sensors present during the test. The input signal was a sinusoid with frequency 16 Hz and twenty-four amplitude steps, ranging from 7.812 mV to 22.6 Volts. The results are shown in Figure 3.3.1.

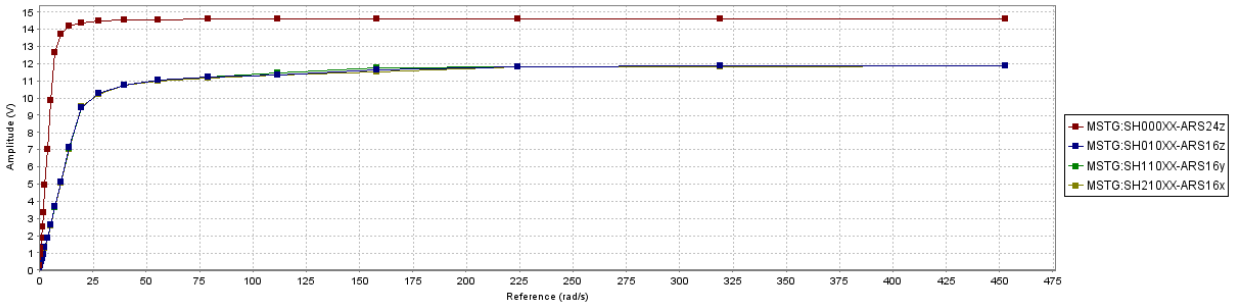

Figure 3.3.1 Rotation rate sensor linearity test results of voltage output versus input rotation rate.

The range of rotation rates spans 0.21 radians/second to 452.5 radians/second. Figure 3.3.2 is a plot of the estimated sensitivity of each rotation rate sensor at each test amplitude step.

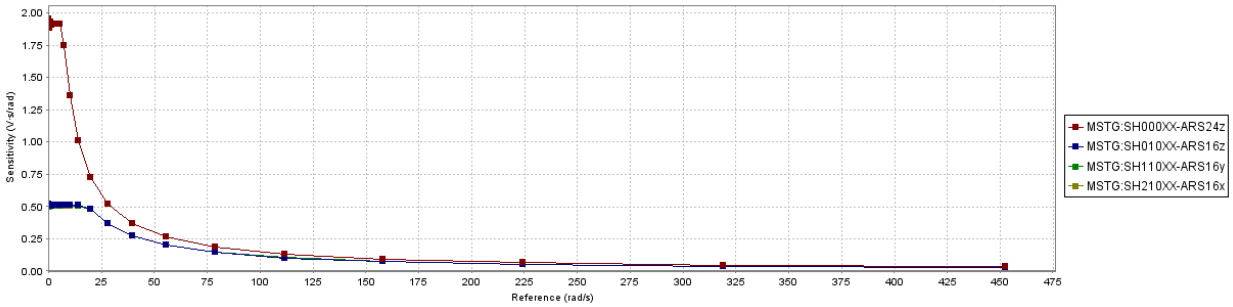

Figure 3.3.2 Rotation rate sensor linearity test results of sensitivity (V/radian/second) versus input rotation rate (radian/second) for ARS16 and ARS24.

The ARS16 sensors maintained a linear output up to 14.0 radians/second, where 14.0 radians/second is the full-scale output of the ARS16 at 16 Hz. Table 3.3.1 lists the average sensitivities for the ARS16 within its linear range of 0.21 to 14.0 radians/second. The ARS24 sensor maintained a linear output up to 5.14 rad/s, where 5.14 radians/second is the full-scale output of the ARS24 at 16 Hz. Table 3.3.2 gives the average sensitivity for the ARS24 within its linear range of 0.21 to 5.14 radians/second.

Sensor ID	Average Sensitivity (V/radian/second)	Standard Deviation (V/radian/second)
ARS16z	507.01	2.61
ARS16y	505.90	2.45
ARS16x	499.95	2.27

Table 3.3.1 Summary of ARS16 average sensitivity values for linearity test.

Sensor ID	Average Sensitivity (V/radian/second)	Standard Deviation (V/radian/second)
ARS24z	1910.2	10.8

Table 3.3.2 Summary of ARS24 average sensitivity values for linearity test.

3.4 Response Verification

Test description: A sensor with a known instrument response model is used as a reference for this test. The Fiber Optic Gyro (FOG) model 103LN serial number 035676 was used as the reference sensor. A sequence of sinusoids were generated from 0.353 to 64 Hz in ¼ octave bands with an amplitude of 1.7e-3 radian/second. This signal was fed to the USGS rotation rate table. The data from the sensors under test were corrected for their individual instrument response models converting all the records to rotation rate (radians/second).

The recorded data from the reference sensor and the sensors under test were processed for coherence, relative gain, and relative phase. The coherence was computed using the technique described by Holcomb, 1989, under the distributed noise model assumption. The spectra (power spectral density estimates or PSDs) were computed using block-by-block DC removal, Hann windowing, 64k FFT length and 5/8 window overlap. With the amount of data processed this provided a 90% confidence interval of 2.69 dB. The results are shown in Figure 3.4.1.

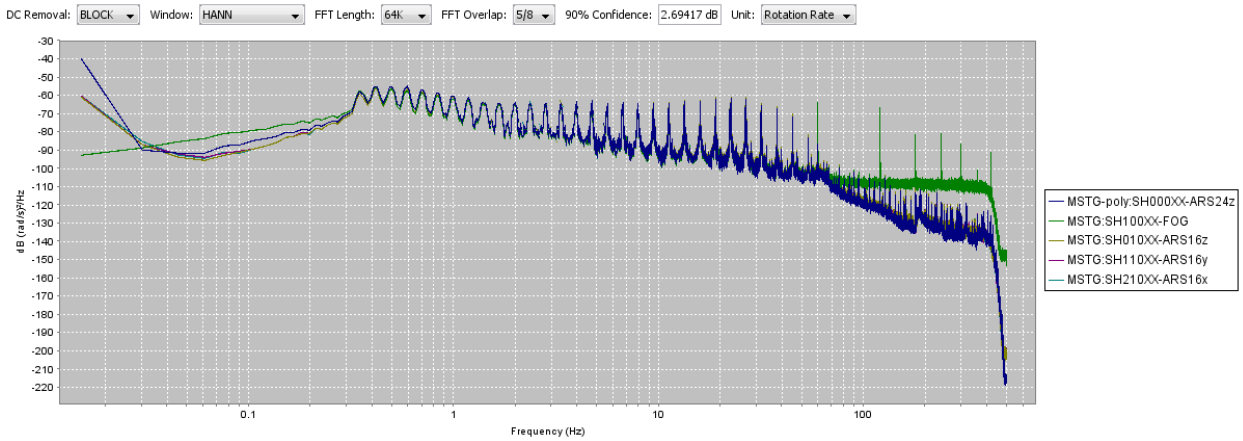

Figure 3.4.1 PSDs of the response verification test.

The PSDs show good broadband agreement with the FOG reference sensor from 0.353 to 64 Hz. To interpret the results of the test we need to review the coherence, relative gain and relative phase. The computed mean-squared coherence values between the reference FOG and each of the sensors under evaluation are plotted in Figure 3.4.2.

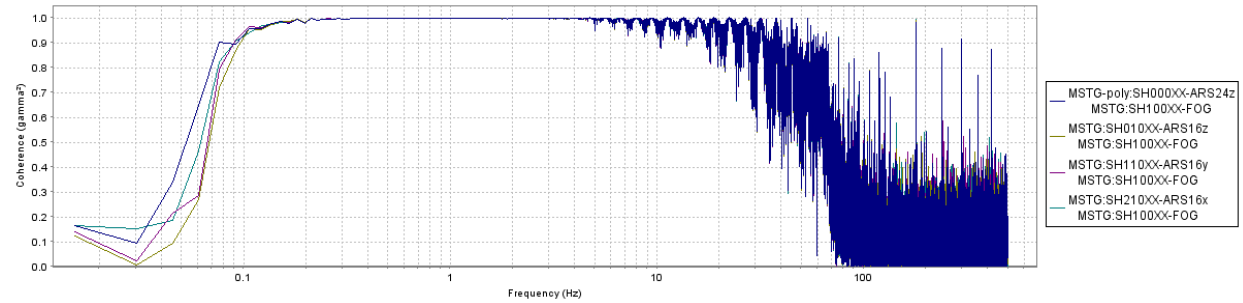

Figure 3.4.2 the coherence between the reference FOG and the ARS16x, ARS16y, ARS16z and ARS24z sensors under evaluation.

The high coherence, 0.9 or higher, from 0.1 to 20 Hz allows us to confidently interpret the relative gain and relative phase results across this broad frequency range. The relative gain is shown in Figure 3.4.3.

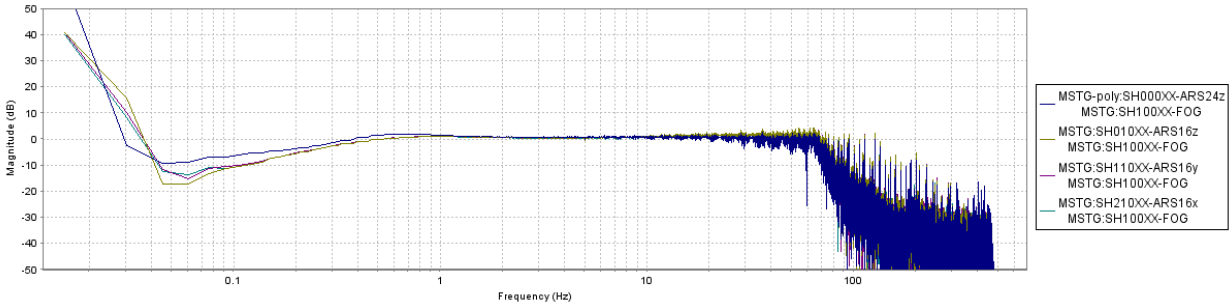

Figure 3.4.3 the relative gain between the reference FOG and the ARS16x, ARS16y, ARS16z and ARS24z sensors under evaluation.

From the relative gain results we observe the 16 Hz sensitivity scaling provides a low relative gain residual, with the ARS24z at 0.5 dB, ARS16x at 0.6 dB and the ARS16y and ARS16z at 0.7 dB. Below 2 Hz, we observe a gradual roll-off; which indicates the models used to describe the low frequency filtering effects are under estimating the amplitude response. The self-noise of the reference FOG sensor limits the interpretation of results above 60 Hz, as noted by degradation of coherence in Figure 3.4.1 and roll-off of the relative gain in Figure 3.4.3 above 60 Hz.
The relative phase is shown in Figure 3.4.4.

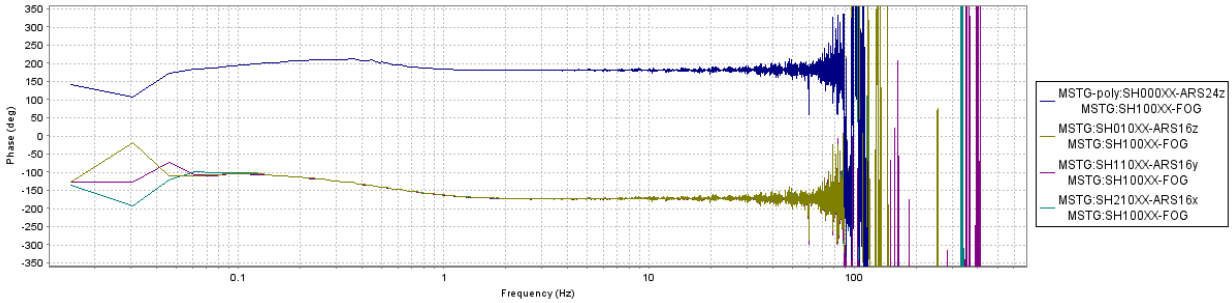

Figure 3.4.4 the relative phase between the FOG and the ARS16x, ARS16y, ARS16z and ARS24z sensors under evaluation.

From the relative phase plot shown in Figure 3.4.4, we note that significant phase variation exists between the FOG and these sensors. The main difference between the ARS16 and the FOG is approximately -175 degrees between 2 and 60 Hz. The three ARS16 transducers are well phase-matched, exhibiting less than 0.5 degrees of variation between 0.02 and 60 Hz. The ARS24 showed a +180 degree phase residual relative to the reference FOG between 2 and 60 Hz. The results imply that there is a polarity convention difference between the ARS16 and FOG and the ARS24 and FOG. Below 2 Hz, the phase residuals increase for the ARS16 and ARS24 sensors, indicating an improved instrument response model would be needed to work in this frequency range.

3.5 Sensor Self-Noise: Isolation Noise Test

Test Description: The purpose of the isolation noise test is to provide an environment with minimal influence of seismic rotation rate background; allowing for the evaluation of the sensors

electronics and transducer noise under conditions of minimal excitation. The USGS ASL East Tunnel was used for this test. Test data was recorded on Q330S digitizers. This test was run overnight and the data collected and reviewed prior to processing.

By selecting a common time window the self–noise spectra were estimated. The results are shown in Figure 3.5.1.

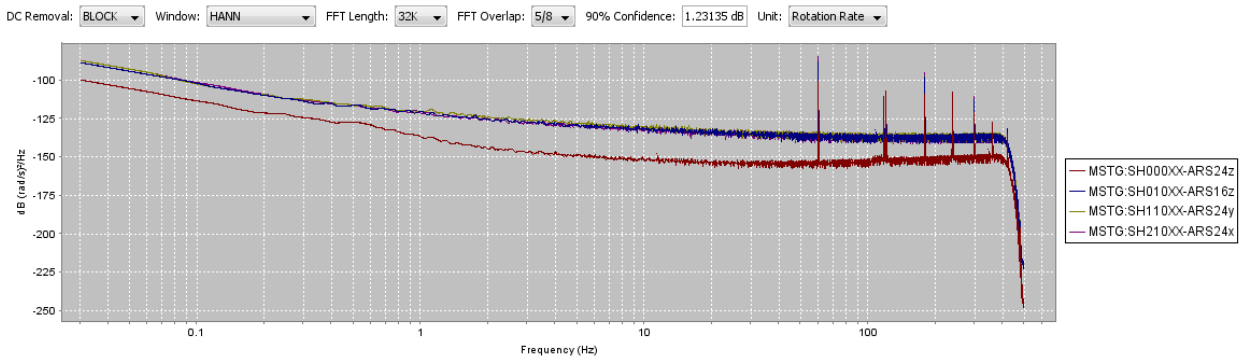

Figure 3.5.1 ARS16 and ARS24 sensor self-noise estimates for an isolation noise test on November 11, 2012.

Note that sensor ARS24 has the best noise model of the two sensors designs tested. Also, the amount of variation in the three ARS16 sensors self-noise spectra was minimal; at 10 Hz the sensors have noise values -132 dB. The ARS24 has a 10 Hz noise value of -152 dB. Table 3.5.1 summarizes the RMS noise for two passbands 0.1-10 Hz, and 1 to 300 Hz.

Waveform	0.1 Hz - 10 Hz	1 Hz - 300 Hz
ARS24z	0.560 rms_µrad/s	3.12 rms_µrad/s
ARS16z	2.26 rms_µrad/s	10.80 rms_µrad/s
ARS16y	2.41 rms_µrad/s	11.28 rms_µrad/s
ARS16x	2.38 rms_µrad/s	15.41 rms_µrad/s

Table 3.5.1 Summary of RMS noise for three passbands.

The ATA sensors full-scale voltage output is a function of supply voltage (Vs). The ARS16 and ARS24 full-scale voltage output range is –Vs + 2Volts (negative supply) and +Vs – 2Volts for the positive supply. For our testing Vs equals 12 Volts, so the full-scale output voltage is ±10 Volts. Dynamic range is computed by 20 times log base 10 of the ratio between the RMS full-scale rotation-rate and the RMS of the Noise for a specified passband. The dynamic range can be estimated for the same two passbands. The results are summarized in Table 3.5.2.

Waveform	0.1 Hz - 10 Hz	1 Hz - 300 Hz
ARS24z	76.4 dB	61.5 dB
ARS16z	76.3 dB	62.7 dB
ARS16y	75.7 dB	62.3 dB
ARS16x	75.8 dB	59.6 dB

Table 3.5.2 Summary of Dynamic Range estimates for three passbands.

3.6 Cross-Axis Sensitivity

Test Description: Measure the amount of cross-axis coupling by an input orthogonal to the primary input axis of a sensor.

For this test the ARS16 sensor module was attached to an L-bracket and the L-bracket attached to the ASL rotation rate table. Figure 3.6.1 shows how the ARS16 and L-bracket were attached to the ASL rotation rate table with ARS24 in background. Complete test setup is shown in Figure 3.6.2. This had the effect of reorienting the sensor transducers from rotation rate about the Z-axis to rotation rate about the E-axis. The ARS24 and FOG sensors were not changed, and maintained alignment to the Z-axis. A high amplitude (0.0057 radians/second) sinusoid signal was used as the input to the test. The spectra (power spectral density estimates or PSDs) were computed using block-by-block DC removal, Hann windowing, 64k FFT length and 5/8 window overlap. With the amount of data processed this provided a 90% confidence interval of 2.69 dB. The ratio between the peak amplitude observed by the reference and that observed by the realigned sensor is the cross-axis sensitivity. The results are shown in Table 3.6.1.

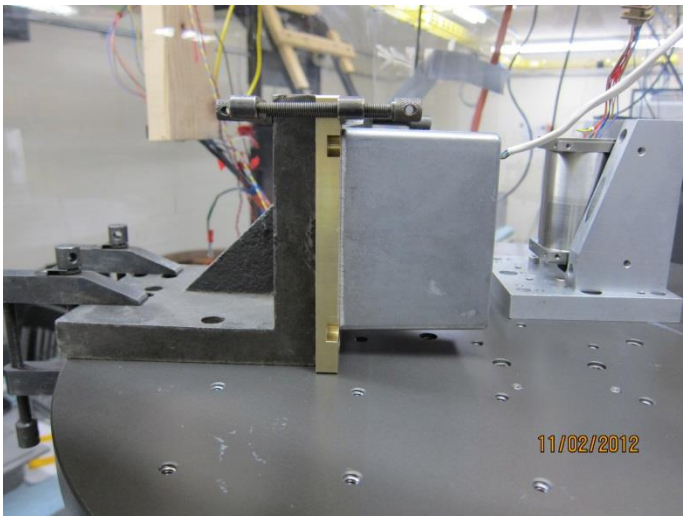

Figure 3.6.1 ARS16 sensor module bolted to L-bracket and attached to ASL rotation rate table for Cross-Axis Sensitivity test.

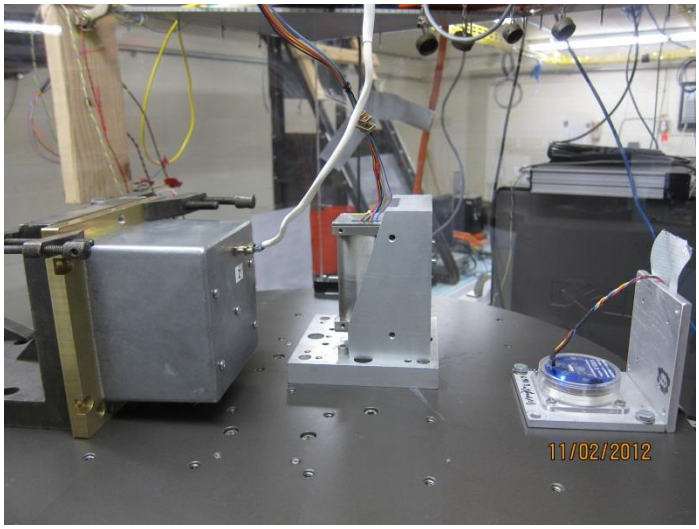

Figure 3.6.2 Cross-Axis Sensitivity test configuration, showing ARS16 sensor module, ARS24 and FOG (from left to right).

Waveform	4 Hz Peak RMS Amplitude	Cross-Axis Sensitivity (dB)
FOG	0.00373 rms_rad/s	-
ARS16z	5.601 rms_µrad/s	56.5
ARS16y	2.884 rms_µrad/s	62.2
ARS16x	3.829 rms_µrad/s	59.8

Table 3.6.1 Summary of Cross-Axis Sensitivity.

Note that the Cross-Axis Sensitivities is on the order as the Dynamic Range estimates.

4 REFERENCES

1. IEEE Standard for Digitizing Waveform Recorders, IEEE Std. 1057-1994.

2. IEEE Standard for Analog to Digital Converters, IEEE Std. 1241-2001.

3. Kromer, Richard P., Hart, Darren M. and J. Mark Harris (2007), 'Test Definition for the Evaluation of Seismic Sensors Version 1.0, SAND2007-5038.

4. Holcomb, Gary L. (1989),'A Direct Method for calculating Instrument Noise Levels in Side-by-Side Seismometer Evaluations', DOI USGS Open-File Report 89-214.

5 DISTRIBUTION

1 Ann Shubert
Applied Technology Associates
1300 Britt St. SE
Albuquerque, NM 87123

1 Dennis Smith
Applied Technology Associates
1300 Britt St. SE
Albuquerque, NM 87123

1	MS0404	Robert Abbott	06913
1	MS0404	Amy Halloran	06913
1	MS0404	Darren Hart	05736
1	MS0404	Tim McDonald	05736
1	MS0404	John Merchant	05736
1	MS0899	RIM-Reports Management (electronic copy)	9532


Sandia National Laboratories

ATTACHMENT C: OBSERVATIONS USING ROTATIONAL SEISMOMETERS

Observations of Volcanic Activity at Kilauea Volcano, Hawaii, Using Rotational Seismometers

Robert E. Abbott, Darren Hart, *Sandia National Laboratories,* Albuquerque, NM
Weston A. Thelen, *Hawaiian Volcano Observatory*, Hawaii National Park, HI

ATTACHMENT C

Abstract

We present data and analysis from a multi-week deployment of two rotational seismometers at Uwekahuna, Hawaii, on Kilauea Volcano. The rotational seismometers are ATA models ARS-16 (three instruments in ZNE configuration), and ARS-24 (two instruments in vertical orientation). These instruments utilize magnetohydrodynamics to measure particle rotation rate with negligible sensitivity to translational motion. The instruments were paired with a Kinemetrics EpiSensor tri-axial accelerometer to create a six degree-of-freedom (6DOF) instrument (three orientations for translational motion and three for rotation rate). Controlled testing shows that instrument self noise for the ARS-24 and ARS-16 were 2.2 and 11.7 e-6 radians/s rms, respectively. Ambient noise at Uwekahuna appears to be 10-15 dB lower than the quieter ARS-24. Many high-amplitude events were recorded with significant signal-to-noise ratio, however. These include a magnitude 2 event within 2 km epicentral distance and a magnitude 3.3 event 20 km distant. 6DOF processing of these event data to determine back-azimuth had highly variable results, even though cross correlations between vertical-axis rotation rate and transverse horizontal acceleration were high. This is likely caused by the great degree of scattering (short mean free path) at Kilauea Volcano. 6DOF processing to determine *in situ* shear velocity is not sensitive to scattering, and yielded shear wave velocities of 350-450 m/s at 10 Hz. This is in agreement with previous studies.

Instrument Testing

We tested four rotational seismometers destined for the UWE deployment. Three of the instruments were ATA model 16s, and one was ATA model 24. All testing was conducted at the USGS Albuquerque Seismological Laboratory (ASL), aided by Bob Hutt and John Evans. Active testing utilized ASL's rotational stage, and passive testing overnight was conducted in the ASL tunnel. Tests included swept frequency with constant amplitude, constant frequency with increasing amplitude, long-duration dwells at a single frequency, cross-axis sensitivity, and sensor self-noise tests. The results are documented in a Sandia Report (in preperation). Select results are below.

ARS-24 Instrument Response

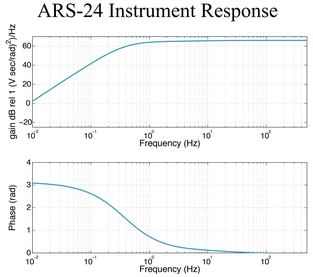

Sensitivities

	Sensitivity (V/rad/sec)	Standard Dev (V/rad/sec)
ARS24	1910.2	10.8
ARS16Z	507.01	2.61
ARS16Y	505.9	2.45
ARS16X	499.95	2.27

Self-Noise

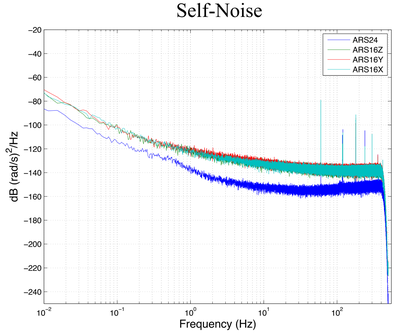

Recorded Data

We deployed two ARS-24 rotational seismometers in vertical orientation, 3 ARS-16 rotational seismometers in tri-axial orientation, and one tri-axial Kinemetrics Episensor accelerometer in the vault at Uwekahuna, on Kilauea Volcano. The instruments were active between and December 12th and February 14, 2013. During that time, a number of high-amplitude events were detected. None of the rotational instruments were able to resolve ambient background noise above it's own self-noise. Unfortunately, the two ARS-24 units began to malfunction a few days after deployment, and only operated until the 18th of December. This was not caught due to problems with telemetry. We think the problem was related to a power supply common to both instruments. The three ARS-16's performed well throughout the deployment (and were on a different power supply).

Map of Recorded Events

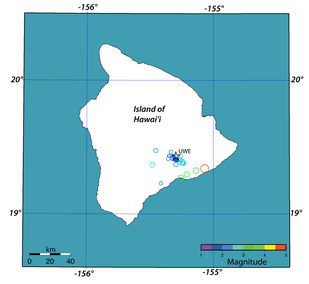

Table of Recorded Events

EventID	Day	Time	Lat	Long	Mag	Dist	ARS-24 Quality	ARS16-Quality
60440896	Dec 13, 2012	17:17:03.680	19.4092	-155.3050	2.13	2.0	Good	Good
60440876	Dec 13, 2012	15:30:47.710	19.4355	-155.3498	1.73	6.5	Marginal	Not Seen
60441106	Dec 14, 2012	8:17:37.680	19.4022	-155.2837	2.01	2.1	Good	Marginal
60440981	Dec 14, 2012	2:24:36.430	19.3255	-155.1352	3.18	19.3	Good	Not Seen
60441331	Dec 15, 2012	15:49:45.640	19.3698	-155.4818	2.81	20.9	Good	Marginal
60441716	Dec 15, 2012	2:30:50.830	19.4083	-155.3000	1.21	1.7	Marginal	Not Seen
60441476	Dec 16, 2012	4:06:41.870	19.4052	-155.2865	2.02	1.7	Marginal	Not Seen
60441966	Dec 17, 2012	23:09:06.510	19.2293	-155.4127	2.11	24.8	Marginal	Not Seen
60442321	Dec 18, 2012	19:58:08.940	19.4128	-155.2920	1.85	0.8	Good	Good
60442266	Dec 18, 2012	10:39:14.700	19.2960	-155.2115	3.06	16.0	Good	Marginal
60443341	Dec 22, 2012	12:59:40.570	19.2703	-155.2557	3.10	17.0	N/A	Good
60443996	Dec 24, 2012	9:51:44.230	19.3707	-155.2952	2.49	5.5	N/A	Marginal
60447191	Jan 5, 2013	14:37:18.080	19.3402	-155.0682	4.55	24.9	N/A	Good
60447491	Jan 6, 2013	4:43:10.500	19.4342	-155.2587	2.55	3.6	N/A	Marginal
60450231	Jan 13, 2013	14:28:57.540	19.3885	-155.2475	3.17	5.7	N/A	Good
60452726	Jan 16, 2013	3:15:23.560	19.3858	-155.2407	2.69	6.4	N/A	Good
60458226	Jan 22, 2013	0:55:23.620	19.4650	-155.3360	2.01	6.9	N/A	Marginal
60458931	Jan 26, 2013	10:08:41.370	19.3818	-155.2363	2.89	7.0	N/A	Good
60458926	Jan 26, 2013	10:08:33.050	19.3780	-155.2417	2.10	6.9	N/A	Marginal
60459671	Jan 27, 2013	14:00:08.570	19.4138	-155.3557	2.20	6.9	N/A	Marginal
60459531	Jan 27, 2013	4:15:57.420	19.4065	-155.2635	2.34	3.2	N/A	Marginal
60460891	Jan 29, 2013	14:43:55.880	19.4155	-155.3255	2.17	3.8	N/A	Marginal
60460396	Jan 29, 2013	11:44:01.010	19.4142	-155.3172	2.34	2.9	N/A	Marginal
60460181	Jan 29, 2013	6:09:35.320	19.4745	-155.4553	2.30	18.3	N/A	Marginal
60461636	Jan 31, 2013	13:51:13.040	19.4038	-155.2970	1.83	1.9	N/A	Marginal
60449182	Feb 12, 2013	4:10:33.390	19.4267	-155.3132	1.66	2.5	N/A	Good
60449712	Feb 13, 2013	19:56:57.280	19.4308	-155.3128	2.47	2.7	N/A	Marginal

Example Signals

Event 60442321 (1-60 Hz Bandpass)

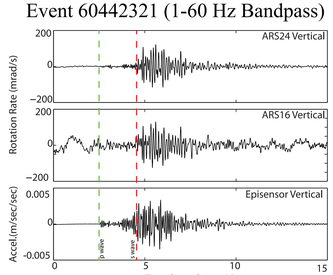

The plot above shows vertical rotation rate and acceleration signals for a magnitude 1.85 event, 0.8 km distant. Notice the relative noise on the two rotation instruments, as well as relative lack of signal before the S wave. All of the signal before the S wave is caused by mode conversions from P to S, as sensitivity to translational motion on the rotational seismometers is essentially nil.

Example Signals

Event 60450231 (1-30 Hz Bandpass)

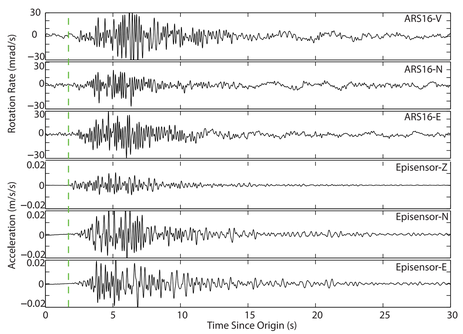

This is a magnitude 3.17 event, 5.7 km away. Rotation-rate traces show little horizontal to vertical magnification, while acceleration traces show significantly higher amplitudes on the horizontals.

Theory

Consider a plane wave propagating in direction of unit vector **n** with speed c. The particle displacement vector **u**(x,t) is given by

$$\bar{u}(\bar{x},t) = U\hat{p}w\left(t - \frac{\bar{x}\cdot\hat{n}}{c}\right), \qquad (1)$$

where U is the displacement amplitude scalar, $\boldsymbol{p}$ is a dimensionless unit polarization vector, and **w**(**x**,t) is the displacement waveform. For a plane shear wave p·n = 0 and c = β, for a plane compressional wave $\boldsymbol{p} = \boldsymbol{n}$ and $c = \alpha$. Since our instrumentation measures particle acceleration and rotation rate, we need expressions for those quantities. The associated particle acceleration vector **a**(**x**,t) is given by

$$\bar{a}(\bar{x},t) = U\hat{p}\ddot{w}\left(t - \frac{\bar{x}\cdot\hat{n}}{c}\right), \qquad (2)$$

and the particle rotation rate vector is given by the time derivative of *curl* **u**(**x**,t)

$$\dot{\bar{\omega}}(\bar{x},t) = \frac{U}{c}\ddot{w}\left(t - \frac{\bar{x}\cdot\hat{n}}{c}\right)(\hat{p}\times\hat{n}). \qquad (3)$$

Note that particle rotation rate is a dimensionless quantity, and is perpendicular to both $\boldsymbol{p}$ and $\boldsymbol{n}$.

The vector product of (2) and (3) via the "Bac-Cab" Rule is:

$$\bar{a}(\bar{x},t)\times\dot{\bar{\omega}}(\bar{x},t) = \frac{U^2}{c}\left(\ddot{w}\left(t - \frac{\bar{x}\cdot\hat{n}}{c}\right)\right)^2[(\hat{p}\cdot\hat{n})\hat{p} - \hat{n}]. \qquad (4)$$

For a shear wave **p** · **n** = 0, leading to

$$\bar{a}(\bar{x},t)\times\dot{\bar{w}}(\bar{x},t) = -\frac{U^2}{c}\left(\ddot{w}\left(t - \frac{\bar{x}\cdot\hat{n}}{c}\right)\right)^2\hat{n}, \qquad (5)$$

and

$$\frac{\|\bar{a}(\bar{x},t)\|}{\|\dot{\bar{w}}(\bar{x},t)\|} = \hat{n}\times\frac{\bar{a}(\bar{x},t)\times\dot{\bar{w}}(\bar{x},t)}{\|\bar{a}(\bar{x},t)\times\dot{\bar{w}}(\bar{x},t)\|} = c = \beta. \qquad (6)$$

Thus, measurement of both acceleration and rotation rate at the same receiver location allows the determination of the propagation direction of the incident wave. Furthermore, using equations (2) and (3), the wavespeed of the incident wave is given by

$$\frac{\|\bar{a}(\bar{x},t)\|}{\|\dot{\bar{w}}(\bar{x},t)\|} = c = \beta. \qquad (7)$$

Results

Back-Azimuth Determination

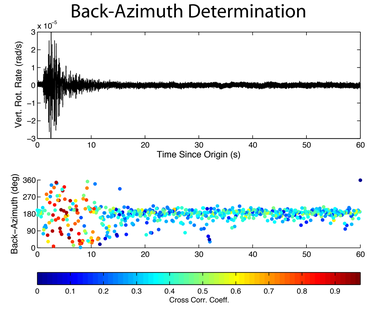

Equations (6) and (7) are valid for the situation where **p** · **n** = 0 (polarization is perpendicular to propagation). For those equations to be valid, the measuring point must be aligned such that the back-azimuth to the source is colinear with the unit propagation **n**. This can be functionally achieved by rotating the horizontal components of acceleration to radial and transverse orientations. When these two horizontal acceleration time-series are rotated to radial and transverse positions, equation (5) is maximized. It can be shown that this is equivalent to maximizing the zero lag cross-correlation of transverse acceleration and vertical-axis rotation rate. In practice we compute the cross-correlations at 1 degree increments (for a total of 360 cross correlations). Presented above is the results of the analysis for event 60440896 (M = 2.13, 2.0 km). Notice that the crosscorrelation coefficients only reach significant value during the event, but that the back-azimuths vary widely. We feel that the analysis is failing because Kilauea is characterized by highly-scattering geology. Non-interfering plane waves are the starting place for the theory, and while the plane wave approximation probably holds, there are too many overlapping phases for a clean comparison of vertical rotation rate and transverse acceleration.

Below are the results for all high signal-to-noise events recorded by the ARS-24 and ARS-16 before the eventual malfunction of the ARS-24. Not all events of this subset have high S/N on the noisier ARS-16. Green and red lines are P- and S-wave picks. The black line is the theoretical back azimuth computed from the map coordinates. Only cross correlations greater than 0.75 are plotted. The progressive increase in high correlations on the ARS24 are the result of harmonic noise contaminating the signal before it eventually became dominant.

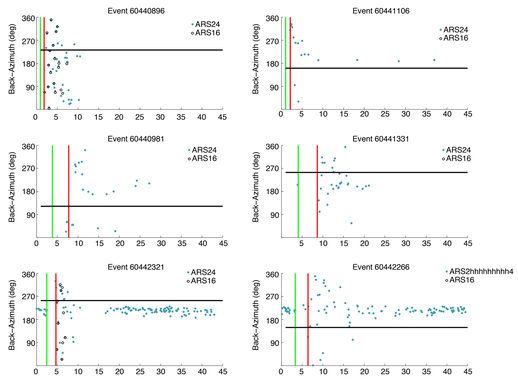

Results

Calculated Shear Velocity at UWE

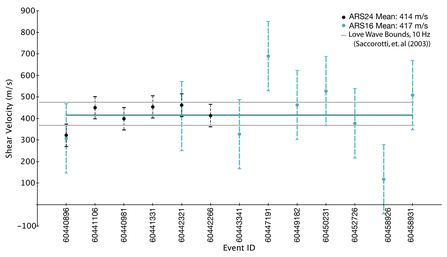

For all events with signal-to-noise ratio of four or greater, we used equation (7) to find the in situ shear velocity. The analytic-signal instantaneous amplitude (absolute value of Hilbert transform) was found for vertical-axis rotation rate, and both horizontal acceleration components. Since we do not have a dominant back-azimuth to rotate to, the two horizontal components were averaged. In the following equation, $f(\beta)$ was minimized.

$$f(\beta) = \text{norm}\left(\frac{\|H(\bar{a}(\bar{x},t))\| + \|H(\bar{a}(\bar{y},t))\|}{2} - \beta\|H(\bar{\omega}(\bar{z},t))\|\right)$$

The overall mean shear velocity using both instruments was virtually identical, although the ARS-16 results show considerably more scatter. This is not surprising, as we do not have as good an intrument model for the ARS-16, and it is a noisier instrument. The results compare very favorably with Saccorotti et al. (2003) results derived at Kilauea using array measurements.

Something Completely Different in Albuquerque

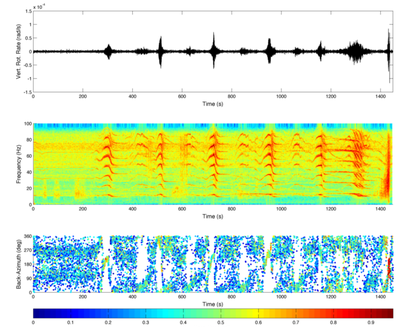

The same instrument setup was tested at Sandia and captured this recording of circling helicopters. Notice that back-azimuth calculations are stable and show smoothly varying back-azimuths with time. In contrast to the UWE data, these signals are more continous in nature, and the geology is simpler (sedimentary basin). The broadband event at 1425 seconds is unexplained, but produced the best cross-correlations.

Acknowledgements

We would like to thank our partners and colleagues at ATA (Dennis Smith, Darren Laughlin, Bob Pierson, Ann Schubert) for the loan of the rotational seismometers. Bob Hutt and John Evans at the USGS ASL graciously allowed the use of their rotational stage. This work was funded under the U.S. Department of Energy's Energy Efficiency and Renewable Energy Geothermal Technologies Office.

ATTACHMENT C

Sandia is a multi-program laboratory operated by Sandia Corporation, a Lockheed Martin Company, for the United States Department of Energy's National Nuclear Security Administration under contract DE-AC04-95AL85000

ATTACHMENT D: SMHD HIGH-TEMPERATURE MATERIAL ANALYSIS

This attachment was deemed to include both ATA Proprietary information as well as material potentially subject to International Traffic and Arms Regulations (ITAR) control. Therefore, the attachment was removed from this final report and is available from ATA for authorized government reviewers for purposes of review and evaluation.

ATTACHMENT E: SMHD VS. LFITS TECHNOLOGY TRADE STUDY

Document Description:	Document Number:	Applied Technology Associates Albuquerque, New Mexico
SMHD-LFITS Trade Study	0230000131	
Model:	**CAGE Code:**	
SMHD, LFITS	6M566	

SMHD-LFITS Trade Study

Rev.	ECO #	Description	Date	Approved
A	1205	Original Release	10/10/2013	B. Pierson

APPROVALS	
PRINCIPAL INVESTIGATOR:	**Date:**
Darren Laughlin	10/10/2013
PROGRAM MANAGER:	**Date:**
Bob Pierson	10/10/2013
QUALITY MANAGER:	**Date:**
Trish Kiker	10/10/2013

Table of Contents

List of Figures

1.0 SCOPE

Under a grant from the US Department of Energy, Applied Technology Associates (ATA) is comparing two angular motion sensors that are being considered for inclusion in a 7degree-of-freedom (7DOF) sensor package being proposed for locating and characterizing hard rock fracturing during geothermal well development (Enhanced Geothermal Systems – EGS). This analysis seeks to examine the two sensor technologies and assess their suitability for the application. The most appropriate sensor will be developed in Phase 2 of this effort.

The two sensors are ATA's Low-Frequency Improved Torsional Seismometer (LFITS), and ATA's magnetohydrodynamic (MHD) sensor, specifically a seismic adaptation of the MHD technology (SMHD). The MHD angular rate sensors have been developed previously for military and space applications where the temperature range is typically -55ºC to +85ºC. The LFITS technology is being developed under the Phase 1 grant and has only been used in laboratory applications. In addition to three angular sensors, the 7-DOF package will include three linear motion sensors, and a pressure sensor. Temperatures in geothermal wells often exceed 400ºC but the goal of this 7-DOF instrument development is to be able to operate for extended periods of time at 200ºC or higher by placing the instrument at a higher elevation in the borehole.

The expected geothermal motion environment is presented in the "Draft Specification Notes for a 7-DOF Seismometer" document and strongly influences the analysis, in particular because the motion is dominated by frequencies greater than 100 Hz. A materials analysis was performed for each sensor and their electronics were assessed to estimate the impact of the high-temperature environment on performance and reliability.

2.0 Instrument specification

2.1 Summary

Essentially all seismic measurements are currently acquired using linear seismometers and pressure sensors. Rotation is often calculated using the linear sensors but it is widely accepted that direct rotational measurements would provide additional information and utility. However, to date, no suitable rotational sensor has been developed. The purpose of this program is to define and demonstrate a 7-degree of freedom (7-DOF) motion measurement system (three linear sensors, three rotational sensors, plus pressure) designed for geothermal environments. The "Draft Specification Notes for a 7-DOF Seismometer" document attempts to capture the key requirements for the final downhole sensor suite. The Phase 1 effort produced two candidate instruments; a Seismic MagnetoHydroDynamic angular rate sensor (SMHD) (similar to ATA's ARS-24 but specifically designed only for down-hole seismic measurements) and a Low-Frequency Improved Torsional Seismometer (LFITS) based on a capacitive sensing approach. These angular sensors were performance tested in laboratory conditions. It is planned in Phase 2 for the angular sensor best suited for this application to be upgraded to include high-temperature electronics and materials and then be combined with high-temperature linear motion sensors (accelerometers or geophones) and a pressure sensor to create a 7-DOF sensor package for monitoring downhole geothermal environments. Opportunities will be sought in Phase 2 to make in-situ measurements with the prototype unit.

2.2 Interface Requirements

2.2.1 Electrical Interfaces

The trade evaluation concerning electrical interfaces included consideration of input power characteristics, output signal characteristics, discrete commands, programming interface, and test interfaces. Though there was large uncertainty about the exact nature of many of the parameters, it was determined that both the SMHD and LFITS were equally capable of meeting the specification.

2.2.2 Mechanical Interfaces

The physical size and mechanical interface of the rotational sensor was identified in the Specification as a Key System Attribute (KSA). The 7-DOF instrument will be lowered into a borehole on the end of a cable and will be in a housing that provides mounting locations for all 7 sensors, power supplies, signal conditioning and data acquisition, and a method to lock the sensor into the borehole or casing to enable transmission of high-frequency motion to the sensors. The primary mechanical interface constraint is physical size because the 7-DoF sensor package must fit inside the borehole. The largest hole-lock housing identified during the Phase 1 effort was the one manufactured and distributed by Nanometrics with an internal diameter of 5.5 inches (14 cm) so that sets the practical limit on sensor size because the length of the housing can be increased somewhat so the three sensors can

be placed in a linear orientation, one above the other. Two of the sensors will be oriented horizontally and the other vertically. The smaller SMHD holds a clear advantage over the current TRL3 design of the LFITS which is much larger. The SMHD is also much more customizable than the LFITS so the sensor can be made to fit in the available space. It is not clear how the LFITS size might be reduced while maintaining its sensitivity and noise level. The size of the prototype LFITS and proposed SMHD are shown in Figure 1 and Figure 2, respectively.

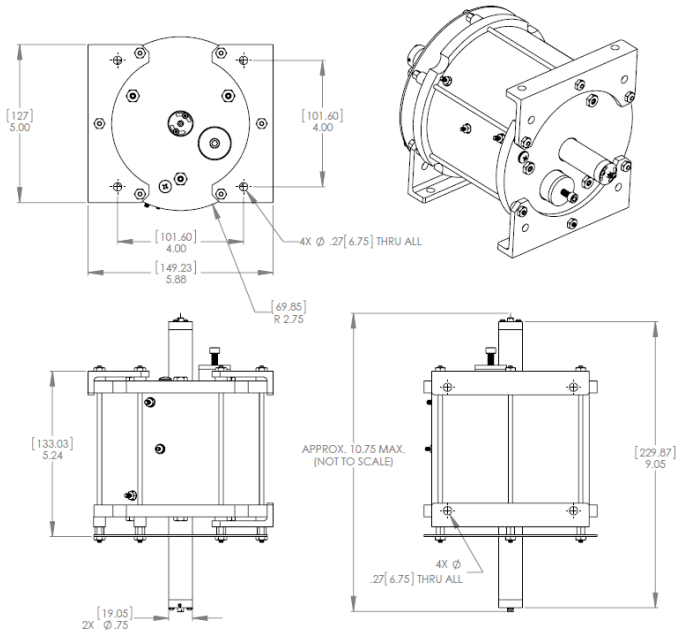

Figure 1. Dimensions of the TRL3 Prototype LFITS

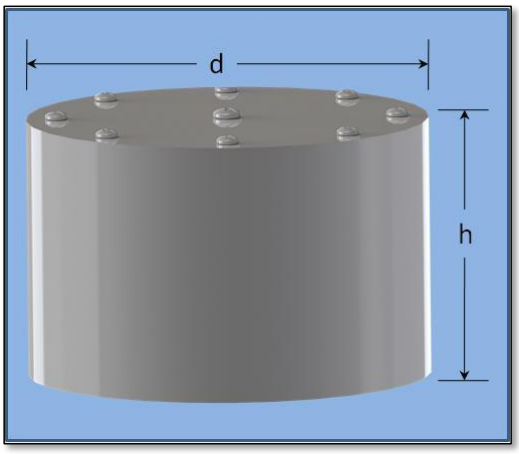

Model	d (in.)	h (in.)
RS-1.6	1.6	1.6
RS-3.8	3.8	3.8

Figure 2. Modeled SMHD Dimensions

2.2.3 Thermal Interfaces

The operating temperature goal for the 7-DoF Instrument is at least 200ºC (392ºF) which is defined as a KSA. This temperature is well above normal operating temperatures for most electronic components and many of the materials normally employed in ATA's sensor products. In addition, even higher temperatures might be encountered under some circumstances that would require the 7-DoF instrument to survive but not necessarily operate.

To assess the likelihood that either the SMHD could be engineered to operate for thousands of hours at 200ºC a detailed analysis of SMHD materials was performed. Each material and process was evaluated for heat-induced degradation, differential thermal expansion issues, and thermal performance variations (e.g. changing magnet strength). A number of material degradation issues were identified, none of which appeared to be insurmountable but a significant amount of engineering will be required to overcome existing design shortcomings. The results of the analysis are presented in the "Seismological Magneto-Hydrodynamic (SMHD) Senor High Temperature Analysis" document. The maturity of the LFITS design limited the scope and usefulness of the same kind of thermal review. However, several problems are evident from cursory observation. The fluid in the LFITS would need to be replaced and the CTE mismatch problems combined with the size of the LFITS would be significant.

The electronic component parts lists for the SMHD are shown in Figure 3 and for the LFITS in Figure 4. Each of the components will need to be assessed for thermal survival and performance, with particular attention paid to the active components, designated with U1, U2, etc. The part count for the SMHD is 5 capacitors, 5 resistors, and 1 active (op-amp). The LFITS has 9 times as many capacitors and resistors as the SMHD and 10 times as many active components. Simply on the basis of part count, the LFITS will be 10 times more difficult to engineer for high temperature and 10 times as likely to fail. The added complexity of the LFITS active components will likely increase the difficulty in finding suitable high-temperature replacements.

ATA PN	MFG PN	REFERENCE DESIGNATOR	DESCRIPTION	QTY
0223000102	NA		Printed Circuit Board, ARS-16	1
0209000478	GRM155F51E104ZA01D (Murata)	C1, C2	Capacitor, SM(0402), 0.1uF, 25V, -20%, +80%, Y5V (100nF)	2
0209000479	C0402C103K5RACTU (KEMET)	C3	Capacitor, SM(0402), 0.01uF, 50V, 10%, X7R (10nF)	1
	C1608X7R1H332K (TDK)	C4	Capacitor, SM(0603) 3300pF 50V 5%	1
0209000481	EMK107BJ105KA-TR (Taiyo Yuden)	C5	Capacitor, SM(0603), 1uF 16V 10%	1
0214F00485	NK-2H2-009-235-TH00 (AirBorn)	J2	Conn, Socket, 9 pin Straight, PC Mount	1
	RC0603FR-07100KL (Yageo)	R1	Resistor, SM(0603), 100k ohm, 1/10W, 0.5%	1
0208000500	M55342K06B10D0R (ROHM)	R2, R4	Resistor, SM(0603), 10 ohm, 1/10W, 0.5%	2
0208000501	MCR03EZPFX1002 (ROHM)	R3	Resistor, SM(0603), 10k ohm, 1/10W, 1%	1
0208000065	M55342K06B1F00R	R5	Resistor, SM(0705), 1M ohm, 1/10W, 1%, MIL-PRF-55342	1
0211000036	LT1028CS8 (Linear Technology)	U1	IC, Single Op Amp, SO8	1
NA	NA	U2	Temperature Sensor	1
0202000441	MS51958-120	NA	Screw, #0-80 X 1/8, 18-8 SS, Pan Head	2

Figure 3. SMHD Electronic Parts List

Designator	Part Description	Mfg. PN	Quantity
C1, C2, C3, C4, C14, C15, C17, C18	CAP CER 680PF 50V 1% NP0 0603	C1608C0G1H681F	8
C5, C8, C10, C12, C20, C23, C25, C27	CAP TANT 6.8UF 35V 10% 2312	T491C685K035AT	8
C6, C7, C9, C11, C13, C39, C44	CAP CER 10000PF 50V 10% X7R 0603	C1608X7R1H103K	7
C16, C19	CAP CER 1000PF 50V 10% X7R 0603	C1608X7R1H102K	2
C21	CAP CER 4700PF 25V 5% NP0 0603	C1608C0G1E472J	1
C22, C24, C26, C28, C30, C31, C33, C34, C35, C36	CAP CER 0.1UF 50V 10% X7R 0603	C1608X7R1H104K	10
C29	CAP CER 3300PF 50V 5% NP0 0603	C1608C0G1H332J	1
C32	CAP CER 8200PF 25V 5% NP0 0603	C1608C0G1E822J	1
C37, C46	CAP CER 470PF 3KV 10% X7R 1812	C1812C471KHRACTU	2
C38, C40, C41, C42, C43, C45	CAP CER 6.8UF 50V 10% X7R 1812	C4532X7R1H685K	6
D1, D2	DIODE SWITCH DUAL 85V SOT23-3	BAV199-7-F	2
R1, R2, R16, R17	RES 47K OHM 1/10W .1% 0603 SMD	ERA-3AEB473V	4
R3	RES 1.00K OHM 1/10W 1% 0603 SMD	ERJ-3EKF1001V	1
R4	RES 604 OHM 1/10W 1% 0603 SMD	ERJ-3EKF6040V	1
R5, R6, R20, R21	RES 7.87K OHM 1/10W .1% 0603 SMD	ERA-3AEB7871V	4
R7	RES 1.07K OHM 1/10W 1% 0603 SMD	CRCW06031K07FKEA	1
R8, R10, R23, R25	RES 232 OHM 1/10W .1% 0603 SMD	ERA-3AEB2320V	4

Designator	Part Description	Mfg. PN	Quantity
R9, R11, R12, R14, R15, R24, R26, R29, R33, R34	RES 0.0 OHM 1/10W 0603 SMD	CRCW06030000Z0EA	10
R13, R18, R27, R32	RES 10.0 OHM 1/10W 1% 0603 SMD	CRCW060310R0FKEA	4
R19, R28, R43, R46	RES 100K OHM .25W 1% 0603 SMD	CRCW0603100KFKEAHP	4
R22	RES 1.13K OHM 1/10W .1% 0603 SMD	ERA-3AEB1131V	1
R30	RES 10.0K OHM 1/8W 1% 0805 SMD	ERJ-6ENF1002V	1
R31	TRIMMER 100 OHM 0.125W SMD	3223W-1-101E	1
R35, R36, R39, R42	RES 2.00K OHM 1/10W 1% 0603 SMD	ERJ-3EKF2001V	4
R37	RES 4.02K OHM 1/10W .1% 0603 SMD	ERA-3AEB4021V	1
R38	RES 9.53K OHM 1/10W .1% 0603 SMD	ERA-3AEB9531V	1
R40	THERMISTOR 2252 OHM +/-0.10 C	PS222J2	1
R41	RES 10.0K OHM 1/10W 1% 0603 SMD	ERJ-3EKF1002V	1
R44, R45	RES 11.5K OHM 1/10W 1% 0603 SMD	ERJ-3EKF1152V	2
U1	Sine Source, 100kHz	QT901S9-100.00kHz	1
U2	IC PREC OP-AMP 28MHZ QUAD 16SOIC	LT1214CS#PBF	1
U3	IC AMP RR I/O 30V SINGLE SOT23-5	LM7321MF/NOPB	1
U4	IC MOD/DEMOD BAL 2MHZ 20-CDIP	AD630BDZ	1
U5	IC OP AMP INSTRUMENTATION 8SOIC	AD8421BRZ	1
U6	IC OP-AMP LOW NOISE SNGL 8-SOIC	LT1128CS8#PBF	1
U7	IC VREF SERIES PREC 2.5V 8-MSOP	ADR431ARMZ	1
U8	IC PRECISION OP-AMP SINGLE 8SOIC	LT1001CS8#PBF	1
U9	IC REG LDO ADJ .15A 14DFN	LT3032EDE#PBF	1
U10	IC CONV DC-DC 15W DUAL 15V PCB	PXB15-24WD15/N	1

Figure 4. LFITS Electronic Parts List

2.3 Rotational Motion

2.3.1 Expected motion

The expected rotational velocity motion is shown in Figure 5 below. The range shown in the shaded area is bounded by the minimum (red) and maximum (blue) expected motion. The minimum motion curve was defined as the smallest event magnitude of interest, Mw = -2, with the maximum expected separation from the event to the instrument, 2 km. The maximum motion curve was defined as the largest expected event magnitude, Mw = +3.5, with the minimum expected separation from the event to the instrument, 1 km. Cases are shown for two different values of Q. The motion is expected to be closer to the estimate with Q closer to 135 but could be higher if the rock is unexpectedly rigid.

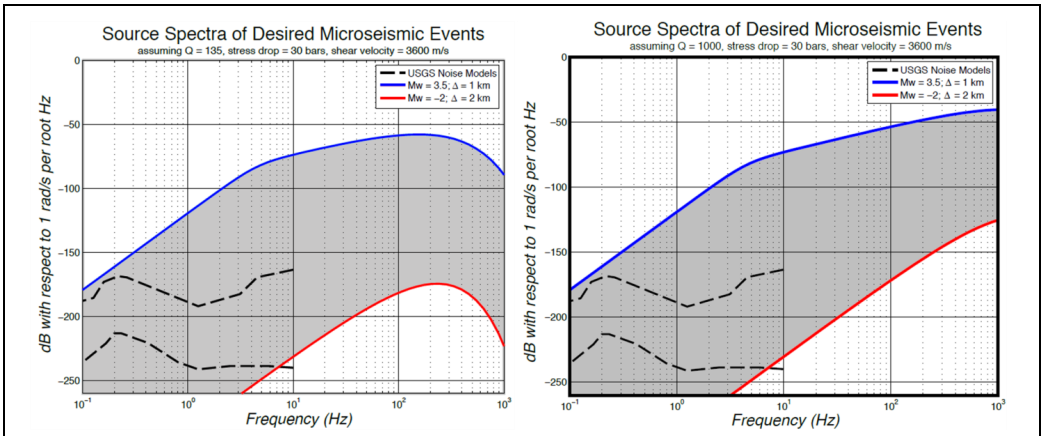

Figure 5. Expected EGS Fracturing Rotational Motion

2.3.2 Motion Measurement Ability

The ability to measure the expected down-hole motion environment in enhanced geothermal system (EGS) development is obviously paramount in this effort. There are three primary components to the measurement that have been identified as Key Performance Parameters (KPP); resolution, bandwidth, and dynamic range. The noise PSDs for the LFITS (modeled and measured) and two sizes of SMHD (modeled) are superimposed on the expected motion PSDs in Figure 6. The TRL-3 maturity of the LFITS leaves the three KPPs listed above not fully characterized. The LFITS frequency response was measured up to10 Hz and the electronic noise was measured from 10 to 1000 Hz. The LFITS is fundamentally a low-frequency angular displacement sensor so it does not match the expected motion environment as well. To improve the noise of the LFITS the sensor might have to be made larger which may reduce bandwidth as internal structures become larger and their resonant frequencies decrease.

The SMHD is a very good match for the majority of the motions to be measured. The resolution of the SMHD can be tailored for the application, subject to the maximum dimensions of the hole-lock container. A 3.8” diameter, 3.8” long SMHD has the resolution to measure the vast majority of the predicted motions but if a smaller SMHD is required to fit the housing it will lose some resolution but will also be able to measure larger motions that would saturate the 3.8” SMHD. The -3dB corner frequencies of the SMHD will be approximately 1Hz at low frequency and greater than 1 kHz at high frequency. The dynamic range between the maximum and minimum expected motion PSDs is approximately 120dB near the peak of the PSDs. The dynamic range of ATA’s MHD sensors is greater than 120dB which matches the requirement well.

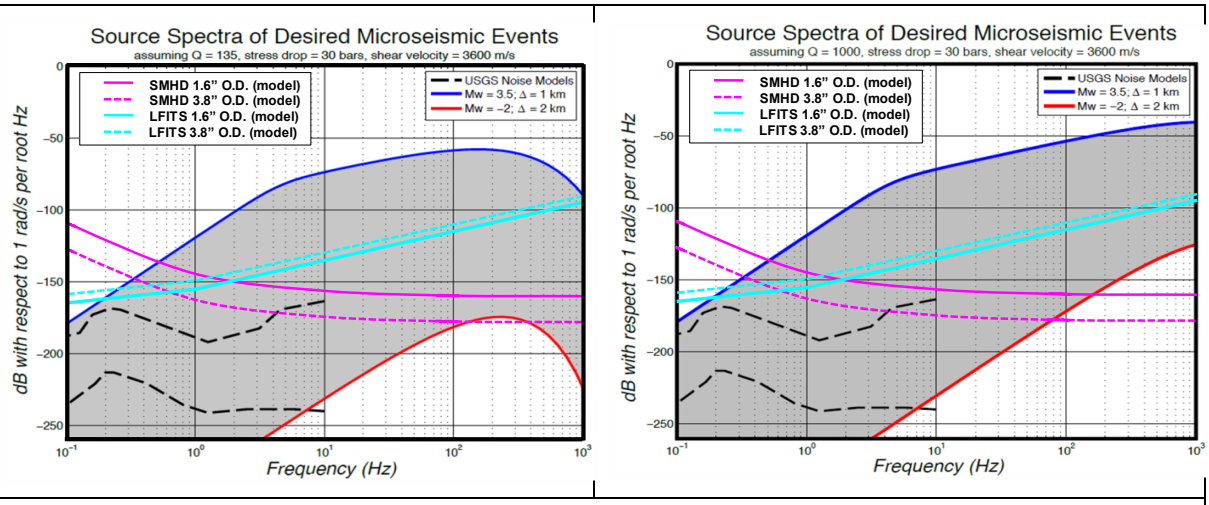

Figure 6. SMHD and LFITS Self-Noise Estimates

2.3.3 Reliability

The down-hole geothermal environment is extremely harsh. High temperature combined with shock and vibration from surface handling and from being lowered into the borehole on a cable creates a challenging environment for most highly sensitive instruments. The LFITS is designed to withstand field handling but would need a shipping lock to constrain the proof mass. Low TRL for the LFITS makes it difficult to predict the level of shock and vibration it would eventually be able to withstand. The SMHD is extremely tough. Similar MHD sensors have been tested to thousands of g's of acceleration with no damage. No special shipping accommodations are required.

The most likely failure for either sensor is high temperature-induced failure of the electronics. As discussed above in the thermal interface section, the simplicity of the SMHD makes it the obvious winner in a reliability trade.

3.0 Summary

An assessment was performed of the relative merits of the LFITS and the SMHD for the high-temperature EGS fracture monitoring application. Key Performance Parameters (KPP) were identified to be measurement resolution, bandwidth, and dynamic range. Key System Attributes (KSA) of size, operational temperature, and reliability were also considered. A simple red, yellow, green system shown in Figure 7 creates a quick visual reference and the best sensor in each category is denoted with a checkmark. Green indicates that the sensor can reasonably be expected to meet all of the requirements in that category. Yellow says that either the sensor does not meet all of the factors or it is not clear that the sensor can meet all of the requirements in that area. Red indicates significant shortfalls in the category with doubtful resolution of the problem.

Figure 7. LFITS - SMHD Trade Summary

3.1 Resolution (KPP)

The SMHD technology measures angular rate. In contrast, the LFITS technology measures angular displacement. Thus, the SMHD has an inherent advantage at high frequency due to lower noise levels. Figure 6 graphically illustrates the performance of the two sensor types relative to expected micro-seismic signal levels. The figure overlays the modeled high-temperature performance of LFITS and SMHD sensors onto the "low Q" (left) and "high Q" predicted micro-seismic signal spectra. The overlay curves for each LFITS and SMHD sensor are their noise floors, so the sensors detect signals above their respective curves. The ideal sensor would have a noise floor curve below the grey shaded area over as wide a frequency band as possible. Thus, the SMHD wins the trade due to its low noise floor at high frequency. However, both sensors are rated yellow. This rating reflects the critical nature of this requirement, the desire to push resolution as far as possible, and the uncertainties involved in defining the seismic signals of interest for such a new technology.

3.2 Bandwidth (KPP)

The bandwidth goal specifies an upper limit of 1,000 Hz. Based on the brassboard, ATA believes it will be much more difficult to design an LFITS sensor that is rigid to high frequency. In addition, ATA is concerned at achieving the combination of adequate rotational sensitivity at high frequency while preventing sensitivity to cross-axis rotational motion and linear acceleration. This combination of concerns led to a yellow rating for the LFITS technology. In contrast, ATA's existing MHD-based sensors have been shown to operate at high frequencies with essentially no sensitivity to cross-axis rotation or linear acceleration. Thus, the related SMHD technology was rated green.

3.3 Dynamic Range (KPP)

Modeling indicated that both sensors can be engineered for large dynamic range so both technologies are rated green and no clear winner is evident.

3.4 Size (KSA)

The sensors are constrained to fit in a package suitable for hole-locked downhole deployment. Modeling indicated a sensor based on the LFITS technology was larger than the SMHD for the same approximate performance over the frequency band of interest. This creates a significant advantage for the SMHD. In addition, work with the brassboards indicates that there are considerable engineering challenges. Though promising work continues on the LFITS for another customer and application, the technology has too low a technology maturity to reliably achieve even the modeled sizes for a geothermal demonstration. Thus the SMHD was rated green and the LFITS given a yellow designation.

3.5 Operational Temperature (KSA)

Analysis of the LFITS during modeling revealed challenges in identifying appropriate dielectric fluids for high-temperature operation. This and other residual engineering component and fabrication uncertainties earned LFITS a red rating. The SMHD was also rated yellow, but with far fewer concerns. ATA has built MHD-based sensors for more than 25 years and tested units up to 150ºC without degrading their performance. During Phase 1, ATA performed a thorough assessment of each of the components of the high-temperature SMHD and demonstrated a test unit based on the proposed Galinstan sense element. As a result, the SMHD technology was considered much lower risk compared to LFITS.

3.6 Reliability (KSA)

Reliability in the EGS environment depends primarily on the ability of the electronics to withstand high temperature. That means both that the electronic circuits have a long mean time to failure at high temperature and that the workmanship and manufacturing techniques are robust enough to prevent mechanical failure of solder joints, wiring connections, and liquid seals. The LFITS sensor would require many more electronic parts in the downhole device than the SMHD. In addition, the SMHD has intrinsic ruggedness due to a lack of moving parts aside from the sense fluid. Thus, although both technologies are rated yellow due to the need for additional qualification work, the SMHD's simplicity and toughness gives it the clear advantage.

3.7 Conclusion

A trade study was conducted to determine whether the LFITS or the SMHD was more suitable for the EGS fracture monitoring application. The study considered performance as measured by resolution, bandwidth, and dynamic range plus the key attributes of size, operating temperature, and reliability. The clear winner of the trade study is the SMHD. Its performance matches the predicted motion profile and its hallmark simplicity and ruggedness indicate that it will meet the requirements of the application much better than the LFITS.

ATTACHMENT F: 7-DOF DOWNHOLE SENSOR MARKET STUDY

Nanometrics

7-DOF Downhole Sensor for the Geothermal Market

Geothermal Market Segmentation

The geothermal market can be segmented into three different segments based on the type of energy, extraction method used. The three methods are low temperature conventional extraction, high temperature conventional extraction, and enhanced geothermal systems.

Low Temperature Conventional Geothermal Market

In low temperature conventional extraction the water extraction temperatures are less than 180 degrees Celsius and the rock has a high permeability. Typically, the energy extracted per well is substantially less than high temperature geothermal systems, and is the range of 3-4 MW per well. One of the characteristics of this type of extraction is that there are very few earthquake and microseismic earthquake events due to steam not being generated downhole and the rock being permeable. Consequently, there is no need for downhole monitoring, nor is there a need for a surface array. The regulatory framework may insist on a single surface seismic station to verify that there are indeed no earthquake events.

Although low temperature geothermal systems produce less energy, there are more of these systems being deployed with the result being that roughly half the added geothermal capacity is for low temperature systems.

The conclusion is that there is no market for downhole instruments for low temperature geothermal systems.

Enhanced Geothermal System Market

There are currently no commercial enhanced geothermal systems operating. The U.S. and Australian governments are investing in this technology since it has the potential to vastly increase the geothermal generating capacity. Enhanced geothermal systems can exploit geothermal resources from low permeability rock by fracturing the rock. These systems will require downhole monitoring to understand the rock fracture structure. While this segment does have future potential, it is probably 5-10 years before there will be significant market available.

In conclusion, there is no market for downhole instruments except for a few instruments required for experimental or demonstration systems sponsored by governments.

High Temperature Conventional Geothermal System Market

High temperature geothermal systems extract water at temperatures above 180 degrees Celsius from high permeability rock. This segment represents half the growth in geothermal capacity or about 300-400 MW per year. Generally, high temperature systems are larger, but there are fewer as compared to low temperature systems. High temperature systems do generate seismic and microseismic events due

to the boiling of the water downhole. Events are generated at the boiling interface. The location of the boiling zone is an important parameter in geothermal fields.

Most high temperature geothermal sites have seismic monitoring that consists of a multi-element surface array distributed over the geothermal field to give good location accuracies. For example, the 1517 MW geysers complex has a 40-station network, the 188 MW Los Azufres station has a 5 element seismic network, the Los Humeros power station has a 6 station seismic network. Typically, these networks consist of a mix of seismometers and accelerometers with data telemetered to a central site. The detection thresholds of these networks are approximately M0.0 to M1.0.

To resolve smaller events down to M-3.0, a microseismic downhole array is required. For example, a 16 station borehole array in the northeast corner of the geysers has a detection threshold of M-0.9. A microseismic array is used for accurate production monitoring rather than seismic hazard mitigation. To resolve microseismic events, the sensors need to be close to the active production zone, requiring a downhole sensing array. However, the science of downhole monitoring has not been proven to be necessary yet. The smaller events are not located as well as the larger events limiting the usefulness of the data. There is a view in the industry that it would be more productive to improve the velocity models rather than identify smaller events. Another factor against microseismic monitoring is that the noise environment around a geothermal field is high and can mask the microseismic events. Lastly, it is very expensive to deploy a downhole microseismic array. It costs about $1M to drill a monitoring well and another $0.5M to deploy instruments to continuously monitor. There needs to be a compelling benefit to spend that amount of money on monitoring in an industry with very tight budgets.

There are some geothermal fields where the surface noise is high. In order to reduce the effects of the surface noise, the instruments can be deployed below the surface. However, this does not create a need for a complete downhole array. Nor is there a need for deep deployments in expensive boreholes. Shallow boreholes may be sufficient.

In examining downhole geothermal sales, companies are selling about ten downhole sensors per year right now.

In conclusion, there is a very limited market for downhole instruments in the high temperature conventional geothermal market. Although 300-400 MW of capacity is being added each year, there is a limited benefit to adding downhole monitoring.

Economics of Geothermal Projects

The economics of geothermal systems need to be compared to oil and gas extraction. Both industries are extracting energy from the ground via drilled wells. However, the energy contained in hot water is 100 times less by volume than oil or gas. Therefore, the commodity coming out of a geothermal well is 100 times less valuable, although the cost of drilling is comparable. If geothermal could set power prices, then it would not be an issue. However, geothermal systems are price takers, meaning the price is set on an open market where geothermal systems are trying to compete with other power generation

technologies. It should not be a surprise that the geothermal industry spends about $10M on monitoring and instrumentation annually, whereas the oil and gas market spends $20B annually.

Geothermal Market Size

The demand for rotational seismometers for geothermal applications is directly related to the rate at which installed geothermal generating capacity is added globally. It will be easier to sell within the USA, so the analysis will be broken down into the demand in the USA and demand in the rest of the world. We are assuming that there is little demand for new sensors in the existing installed production sites. Existing production sites are already instrumented sufficiently (this is an assumption) and would likely replace damaged or failed equipment with similar replacements rather than an entirely new technology, unless there is a compelling cost savings or improvement in performance. It is very challenging to convince a customer to replace working equipment with new technologies and it is probably not worth the marketing effort at this stage. The focus will be on new installations.

Geothermal Capacity in the USA

The USA is the world leader in geothermal generation with an installed capacity of 3187 MW, or 28% of the world capacity of 11224 MW.

Figure 1: Global Context of US Geothermal Installed Capacity 1960 – 2012

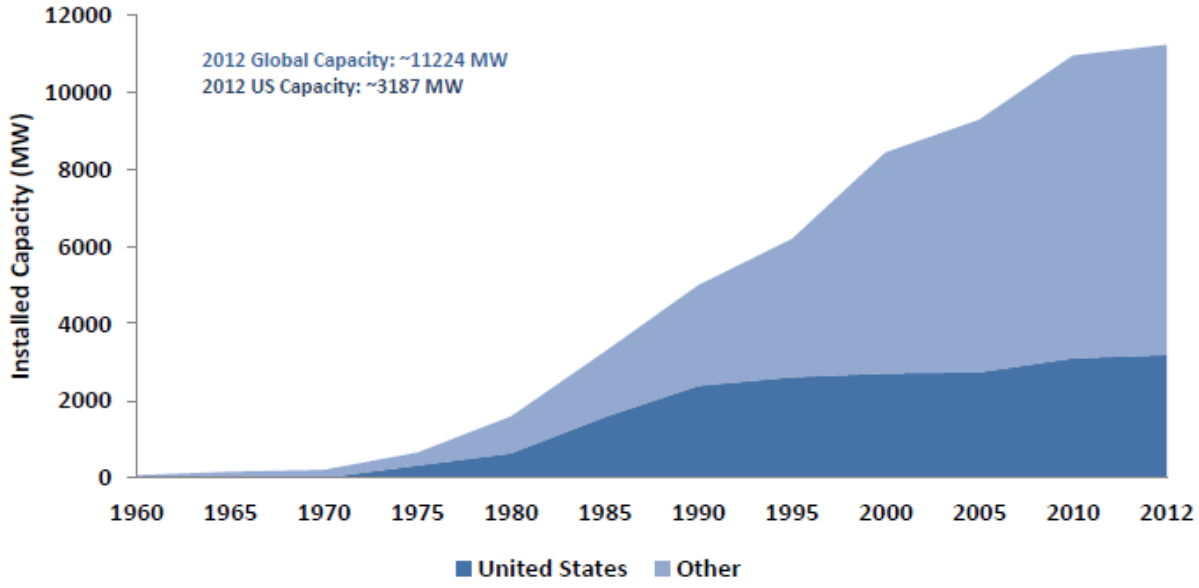

Source: GEA

Figure 1. Global Context of U.S. Geothermal Installed Capacity 1960-2012, Source GEA

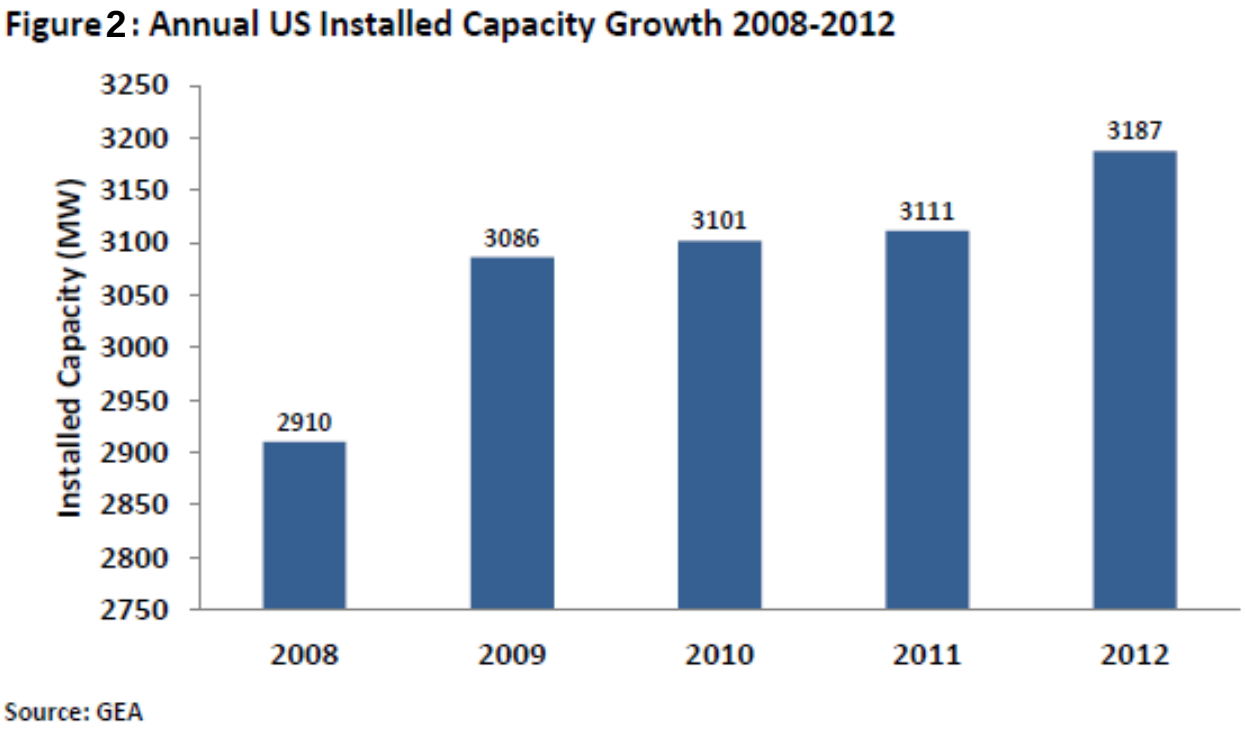

Figure 2. Annual USA Capacity Growth 2008-2012

The installed capacity increased by 5% in 2012, or 147 MW as seven projects came online. This is an increase over 2011, where 10 MW was added with two projects. These projects are listed below:

Projects that came online in 2011

Puna Expansion (HI), Ormat Technologies, 8 MW

Beowawe 2 (NV), Terra-Gen, 1.9 MW

Projects that came online in 2012:

John L. Featherstone Plant (CA), 50 MW

McGinness Hills (NV), 30 MW

Neal Hot Springs (OR), US Geothermal, 30 MW

San Emidio I (NV), US Geothermal, 13 mW

Tuscarora (NV), Ormat, 18 MW

Dixie Valley I (NV), Terra-Gen, 6.2 MW

Florida Canyon Mine (NV), ElectraTherm, 0.1MW

However, these projects should be put in perspective with The Geysers complex owned by Calpine Corp, Silicon Valley power, and Northern California power Agency. The Geysers complex has an installed capacity of 1517 MW from over 350 wells representing half of the installed capacity in the USA. Many of the newer geothermal projects are small-scale projects, which benefits companies offering newer technologies as there is a diversity of customers to pitch to, rather than a few large customers with established methodologies.

Table 1. Total Projects in Development by State

State	Total Projects	Overall Total (MW)
Alaska	6	90
Arizona	1	2
California	31	1859.7-2008.7
Colorado	2	20-25
Hawaii	3	0
Idaho	11	589-664
Louisiana	1	0.05
Nevada	59	2030.15-2250.15
New Mexico	2	115
North Dakota	1	0.25
Oregon	16	319.5-364.5
Texas	1	0.8
Utah	11	190-215
Washington	1	100
Wyoming	1	0.28
Total	**147**	**5317-5836**

Source: GEA

There is a pipeline of future projects as shown in the figure above. However, these figures include all projects at all phases, namely, Phase 1 – resource identification and procurement, Phase 2 – resource exploration and confirmation, Phase 3 – permitting and initial development, Phase 4 – power plant construction and production start. Of the 147 projects, about 100 are in phase 1 and Phase 2, 25 are in Phase 3, and about 25 are in Phase 4. The Phase 4 projects will likely come online over the next four years. Overall, the USA capacity growth will likely be in the range of 120-150 MW per year over a number of smaller scale projects.

World Demand Excluding USA

Current global geothermal production less the USA is 8138 MW and experienced 20% growth from 2005 to 2010. The top ten geothermal producers globally are as follows:

Philippines	1904 MW
Indonesia	1200 MW
Mexico	958 MW
Italy	843 MW
New Zealand	628 MW
Iceland	575 MW
Japan	536 MW
El Salvador	204 MW
Kenya	167 MW
Rest of World	1126 MW

Growth slowed from 2010 to 2012, but will likely increase from 2012 to 2015 based on the number of projects underway globally today. Using GEA estimates, we estimate there will be 8% growth annually in global geothermal capacity over the next 3 years representing 600-800 MW of added capacity each year over the next three years.

Geothermal Market Summary

The geothermal market is growing at approximately 8% per year with an estimated 4-6 new plants coming online per year in the US and 8-12 new plants coming online per year globally. One or two of these plants may require downhole instrument arrays. It would be reasonable to estimate that there is a need for one borehole array per year in the geothermal market.

In summary, the total available market is about 10 instruments per year. A 7-DOF instrument with the right marketing could expect to capture a third to half of the market or 3-5 instruments per year. This is a very small market with very limited market potential.

Non-Geothermal Applications Market Summary

The main alternative market for a 7-DOF instrument is the oil and gas market. The microseismic studies required for geothermal fields are very similar to the microseismic studies required for tight oil and gas extraction. The main difference is the size of the geothermal monitoring market relative to the oil and gas monitoring market. The oil and gas microseismic monitoring market is 10 to 100 times larger than the geothermal monitoring market. However, there needs to be a clear competitive advantage to a 7-DOF instrument over existing instruments used in the oil and gas space. We would suggest that the oil and gas market be pursued in parallel with the geothermal market once the product has been proven in demonstration projects.

Competitive Products and Pricing

There are a number of competitive products in this market. All the competitive products are translational sensors of various types.

Borehole Seismometer

Example Product: Trillium120 Borehole by Nanometrics

This product is a 3 component seismometer with a diameter of 5.7". It includes a holelock and can be deployed at any point in the borehole. The operating temperature range is -20 to 65 Deg C.

High Temperature Vertical Profiling Tools

These tools incorporate a string of high temperature geophones on up to 100 levels. These tools operate up to 150-175 degrees Celsius and typically have small diameters in the range of 40-85mm. Geophone String

Example Products:

Geochain Vertical Seismic Profile Tool by Avalon Science Ltd.

This vertical seismic profile tool uses SM-45VHT geophones, and operates up to 225 Deg C (for several days). The diameter of the tool is 3.25". Up to 100 geophone modules can be used in the string with 50ft or 100ft spacing. Other companies offer competitive products.

High Temperature Optical Accelerometer String

Example Product: OpticSeis by Paulsson Inc.

This is a seismic profile tool that can be used for microseismic studies. The tool uses a fiber optic geophone and can operate up to 300 Deg C. The product has an outer diameter of 2". This is a very new product that is undergoing testing in 2013 with a 150 level 3 component system.

VSI – High Performance Microseismic Acquisition Tool by Schlumberger

This is a vertical seismic profiling tool designed for hydraulic fracture monitoring. It has a 175 degree temperature rating,

Maxiwave Digital downhole seismic array by Sercel

The Maxiwave is a vertical seismic profiling tool with up to 100 levels. It can operate to 175 Deg C, and is 85mm in diameter. Each level has three OYO SMC1850 geophones and a 24-bit digitizer.

Downhole Acquisition Tool by ESG

This is a vertical seismic profiling tool that is 42mm in diameter. It uses a OMNI-2400 geophone

GeoRes downhole seismic system by Geospace Technologies

This tool uses a three axis OMNI-2400 geophone at each level, and can handle up to 48 levels. The temperature rating is 150 Degrees C.

Summary of Competitive Products

The products and methods currently used for downhole monitoring are well-established in the market with the large companies such as Sercel and Schlumberger offering turnkey solutions. Any new tool competing in this space must offer an instrument and methodology that has a clear competitive advantage over existing solutions.

Pricing Discussion

There is not a straight answer to the question of what is the right price for a 7-DOF instrument, it depends on a number of factors. However, as a starting point, we can estimate the minimum price based on the cost such that below that price the product is not economic to produce. This price can be built up using two methods. The first is to use a multiple of part costs, and the second method is to use a multiple of the total costs, meaning the parts costs and the manufacturing labour costs. Typically, an instrument manufacturing company needs to see a parts cost markup of 3-4 times the parts costs or a multiple of 2.5 to 3.3 times the total costs to manufacture.

Parts cost Estimate (assumes dry borehole, low temperature)

	Parts Cost	Labor Cost
3 x rotational sensor elements	6000	24 hrs
3 x geophone elements	600	3 hrs
Pressure sensor	200	2 hrs
Pressure Enclosure	2000	2 hrs
Holelock	3000	4 hrs
Electronics	1000	4 hrs
System testing		8 hrs
Totals	12,800	47 hrs x $80/hr = 3760

Price based on a 3-4 times markup of parts	38,400 – 51,200
Price based on a 2.5-3.3 times total cost	41,400 – 54,648

Using a cost based analysis, the price range is $40,000 to $55,000 per instrument would represent the minimum economic price. This price does not include cabling which will be significant at the typical depths of 1-2km. Cabling costs from $10-$15 per meter, so at 2km the cable cost is in the range of $20,000-$30,000. Nor does the price include installation costs, and the costs of ancillary equipment including surface digitizers.

Pricing Sensitivity

The market acceptance of the product is not going to strongly driven by pricing assuming the price is broadly competitive with existing solutions.

7-DOF Competitive Advantages

In order to be successful in the marketplace any new product must offer clear competitive advantages over existing established products. A competitive advantage can be cost driven, meaning, the new product is substantially cheaper than existing products, or it can provide new information or knowledge that is advantageous to a user.

Early in the program, it was envisioned that the 7-DOF instrument could be used to locate seismic events using a single instrument rather than requiring a downhole array of instruments. Drilling observation wells is expensive ($1-2M per well). The 7-DOF instrument would require a single well, as opposed to an array of 3-10 wells with established instruments. This would save millions in well drilling, representing a compelling competitive advantage.

However, earthquakes are highly directional in their energy dispersion patterns. Some locations can receive almost no seismic energy (a null point), whereas other areas can receive a strong seismic response. Consequently, there is a need to have spacial diversity, and not just a single instrument. This requirement diminishes the principal competitive advantage of a 7-DOF instrument. Further investigation is needed to understand the trade-off between spacial diversity and the addition of rotational data. Perhaps there is an optimal point of fewer instruments with rotational sensors.

A 7-DOF instrument does provide new information, namely the 3 orthogonal rotational signals, that can be used to enhance location accuracies of seismic events. However, this competitive advantage needs to proven with scientific studies.

Without a clear, compelling, and proven competitive advantages, it will be challenging and likely uneconomic to develop a market for a 7-DOF instrument at this time. We suggest that more work needs to be done to demonstrate the performance and benefits of the instrument before introducing to a market.

Desired Specifications

A better understanding of the motion environment gained through modeling or field testing will be required to define instrument specifications.

Barriers to Market Entry

Having a functional rotational 7-DOF seismometer does not necessarily mean that it will be successful in the marketplace. There are a number of external factors that will influence its market acceptance.

1. Acceptance by the scientific community that the sensor works.
2. Processing and Analysis software having the capability to handle rotational data.
3. Being able to sell the product globally.
4. A company having the ability to deliver a turn-key solution.
5. Operational evidence of outperforming translational only solutions.
6. Reliability of the sensor.
7. Use of Mercury in the sensing element

We will address each of these factors and suggest possible solutions to mitigate or eliminate the market limitation.

Acceptance by the Scientific Community that the Sensor Works

This is one of the most important factors towards market acceptance. The geophysics community is a highly technical group that has seen a large number of innovations over the last 30 years, along with a number of significant failures. There is a healthy level of scepticism about radically new technologies based on new science, particularly those technologies that customers cannot readily understand. They realize that many of these new technologies may take many years to reach the level of maturity such that they can be easily deployed in the field. The geophysics community does look to the scientific members in the community to verify the science of new technologies.

This limitation can be overcome by engaging the scientists in the geophysics community and encouraging them to test the product and publish the results, preferably in scientific journals. This is a slow process, but it is a necessary condition towards market acceptance. If the community is actively engaged, this can take anywhere from one to three years to reach a reasonable level of market acceptance. It is important to locate the opinion setters in the industry and engage them to demonstrate the performance of the instrument. This can be done by loaning instruments to a number of organizations for testing and evaluation.

Processing and Analysis Software Having the Capability to Handle Rotational Data

Having a 7-DOF sensor is only part of the solution that an end customer would require. Some components of the rest of the solution are readily available on the open market, namely, digitizers, telemetry equipment, borehole cabling, data collection software. However, there is one critical element that is missing from the solution and that is the processing software to locate events using rotational data. Event location software algorithms are very specialized and highly complex, particularly in the microseismic space. Only a few companies have the capability to write this type of software. Adding rotational processing algorithms into the location software will be challenging, and require extensive testing and field verification. The rotational signals will have different signal to noise ratios as compared

to translational signals requiring different weighting factors that may require a different approach to processing.

The best approach would be to team with a research organization in the early phases, and then find a commercial partner that has the software experience and expertise to bring the solution to market.

Being Able to Sell the Product Globally

The rotational sensor technology has not yet been assessed under the International Traffic in Arms Regulation (ITAR). An ITAR restriction would limit the market to the USA only. However, the USA market is only 17% of the global market. This would restrict sales to an extent that the market is not large enough to be economically viable. This product needs to be sold globally to be economically viable.

An assessment from the U.S. Department of Commerce is required to ensure that the instrument is not covered by ITAR restrictions.

A Company Having the Ability to Deliver a Turn-Key Solution

The power station operators are looking for turn-key solutions to monitor for microseismic events. They will evaluate a solution from end-to-end and compare it to other possible solutions from vendors selling other technologies. Operators are looking for a production tool that delivers answers in real time rather than a scientific tool that may not be an end-to-end solution, or that may or may not deliver the results they are looking for.

The most effective approach would be to team with a company that has experience in delivering turn-key solutions to this market.

Operational Evidence of Outperforming Translational Only Solutions

In evaluating a solution, a power station operator will be looking for evidence that the solution has worked at other geothermal sites. They do not want be the first customer. We should be clear that an operator may be willing to facilitate testing of a new technology, but that is different from purchasing a system for an operational environment. They will evaluate the solution against the solutions that they understand. Rotational motion is not well understood in the community, so there will be a significant hurdle to developing a level of understanding sufficient to accept the technology. There needs to be a compelling benefit for them to switch to this technology as there is risk associated with new technologies.

We suggest teaming with a power company for a demonstration project.

Reliability of the Sensor

It is expensive to deploy a deep borehole sensor. Replacing a sensor due to poor reliability will be costly and highly visible to the end customer. The downtime as a result of the replacement of a sensor may affect production at the geothermal well if there are regulatory requirements to monitor during production. This may impact revenues to the operator. The cost of reliability here is not just the cost of the sensor. It also includes the redeployment costs, and the lost revenues due to the downtime. Consequently, it is vitally important to ensure the sensor is highly reliable for this application.

Reliability is best managed by having a robust design that has been subjected to rigorous testing. The manufacturing should be with an organization that has a proven capability to deliver high quality sensors.

Use of Mercury in the Sensing Element

The 7-DOF sensor contains three magnetohydrodynamic rotational sensors. These sensors use a conductive fluid for the inertial mass. In order to achieve a low noise floor, this fluid must be liquid higher than -30 degrees C, have a high density, have a low viscosity, and have a high electrical conductivity. Currently, the most suitable material is mercury. However, mercury is a hazardous material, and there are a number of issues with it:

Regulatory environment for mercury is highly restrictive

Compliance with regulations is onerous

Product liability costs for borehole products containing mercury may be prohibitive

There are many restrictions on shipping devices containing mercury

Manufacturing costs associated with handling mercury are high

Each of these issues will be explained in more detail.

Regulatory Environment

There is a global effort "to prohibit and phase out all products containing mercury because the adverse impacts of mercury in products outweigh any benefits". Each country is enacting their own laws restricting mercury to varying degrees:

USA

- There is an export ban of mercury
- Federal regulations restrict usage
- Each state is enacting laws restricting mercury use, i.e. California:

AB 2943 is known as the "Mercury Pollution Prevention Act of 2004" and would prohibit the sale of products with added mercury beginning in 2006 at a level of 1,000 milligrams per product, becoming increasing restrictive to a level of 10 milligrams after January 1, 2008. Exemptions would be provide for fluorescent lamps, those products for which added mercury is essential to comply with federal or state health or safety standards and those products for which a manufacturer applies for and receives an exemption, which would include a system for the collection and proper processing of the product at the

end of its useful life. Products with mercury sold after 2006 would also need to be label to indicate the presence of mercury.

European Union

- There is an export ban of mercury
- Measuring devices containing mercury for use by the general public have been restricted from the market.
- "The main mercury product group not covered by Community law is measuring and control equipment. The Commission is due to present proposals to include medical devices and monitoring and control instruments under Directive 2002/95/EC[12], which already covers lighting and other electrical and electronic equipment. The ExIA finds that additional action in this area is appropriate."

Canada

"Exemptions will be included for essential products with no viable alternatives such as certain scientific, medical and industrial products (e.g. reference electrodes). Exempted products will be subject to the regulatory requirements such as labelling, reporting and record-keeping. It will also be possible for manufacturers and importers to apply for permits for new, unforeseen products that contain mercury if they offer human health or environmental benefits."

In summary, industrial products can be sold today with mercury, but the legislation is steadily restricting its usage with the goal of total phase-out of mercury.

Compliance with Regulations is Onerous

A review of the regulations shows that the proposed regulation of mercury will impose a heavy compliance cost on all manufacturers or importers of mercury containing products. For example, one jurisdiction, namely Canada, is proposing the following requirements:

- Under the proposed regulation, the manufacture or import of mercury-containing products would be prohibited, unless the product is listed in the Schedule of the regulation, has received a permit, or mercury is only incidentally present in the product. Also, the proposed regulation will not apply to certain products such as waste, products intended for recycling, drugs, veterinary biologics and military ammunition and explosives.
- It would be the manufacturers' or the importers' responsibility to apply for a permit to manufacture or import a mercury-containing product other than those listed on the Schedule of this regulation.
- Certain conditions would have to be met for a permit to be issued. The product must play an important role in the protection of human health or the environment; there must be no viable alternative product; and there must be an end-of-life management plan for it.
- Manufacturers and importers would be required to appropriately label mercury-containing products, and to ensure that the quantity of mercury in lamps is certified by a Standards Council of Canada accreditation body such as the Canadian Standards Association.

- Manufacturers and importers would also be required to submit annual reports to Environment Canada with information about the quantity of mercury-containing products that were manufactured or imported, and to keep adequate records.
- Anyone who sells to a supplier, wholesaler or retailer would also be subject to record-keeping requirements.

Other jurisdictions intend to have similar protocols and regulations. In summary, it will be expensive to comply with the proposed regulations.

Product Liability Risk

All companies are required to carry product liability insurance to cover potential claims. Product liability insurance is purchased with a stated claim limit. A company is liable for any amount beyond the limit. For example, a product liability policy for $5m and a claim of $15m would result in the insurance company paying $5m and the company paying $10m.

Mercury contamination is a potential product liability risk. A mercury spill on the ground would require decontamination of the affected area. One could imagine this costing 10k to 1m depending on the nature and extent of the spill. A mercury spill underground could leak into an aquifer causing widespread contamination of a water table. One could imagine this costing 1m-100m or more to remediate or compensate, again depending on the nature and extent of the spill

A 7-DOF seismometer is designed to be installed underground in a steel cased borehole. Occasionally, borehole instruments are lost in boreholes due to being jammed in the borehole, lift cables failing, or neglect. Mitigation solutions include:

1. Abandoning the instrument in the borehole

   Potential Long-term leakage of Mercury into the water table

2. Drilling the instrument out of the borehole (pulverizing the instrument)

   Mercury would contaminate the borehole, and the drilling rig and pad

3. Cementing the instrument into the borehole

   Potential longer-term leakage of Mercury into the water table

4. Recovery of the instrument using complex methods

   Safe but expensive recovery of instrument and mercury

There is a significant liability risk with borehole instruments containing mercury due to potential contamination of the water table. This creates a large product liability risk that may render the deployment of the instrument uneconomic.

Restrictive Transportation

There are significant restrictions on the transportation of products containing mercury. Essentially, logistics companies do not want the risk of transporting hazardous materials. For example:

- It is unlawful to transport mercury or mercury-containing products through the U.S. Postal Service.
- Canadian postal service will not transport packages containing mercury
- The transportation of mercury and mercury devices is covered by hazardous materials regulations under the US Department of Transportation (DOT) and International Air Transport Association (IATA) requiring special handling procedures by freight carriers. These procedures require a hazardous material warning label for all air shipments regardless of the amount of mercury, and for land freight in amounts of 1 pound or more. The freight carriers naturally charge a special handling fee for such hazardous materials, which can amount to $10.00 to $65.00 plus regular freight cost. These shipping costs are chargeable to the customer.
- DHL – "Mercury contained in manufactured articles" – not accepted in the Americas, Middle East, Asia Pacific. There is a 5L limit for Europe and Africa

In summary, mercury is a hazardous material with significant restrictions on its transportation.

Manufacturing Costs Associated with Handling Mercury

Mercury is a hazardous material requiring special handling and management. There are occupational exposure limits (OEL) for the organic, inorganic and elemental forms of mercury. These limits apply to workers directly involved with tasks using mercury or products containing mercury, and also to other workers in the workplace who may be exposed to mercury indirectly from these operations. It is important to note that OELs represent standards for the protection of most healthy workers. Steps must be taken to keep mercury levels as low as reasonably practicable in the workplace.

An employer must train workers on the health hazards and the safe work procedures developed by the employer, comply with the requirements for handling and storage of mercury, ensure the need for ventilation is properly assessed and systems that are installed are properly designed and maintained, and provide appropriate personal protective equipment (including respirators).

In summary, it is expensive handling mercury in the workplace.

Overall, these issues illustrate that it is challenging and most likely uneconomic to design a 7-DOF sensor containing mercury. Ideally, a different fluid should be used in a 7-DOF sensor.

Summary of the Strategies to Overcome Barriers to Entry

Below is a summary list of the strategies to overcome the barriers to entry:

1. Engage the geophysical scientific community, particularly opinion setters.
2. Loan instruments to scientific community for testing and evaluation.
3. Ensure instrument is not subject to ITAR restrictions
4. Team with a research organization to write processing software
5. Offer a turn-key solution
6. Publish papers comparing performance to translational only sensors
7. Rigorously test early prototypes to ensure a robust design
8. Eliminate mercury from the sensing elements.
9. Develop manufacturing capability for high reliability